공학박사학위논문

Development of bioelectronic nose using nanovesicle and olfactory receptor-derived peptide

나노베지클과 후각수용체 유래 펩타이드를 이용한 바이오 전자코의 개발

2014 년 2 월

서울대학교 대학원

공과대학 화학생물공학부

임 종 현

Abstract

Development of bioelectronic nose using nanovesicle and olfactory receptor-derived peptide

Jong Hyun Lim

School of Chemical and Biological Engineering

The Graduate School

Seoul National University

Smell is one of the most important senses to perceive environmental conditions. Extensive studies to develop electronic devices that mimic the function of the animal nose have been performed.[1, 2] Most electronic devices consist of an array of several sensors reacting to volatile chemical compounds. Odor is characterized through analyzing the response patterns generated by the sensor array. However, such devices have limitations in terms of sensitivity and selectivity. Hence, a novel concept of sensor device called a bioelectronic nose was suggested.[3, 4] Sensors which use biomolecules as a primary sensing material are generally called bioelectronic noses. The bioelectronic nose is composed of primary and secondary transducers. The primary transducer is an odorant-recognizing biomolecule such as olfactory receptors (ORs). The secondary transducer is a highly sensitive sensor platform that converts biological responses into signals that can be measured.

The objective of this research is to develop bioelectronic noses by functionalizing electronic sensor platforms with ORs. The ORs belong to the

G protein-coupled receptor (GPCR) family.[5] And approximately 390 kinds of ORs exist in human.[6] In this research, ORs were over-expressed in human embryonic kidney (HEK)-293 cells. The function of ORs could be elucidated using OR-expressing cells. Especially, a specific OR recognizing a lung cancer biomarker was determined. Although cells can successfully mimic the function of olfactory sensory neurons, they are unsuitable to be combined with nanomaterial-based sensor platforms due to their large size. Thus, cell-derived nanovesicles were produced from the the cells using cytochalsin B.[7] The nanovesicles contain all membrane proteins and cytosolic components for the signal transduction; therefore, they can be an excellent alternative to the cells. The OR-containing nanovesicles were immobilized on the single-walled carbon nanotube (SWNT) transistors. Odorants first bind to the ORs which are expressed in the membrane of nanovesicles. Then, the nanovesicles generate cellular signals. These signals are amplified and converted into electric responses by SWNT transistors. Through this strategy, the bioelectronic sensor detected the lung cancer biomarker with high sensitivity and selectivity.

ORs have a great selectivity capable of precisely discriminating their ligands among a mixture of other compounds. By virtue of this selectivity, bioelectronic noses can be used for the determination of quality of foods. A canine OR that detects an indicator of food oxidation was used for the functionalization of SWNT transistors in a form of nanovesicle. The developed sensor detected the indicator from the spoiled milk without any pretreatment processes.

A nanovesicle-based bioelectronic nose shows excellent performances as a sensing device in terms of sensitivity and selectivity. However, its stability is insufficient to be used in practical fields because the signaling pathway in the nanovesicle requires unstable signaling components, such as adenosine triphosphate (ATP). Thus, the signaling pathway was modulated to improve

the stability of nanovesicles. By using an OR which was covalently coupled with potassium channels, the nanovesicles can generate cellular signals without the aid of ATPs. Consequently, the stability of nanovesicle-based sensor was remarkably improved.

Whole OR proteins require a lipid membrane for their proper three-dimensional structure. However, OR-derived peptides (ORPs), which mimic odorant-binding pockets of ORs, do not require the lipid membrane; thus, reproducibility and repeatability can be improved. A bioelectronic nose using ORPs and SWNT transistors was developed for determining the degree of seafood decomposition. This bioelectronic sensor specifically detected the odorant generated from decomposed seafood with high sensitivity and selectivity. Therefore, the sensor was able to easily and rapidly determine the degree of seafood decomposition. Moreover, this peptide-based bioelectronic nose was active in a dry condition and detected gaseous odorants.

Bioelectronic noses can be applied for the various purposes, such as the diagnosis of diseases, the monitoring of environmental pollutants, and the determination of food safety. This study offers an optimal fabrication process of bioelectronic noses based on nanovesicles and peptide receptors, and demonstrates the potential for practical applications of the bielectronic nose.

Keywords: bioelectronic nose, nanovesicle, peptide, carbon nanotube, diagnosis, food quality

Student number: 2008-21108

Contents

List of Figures

List of Tables

List of Abbreviations

2M1PROH: 2-methyl-1-propanol

AC: alternating current

AcOH: acetic acid

ADP: adenosine diphosphate

AFM: atomic force microscopy

ATP: adenosine triphosphate

cAMP: cyclic adenosine monophosphate

CPNT: conducting polymer nanotube

DC: direct current

DMA: dimethylamine

DMEM: Dulbecco’s modified Eagle’s medium

dPBS: Dulbecco's phosphate-buffered saline

DW: deionized water

EA: ethylacetate

E. coli: *Escherichia coli*

EIS: electrochemical impedance spectroscopy

EtOH: ethanol

FBS: fetal bovine serum

FET: field-effect transistor

FITC: fluorescein isothiocyanate

GC-MS: gas chromatography-mass spectroscopy

GPCR: G protein-coupled receptor

HCA: hydrocinnamaldehyde

HEK-293: human embryonic kidney-293

HPLC: high-performance liquid chromatography

hPTHR: human parathyroid hormone receptor

ICCOR: ion-channel-coupled olfactory receptor

ICCR: ion-channel-coupled receptor

IMS: ion mobility spectrometry

MCA: methylcinnamaldehyde

MeOH: methanol

MOx: metal oxide

OR: olfactory receptor

ORP: olfactory receptor-derived peptide

OSN: olfactory sensory neuron

OTS: octadecyltrichlorosilane

PCR: polymerase chain reaction

PDL: poly-D-lysine

PDMS: polydimethylsiloxane

PS: penicillin-streptomycin

QCM: quartz-crystal microbalance

RTP1S: receptor-transporting protein 1S

SEM: scanning electron microscope

SD: standard deviation

SPR: surface plasmon resonance

SWNT: single-walled carbon nanotube

TEA: triethylamine

TMA: trimethylamine

Chapter 1.

Research background and objective

Chapter 1. Research background and objective

Human can perceive and discriminate numerous odors using the olfactory system. The specific smell perception is triggered by a binding event between odorants and olfactory receptors (ORs) expressed on the surface of olfactory sensory neurons (OSNs).[5] Once certain odorants bind with specific ORs, the olfactory signal cascade is activated, and olfactory signals are subsequently generated.[8] Finally, the signals are transmitted to the brain, and human become aware of the characteristics of odors such as quality and intensity. Smell perception is basically derived from the odorant-discriminating ability of ORs. In the case of human, approximately 390 kinds of functional ORs exist, and these receptors can recognize odorants with a special selectivity.[6, 9] When biological signals from ORs are transduced into perceptible signals such as electrical or optical signals, the identification of specific odors is possible without the aid of the nose.

Recently, various types of devices called an electronic nose have been developed.[2, 10, 11] These sensors are based on chemical adsorption methods rather than biological mechanisms. Common electronic noses are fabricated as arrays of several sensors providing physical or chemical responses. Such devices discriminate odors through analyzing the response pattern of the sensors. However, they have critical limitations to be applied in practical fields. First of all, the sensitivity of electronic noses is insufficient. Human nose was reported to detect odorants at concentrations lower than ppt level in olfactory sensory tests, whereas the sensitivity of electronic noses was mainly in the ppm or ppb range.[12] Moreover, electronic noses could not specifically distinguish one odorant within a mixture of odorants. Overall,

electronic noses cannot fundamentally mimic biological olfaction because ORs are not used.

A bioelectronic nose is based on OR proteins or cells expressing ORs on their surface. ORs act as an odorant-recognition element, and are combined with sensor devices to convert biological signals into electrical or optical signals.[3] Because ORs provide the odorant-discriminating ability, the bioelectronic nose can closely mimic the natural olfactory system.[12, 13] The concept of odorant analysis using bioelectronic noses fundamentally differs from the odor-discriminating strategy of electronic noses based on the pattern recognition using sensor arrays. Instead, when the ORs are utilized as a primary sensing material, the sensors benefit from their own selectivity towards the odorants, and can precisely distinguish a target molecule among a mixture, similarly to the human nose.[13] In addition, sensors based on ORs are more sensitive than electronic noses. The limit of detection reaches a femto-molar range in liquid conditions and ppt range in gaseous conditions.[12-14]

In spite of these advantages of bioelectronic noses, they are not yet used in extensive fields. This is because their potential for practical applications has not been clearly verified. Moreover, functions of all ORs have not yet been fully elucidated. Therefore, the development of bioelectronic noses which can detect its ligands from practical samples was required. And the relationship between various ORs and odorants needed to be investigated further.

In this research, a specific human OR reacting to a lung cancer biomarker was determined using calcium signaling assay. Then, a bioelectronic nose using nanovesicles and single-walled carbon nanotube

field-effect transistors (SWNT-FETs) was developed. This sensor can detect the lung cancer biomarker from human blood plasma without any pretreatment processes. Also, a nanovesicle-based bioelectronic nose for the assessment of food oxidation was developed. These sensors could detect odorants with high sensitivity and selectivity; however, stability in a non-frozen state was insufficient. Thus, the study for improving the stability of nanovesicles was conducted. In more practical terms, a peptide-based bioelectronic nose for the determination of seafood decomposition was developed. This sensor has high repeatability as well as sensitivity and selectivity.

In summary, the objectives of this study are:

1. The development of bioelectronic noses based on nanovesicles and SWNT-FETs for the detection of lung cancer biomarkers and for the assessment of food oxidation
2. Improvement of nanovesicle stability using ion-channel-coupled ORs
3. The development of a bioelectronic nose based on OR-derived peptides and SWNT-FETs for the reproducible and repetitive detection of trimethylamine (TMA), an indicator of seafood decomposition
4. Fabrication of a detection system for the sensing of gaseous odorants

Bioelectronic noses have excellent characteristics as a sensing device. They can sensitively and selectively detect its ligands from practical samples, such as blood or foods. Therefore, bioelectronic noses will be readily applied

in various fields such as the diagnosis of disease, the assessment of food safety, and the monitoring of environments.

Chapter 2.

Literature review

Chapter 2. Literature review

2.1 History of artificial smelling methods

2.1.1 Trained animal

Sense of smell is the most mysterious sense among five senses, and its biological mechanism was revealed relatively later than other senses. This sense has been instinctually used for the perception of dangerous situations or subtle changes in the environment. For instance, fire can easily be recognized through the smell of smoke, and the spoilage of food can be determined by their putrid odors. However, humans have insensitive noses. Non-human vertebrates such as dogs and mice have more types and numbers of olfactory sensory neurons (OSNs) in their noses.[15-17] This makes them more sensitively smell something out than human beings. In airports, the scene of trained dogs sniffing for explosives and drugs is quite natural.

Many animal trainers and scientists have attempted to train animals for various purposes. Dogs have been trained to detect illegal narcotics and explosives, and their reliability has been examined by many scientists.[18, 19] Trained dogs are able to find narcotics and explosives with very high accuracy.[20, 21] Therefore, they are commonly used in various places such as customs. More recently, dogs have been trained for the diagnosis of diseases. Various types of intractable diseases such as lung, bladder, and breast cancers require early diagnosis. These diseases cause tiny changes in body or urine odors. Although people cannot perceive such small changes, dogs can.[22-24] Mice and rats are also good odor detectors.[25-28] They can recognize

compounds which are regarded as odorless, such as carbon dioxide.[29] For these advantages, animals are still trained as alternatives to the human nose.

Even though animals can smell with high sensitivity and reliability, they have significant limitations as odor detectors. For instance, training and maintenance require high costs. Also, various external parameters such as illness and disorders can affect their smelling abilities. Most of all, after finishing their smelling work, they require rest for a long time before working again because their ability is easily and rapidly lost. This olfactory adaptation is a severe problem with the exploitation of animal noses.[30, 31]

2.1.2 Electronic nose

Electronic noses were first suggested in 1982.[1] A novel smelling device was constructed using semiconductor-based transducers, and it was demonstrated that the sensor was able to reproducibly discriminate various odors. Following this achievement, many studies have been performed to find new and more advanced materials for smelling devices.[32-35] Important studies supporting the scientific background of electronic noses have been reported. In the early 1990s, L. B. Buck and R. Axel revealed the olfactory mechanism.[5, 36] In the nasal cavity, there are numerous OSNs, which are the primary odor-sensing cells. Each OSN expresses a single type of OR on its surface membrane.[8] ORs have an excellent selectivity capable of precisely discriminating ligand molecules among a mixture of analogous compounds.[37] Once a certain odorants bind with specific ORs, a signal cascade is activated and olfactory signals are generated.[8] The generated

signals are transmitted to the brain, and a person becomes aware of the characteristics of odors using the combination of activated OSNs.[38]

The odor-discriminating mechanism of the natural olfactory system is very similar to that of electronic noses. Electronic noses are commonly composed of an array of several sensors. Each sensor produces specific responses by reacting to chemical compounds. Thus, an electronic nose can generate 'odor fingerprints' which are unique patterns of odorants.[39] Odorants can be identified by analyzing the response pattern. The stimulation of odorants generates specific response patterns from olfactory cells in the natural olfactory system or sensor arrays in the electronic nose.[40] The generated patterns are analyzed as a specific characteristic of odors in the brain or electric devices. Both human and electronic noses recognize odors through this process.

Many compounds have been used as a sensor material for the development of electronic noses. Metal oxide (MOx)-based sensors have mostly been developed.[41-45] The surface of MOx is modified with diverse chemical compounds. An array of MOx allows the sensor to generate specific response patterns. Conducting polymers or field-effect transistors have also been applied to electronic nose systems.[46-48] Such devices have been utilized in many fields requiring the detection of toxic molecules such as amines, alcohols, and sulfur compounds. Also, surface acoustic wave transducers with an array of polymer layers have been extensively used for the development of electronic noses.[49-52]

However, electronic noses have critical limitations for applications in practical fields. First, the sensitivity is insufficient. It was reported that people can detect odorants at concentrations lower than the ppt level,

whereas the sensitivity of electronic noses has mainly been in the ppm or ppb range. Electronic noses could not specifically distinguish one odorant within a mixture of odorants. Moreover, electronic noses cannot fundamentally mimic the human biological olfaction due to the absence of odorant-recognizing biomolecules.

2.1.3 Bioelectronic nose

In the late 1990s, a novel and more advanced concept of sensor devices was suggested.[4] The challenge was to use ORs as a sensing material in order to mimic the human or animal olfactory system. This new device is called a 'bioelectronic nose'. The bioelectronic nose is based on OR proteins or cells expressing ORs on their surface membrane. ORs are odorant-recognition elements, and are combined with sensor devices that convert biological signals into electrical or optical signals.

Since ORs provide odorant-discriminating ability, the bioelectronic nose can closely mimic the human or animal olfactory system. The concept of odorant analysis using a bioelectronic nose fundamentally differs from the odor-discriminating strategy of electronic noses based on pattern recognition using sensor arrays. When the ORs are utilized as a primary sensing material, the sensors can precisely distinguish a target molecule among a mixture of various compounds. In addition, sensors based on ORs are more sensitive than electronic noses. The limit of detection reaches the femto-molar range in liquid conditions and the ppt range in gaseous conditions, which is similar to that of the human nose.[12, 13] By virtue of these excellent characteristics, the bioelectronic nose is now receiving great attention from diverse fields

such as disease diagnosis, food safety assessment, and environmental monitoring.

2.2 Concept of bioelectronic nose

2.2.1 Biological recognition element

A bioelectronic nose consists of two main parts: an odorant-recognition element and a signal transducer.[3] For the odorant-recognition, cells expressing ORs in their surface membrane, OR proteins, and nanovesicles have generally been used. In the human nose, approximately 390 different types of functional ORs exist.[53] However, humans can discriminate thousands of types of odors. This asymmetry originates from the excellent odorant-recognition ability of ORs, which are capable of distinguishing between their specific ligands and partial ligands, as well as irrelevant molecules.[8, 38] A single odorant activates various types of ORs, and one OR is activated by several odorants. Thus, numerous combinations of activated ORs can be generated. These combinations are recognized as a unique property of an odor in the brain.[53]

A bioelectronic nose utilizes this odor-discriminating ability of ORs. Thus, they can detect specific odors with great selectivity. For instance, the odor from decomposed seafood can be easily distinguished among other odors from various spoiled foods when a bioelectronic nose is functionalized with receptors that can selectively detect the odor of spoiled seafood.[54] However, problems still remain to be overcome. ORs have a seven-transmembrane structure with a high hydrophobicity in the transmembrane

region, which makes the expression of ORs in a heterologous system very difficult.[55] Several attempts have been made to achieve functional expression in various heterologous systems. Among various systems, human embryonic kidney (HEK)-293 cells are broadly used because they allow for a relatively high expression level.[56-58] The identification of membrane-targeting tags and accessary proteins assisting the membrane expression, such as rho-tag and receptor-transporting protein 1S (RTP1S), facilitated the high-level expression of ORs in mammalian cells.[59-61] Insect cells, such as SF9 cells, have also been used for the functional expression of ORs.[62, 63] *Saccharomyces cerevisiae* and *Escherichia coli* are also good OR expression systems.[64, 65] These systems allow for mass production and efficient purification processes. Thus, they are effectively being used to produce OR proteins for bioelectronic noses.

2.2.1.1 Receptor-based bioelectronic nose

The type of the bioelectronic nose can be classified on the basis of the biological recognition elements. The bioelectronic noses can be functionalized with OR proteins. The receptor proteins can be obtained from all types of expression systems, such as mammalian cells, *Saccharomyces cerevisiae*, and *E. coli*. Then, the proteins are combined with diverse types of secondary transducers, such as quartz-crystal microbalances (QCMs),[66-70] surface plasmon resonances (SPR),[71-73] and field-effect transistors (FETs) [45, 46, 70-72].[12-14, 74, 75] The binding event between ORs and odorants induces a mass change in ORs. This change is converted into measurable signals through QCMs. The binding can also be monitored using SPR-based

devices by measuring the change in optical properties that occurs on a metal surface coated with ORs. The sensing mechanism of an FET-based sensor is based on the change in charge of the ORs. When OR binds with odorants, its conformation changes. By the conformational change of the OR, the net charge of the OR protein subsequently changes.[13, 76] The change in charge acts as a gate potential to FET devices, and the odorants are detected.

Receptor-based bioelectronic noses have many advantages as a practical sensor, although additional studies on protein quality control are still required due to the complex structure of ORs. Most of all, they have excellent selectivity of ORs, because the whole protein is used. Therefore, the sensor can precisely discriminate its ligand from other analogous compounds.[13] In addition, the mass production of ORs is possible, and storage is relatively easy.[65] Furthermore, OR proteins expressed in *E. coli* were reported to still be active in dry conditions, which allowed for a biosensor that detects gaseous odorants to be developed.[12]

2.2.1.2 Cell-based bioelectronic nose

Bioelectronic noses based on cells which express ORs on their surface are classified as cell-based bioelectronic noses. The cells can generate cellular signals. The binding event between ORs and odorants triggers the olfactory signaling cascade, and positive ions flow into the cells from the outside.[66, 77] The electrical potential of the cells consequently changes. The potential change can be measured by various sensing methods, such as fluorescent dyes, SPRs, and planar microelectrodes.[77-81]

One of the most important characteristics of cell-based bioelectronic noses is that the cells containing ORs produce the olfactory signals, which may be identical to the signals generated by OSNs. Because the isolation and *in vitro* culture of OSNs are very difficult, the practical use of OSNs is realistically impossible. Therefore, as an alternative to OSNs, OR-containing cells have been effectively utilized. The function of each OR has not yet been fully identified, and has to be elucidated to understand the mystery of the sense of smell. Cell-based bioelectronic noses can be effectively used for the identification of the unrevealed function of ORs.

2.2.1.3 Nanovesicle-based bioelectronic nose

The concept of using nanovesicles lies between those of cells and protein. Nanovesicles can generate cellular signals similar to those produced by cells. They are produced from the cell surface by treatment with a chemical compound that destabilizes the cellular membrane.[7] When nanovesicles are isolated from cells, all membrane proteins and cytosolic components for the signal transduction are still contained in the nanovesicles. Therefore, the nanovesicle can have cell-like properties. In addition, nanovesicles have advantages as a protein-like material in terms of long-time storage and mass production.

The nanovesicle is especially suitable to be combined with nano-materials by virtue of its small size. Therefore, nanovesicles have been effectively used for the functionalization of FETs. The nanovesicle-based bioelectronic nose was first developed in 2012.[82] H. J. Jin *et al.* demonstrated that the odorants can be selectively and sensitively detected through the

olfactory signaling pathway in nanovesicles. Nanovesicle-based sensors have been applied in diverse fields, such as in the assessment of food quality and the diagnosis of diseases.[83]

2.2.2 Signal transducer

The biological responses generated from ORs are mainly divided into three types: conformational changes in ORs, dissociation of the α-subunit of G proteins from activated ORs, and ion influx caused by the signal transduction in cells. These biological responses should be converted into signals that can be measured. Devices for this role are called signal transducers or secondary transducers.[3]

2.2.2.1 Quartz crystal microbalance (QCM)

QCMs have been used for the development of receptor-based bioelectronic noses.[66-70] The functionalized surface of quartz crystals is coated with ORs. The whole mass of ORs increases by the binding between ORs and odorants. QCM can specifically detect this change. The adsorption of specific molecules onto the surface of quartz crystals coated with ORs results in the reduction of the resonance frequency of the quartz crystal. Odorants can be detected using this principle.

Research on QCM-based bioelectronic noses using ORs isolated from bullfrogs was reported in 1999.[70] The specific recognition of odorants could be monitored in real-time using the QCM device. It was demonstrated that the ORs over-expressed in *E. coli* and in mammalian cells could also be

utilized for the functionalization of QCM chips.[66, 69] These studies represent that the piezoelectric method can be used for the development of highly sensitive and selective bioelectronic noses. However, QCM devices have an issue that must be overcome. The oscillation frequency of quartz crystals can be easily affected by various external factors, such as electromagnetic fields and pressure. Hence, non-specific noise signals are frequently generated.[84, 85]

2.2.2.2 Surface plasmon resonance (SPR)

SPR has been broadly used to measure the association and dissociation of analytes on a surface. The SPR is an optical phenomenon that occurs when p-polarized light hits a prism covered with a metal surface.[86] At a specific incident angle, the intensity of the reflected light is reduced due to resonance energy transfer. This resonance angle is affected by the adsorption of specific molecules onto the metal surface. When the surface of SPR is coated with ORs, the binding of odorants to ORs influences the resonance angle.

In olfactory signaling, the activated ORs induce the dissociation of the α-subunit of G proteins. In order to utilize this event, ORs and $G\alpha_{olf}$ proteins were immobilized onto the chip of SPRs and can be used to analyze the association and dissociation of ligands.[72, 73] The activation of ORs could be monitored by measuring the release of Gα subunits. SPRs have also been utilized for the development of cell-based bioelectronic noses.[78, 81] The cells were cultured on SPR chips. Then, the inflow of ions into the cells was measured. The influx of calcium ions that occurs by the olfactory signaling

affects the resonance angle of the SPR chip, and the odorants could be detected.

2.2.2.3 Electrochemical impedance spectroscopy (EIS)

EIS is an effective technique to characterize electrodes functionalized with biomolecules. EIS technique commonly requires counter, reference, and working electrodes. And the chemical reaction on the working electrodes was detected through analyzing the electrical impedance spectrum on the devices. For bioelectronic noses, the surface of the working electrode was immobilized with ORs. The binding of odorants to ORs was recognized as a kind of chemical reactions, and affected the impedance value. Consequently, the odorants were measured by recoding the experimental impedance spectrum. Using this principle, EIS-based bioelectronic noses have been successfully developed.[87, 88]

2.2.2.4 Planar microelectrode

Planar microelectrodes have also been used to develop cell-based bioelectronic noses.[79] The cells expressing olfactory receptors are cultured in a chip patterned with planar microelectrodes. After treatment with specific odorants, positive ions flow into the cells. The influx of ions is subsequently transduced into electrical signals through planar electrodes. In addition, the signals could be amplified by electrical stimulation.[80] These results demonstrated the possibility of developing cell-based bioelectronic noses using planar microelectrodes.

2.2.2.5 Field-effect transistor (FET)

Nanomaterial-based field-effect transistors (FETs) have been used for the development of bioelectronic noses. FET sensors react to the event of changes in charge that occur near the sensing channels, and generate highly sensitive responses (Figure 2.1). In order to improve selectivity, FETs are generally functionalized with diverse types of biomaterials such as OR proteins,[12-14, 74, 75] nanovesicles,[82, 83] and OR-derived peptides.[54] The binding event between OR and odorant induces changes in charge of the ORs. This change is subsequently converted into highly sensitive electrical signals through nanomaterials.[13] Nanomaterials with semi-conducting properties have often been utilized to fabricate the sensing channels of FETs, such as single-walled carbon nanotubes (SWNTs), conducting polymer nanotubes (CPNTs), and graphene. Such sensors were able to detect target odorants in the femto-molar range.

Carbon-based nanomaterials such as SWNTs and graphene have been used for bioelectronic noses. SWNTs and graphene-based FETs have excellent properties in terms of sensitivity. The limit of detection of graphene-based bioelectronic noses has reached 40 aM.[14] They can be fabricated through a self-assembly process, which means that large-scale production is possible.[89] In 2009, T. H. Kim *et al*. first reported a SWNT-based bioelectronic nose.[13] They demonstrated the sensitivity and selectivity of the SWNT-based sensor. Following this research, many studies to improve the activity of the sensor and to apply to various fields are now being conducted.[54, 75, 82, 83]

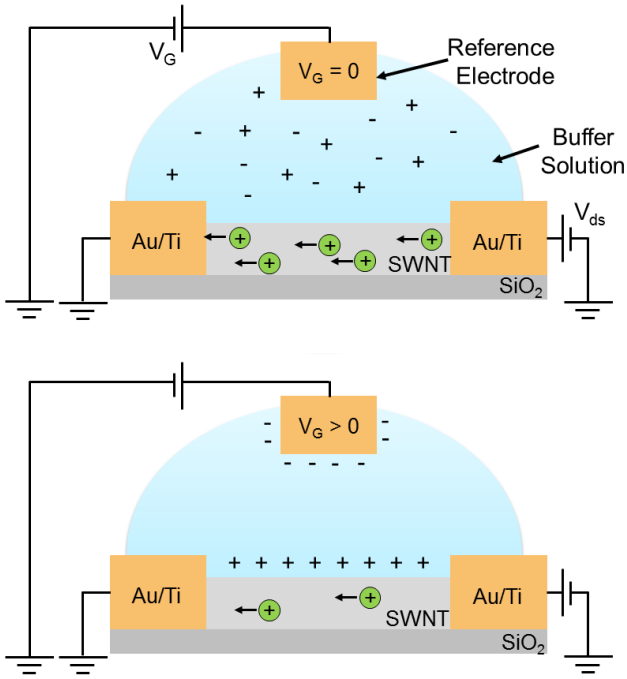

Figure 2.1 A concept of SWNT-FETs. Because SWNT-FETs exhibit *p*-type characteristics, holes are dominant charge carriers. When a positive voltage is applied to a gate electrode (V_G), the number of hole carriers in the SWNT channel decreases. Consequently, the conductance of the SWNT-FET decreases.

Conducting polymers are also very effective sensing materials. In 2009, polypyrrole nanotubes were first used for the development of a bioelectronic nose.[74] Polypyrrole nanotubes were able to convert the conformational change of ORs into highly sensitive electrical signals. There are many advantages in using conducting polymers as a secondary transducer. The immobilization of biomaterials becomes easier because functional groups such as carboxyl or amine group can be easily incorporated during the polymerization process. Moreover, the conformation of conducting polymers can be effectively modified to enhance the conducting properties of materials. For instance, conducting polymer nanoparticles, rather than nanotubes, have also been utilized to fabricate biosensors.[90] Lastly, conducting polymer is very stable against non-specific influences, which means conducting polymer-based sensors are suitable for practical applications requiring the detection of analytes from real samples.[91]

2.3 Characteristics of bioelectronic nose

2.3.1 Sensitivity

The sensitivity toward a specific ligand is one of the most important characteristics of sensors. Artificial olfactory sensors need to be just as sensitive as the human nose. Otherwise, direct sniffing may be more advantageous in terms of sensitivity than using complex equipment. Because the smelling ability of a person is quite excellent, it is a challenge to achieve better sensitivity.

In bioelectronic noses, ORs assist the accumulation of odorants very close to the secondary transducers and produce primary biological signals. Thus, odorants can be more sensitively detected compared to the sensors without ORs. The sensitivity of bioelectronic noses is dependent on the type of secondary transducers. Nanomaterial-based secondary transducers generally show extremely high sensitivity. T. H. Kim *et al.* first reported on an ultrasensitive bioelectronic nose with a detection limit in the femtomolar range by functionalizing SWNT-FETs with human ORs.[13] The binding of odorants to ORs induces the conformational change of ORs, and this conformational change results in changes in the electrical charge. This consequently affects the current of FET sensors. When conducting polymer nanotubes were used as a secondary transducer, the sensitivity was even more improved.[74] The sensitivity of a nanovesicle-based sensor is also very high because the nanovesicles effectively induce the accumulation of charged ions close to the sensing channel. The sensitivity of nanovesicle-based bioelectronic noses reached 1 fM.[82, 83]

Recently, 40 aM detection was possible using human ORs and graphene-based FET platforms.[14] Graphene was treated with oxygen and ammonia plasma to control the bandgap of graphene. Then, OR was conjugated with oxygen plasma-treated and ammonia plasma-treated graphenes. Once the conformation of OR changes to an active form, the charge of OR also changes. The odorants were detected by measuring the change in charge using a graphene-FET. The sensor was able to detect 0.04 fM of amyl butyrate, a specific ligand of the OR used.

In the case of gas-sensing bioelectronic noses, the most sensitive sensor was reported by S. H. Lee *et al*. in 2012. The sensor was fabricated with

human ORs and CPNT-FETs, and was able to detect 0.02 parts-per-trillion (ppt) of gaseous odorants.[12] This sensitivity was comparable to that of a human expert.

2.3.2 Selectivity

The advantage of biosensors is commonly regarded to be selectivity, the ability to specifically detect target molecules. Bioelectronic noses are able to selectively detect their ligand molecules among a mixture of other compounds. The selectivity is derived from the characteristics of ORs. Compared to other biomolecules, ORs have a higher capability to discriminate small chemicals. They can even distinguish the difference of one carbon atom.[13] The sensor developed by T. H. Kim *et al*. precisely recognizes amyl butyrate, a specific ligand of the OR used, from other analogous compounds such as butyl butyrate, propyl butyrate, and pentyl valerate.[13] The only difference between amyl butyrate and the analogous molecules is their alkyl chain length. The selectivity of cell-based or nanovesicle-based bioelectronic noses is also excellent because they generate responses through the original olfactory signaling pathway, as well as utilize the membrane-integrated intact OR proteins.[82]

2.3.3 Human-like behavior

Since the bioelectronic nose utilizes the original ORs, it shows human-like behaviors. S. H. Lee *et al*. functionalized CPNT-based FETs with human ORs, and demonstrated that the sensor was able to recognize odorants with human nose-like characteristics.[12] First, they compared sensor responses generated by the OR-based bioelectronic nose to the normalized cell responses generated by the cellular signal transduction. The recognition pattern by the sensor against several odorants is very similar to that by the cellular signals. Because the signals generated from the cells represent the natural odor response of the human nose, it was verified that the sensor was able to recognize the odorants with human nose-like characteristics. The antagonism of ORs was also demonstrated. ORs can modulate more complex reactions such as antagonism.[92] The binding between OR proteins and agonists, a specific ligand, is interrupted by antagonists. The methylcinnamaldehyde (MCA) and hydrocinnamaldehyde (HCA) are the antagonists of the OR that were used.[93] The response intensities measured by the bioelectronic nose decreased with an increase in concentrations of MCA and HCA. This result clearly represents that the antagonism can occur in the bioelectronic nose, and that the function of the OR remained entirely in the sensor system.

Human-like bioelectronic tongues have also been developed using human bitter taste receptor.[91, 94] The structure of bitter taste receptors is very similar to that of ORs. Thus, a bioelectronic tongue can be fabricated through the same process as that of the bioelectronic nose. The bitter taste receptor was produced from *E. coli*, and used for the functionalization of

nanomaterial-based FETs. When human bitter taste receptor was used as a primary sensing element, the sensor also showed human tongue-like behaviors. The sensor was able to not only selectively discriminate bitter substances, but also quantitatively measure the bitterness of vegetables.[91] These human-like behaviors are unique characteristics that electronic devices can never have if biological receptors are not utilized.

Chapter 3.

Experimental procedures

Chapter 3. Experimental procedures

3.1 Gene cloning

All of human OR genes were amplified by polymerase chain reaction (PCR) from a human genomic DNA library. Then, OR genes were inserted into an expression vector, pcDNA3 (Invitrogen, USA). Flag-tag and rho-tag were fused at the N-terminus of OR genes for the immunoblot assay of ORs and the membrane expression, respectively. The flag-tag and rho-tag sequences are DYKDD DDK and MNGTE GPNFY VPFSN KTGVV.

Human receptor transporting protein 1S (RTP1S) genes were inserted into pcDNA3 vector (Invitrogen, USA). Human $G\alpha_{olf}$ gene was inserted into pcDNA3.1 vector (Invitrogen, USA).

Gene of cfOR5269, one of canine ORs, was inserted pIRES vector encoding influenza virus leader peptide and myelocytomatosis cellular oncogene (cMyc) epitope-tag (received from Prof. Francis Galibert). The influenza virus leader peptide and the cMyc-tag were incorporated for the membrane localization and the immunoblot assay of cfOR5269, respectively.

Kir6.2 channel was fused at the end of C-terminus of hOR2AG1. 25 N-terminal sequences of the Kir6.2 channel were excluded for the effective conformational change of the channel. Flag-tag and Rho-tag were fused at the N-terminus of hOR2AG1. Kir6.2 channel-fused hOR2AG1 was inserted into pcDNA3 vector.

3.2 Expression of ORs in HEK-293 cell

3.2.1 Electroporation

HEK-293 cells were cultured in Dulbecco's modified Eagle's medium (DMEM; WelGENE, South Korea) supplemented with 10% fetal bovine serum (FBS; Gibco, USA) and 1% penicillin-streptomycin (PS, Gibco, USA) at 37 ˚C and 5% CO_2. Transfection was carried out using a Neon Transfection System (Invitrogen, USA). The cells were harvested and resuspended to a density of 1.5×10^7 cells mL^{-1}. Afterwards, the 100 μL of cell solution was mixed with 5 μg of pcDNA3 plasmids encoding Rho-tag-fused OR genes. 1 μg and 0.5 μg of plasmids encoding $G\alpha_{olf}$ and RTP1S genes, respectively, were additionally mixed according to the experimental purposes. After the mixing process, electric pulses (1100 V, three times, and 10 ms) were applied. The cells were subsequently cultured for 48 h.

3.2.2 Lipofection

HEK-293 cells were cultured in DMEM containing 10% FBS and 1% PS at 37 ˚C in 5% CO_2 environment. The cells (>90% confluent) were transfected with 4 μg of pIRES plasmids encoding influenza virus leader peptide, cMyc-tag, and cfOR5269 using lipofectamine2000 reagent (Invitrogen, USA) according to the manufacturer's protocol. The transfected cells were subsequently cultivated again for 48 h.

3.2.3 Production of nanovesicle

Nanovesicles were produced from the OR-expressing cells by incubating the cells in DMEM containing 10 μg mL^{-1} of cytochalasin B (Sigma, USA) with agitation at 37 ˚C for 25 min. The parent cells were separated from the nanovesicles by centrifugation at 500 g for 10 min in Eppendorf tubes, and the supernatant was then further centrifuged to collect the nanovesicles at 15000 g for 30 min. The nanovesicles were finally resuspended in Dulbecco's phosphate-buffered saline (dPBS; Gibco, USA) with 1000 ng mL^{-1} of total protein concentration. Nanovesicles were stored in a frozen state at -70 ˚C, and were melted immediately before being used.

3.2.4 Immunoblot analysis

Cells and nanovesicles were lysed by sonication (2 s on/off, 5 min), and the supernatant and pellet fractions were separated by centrifugation at 15000 g for 30 min. In order to concentrate the proteins, supernatant fractions were lyophilized and then resuspened. Supernatant and pellet fractions with 1 mg mL^{-1} of a total protein concentration were used to confirm the expression of $G\alpha_{olf}$ proteins and OR proteins, respectively. Prepared protein samples were separated by sodium dodecyl sulfate-polyacrylamide gel electrophoresis and transferred to polyvinylidene fluoride membranes (Bio-Rad, USA) under 0.15 A of constant current condition for 60 min. The membranes were incubated in PBS containing 5 wt% skim milk and 0.1 vol% Tween-20 for 2 h, and then incubated in the solution of 1:1000-diluted primary antibodies for 2 h. The primary

antibodies were anti-rho rabbit antibody (GenScript, USA) and anti-$G\alpha_{olf}$ goat antibody (Santa Cruz Biotechnology, USA). The membrane was then incubated in the solution of 1:1000-diluted secondary antibodies for 2 h. Anti-rabbit IgG (Amersham-Pharmacia Biotech, UK) and anti-goat IgG (Millipore, USA) conjugated with horseradish peroxidase were used as a secondary antibody. Luminescence was measured using enhanced chemiluminescence detection kits (Amersham Pharmacia Biotech, UK).

3.3 Calcium signaling assay

Fura-2, a calcium ion-sensitive fluorescent dye, was loaded into OR-expressing cells by incubating the cells in Ringer's solution (140 mM NaCl, 1 mM $MgCl_2$, 1.8 mM $CaCl_2$, 5 mM KCl, 5 mM glucose, and 10 mM HEPES (pH 7.4)) containing 10 mM Fura-2/AM (Invitrogen, USA) at 37 ˚C for 30 min. After the Fura-2-containing solution was replaced with fresh Ringer's solution, fluorescence intensities were measured using a GENios Pro microplate reader (Tecan, Germany). Excitation alternating between 340 and 380 nm was applied, and the amount of fluorescence emitted at 510 nm was recorded. The amount of intracellular Ca^{2+} was measured from the ratio of fluorescence emissions (excitation at 340/380 nm). In order to measure the calcium signaling in nanovesicles, Fura-2-loaded nanovesicles were produced. The Fura-2 loaded nanovesicles were immobilized on a 96-well plate (Nunc, Denmark) pre-coated with 0.1 mg mL^{-1} poly-D-lysine (PDL). The amount of fluorescence from the nanovesicles was measured using the same method described above.

3.4 Preparation of peptide receptor

Olfactory receptor-derived peptide (ORP; NQLSN LSFSD LCFFF) and four kinds of fluorescein isothiocyanate (FITC)-conjugated peptides (GG, GGF, GGFF, and GGFFF) were synthesized by PEPTRON (www.peptron.com) with purity greater than 90%. The ORP were suspended at 1 mg mL^{-1} in DW. Four FITC-peptides were suspended at the same molar concentration (1 mM). The suspended peptides were kept frozen at -20 ˚C, and were melted right before they were used.

3.5 Fabrication of bioelectronic nose

3.5.1 Fabrication of SWNT-FET

SWNT-FETs were fabricated using photolithography technique. First, methyl-terminated octadecyltrichlorosilane (OTS) was patterned on a SiO_2 wafer using the photolithography method. The OTS-patterned wafer was then dipped into SWNT suspensions (0.05 mg mL^{-1} in dichlorobenzene) for approximately 10 s. During the dipping process, SWNT networks were self-assembled on the exposed SiO_2 surface. Ti (10 nm)/Au (30 nm) electrodes were deposited using the photolithography method, and were covered with an insulating photoresist (DNR) to block contact with the solutions.

3.5.2 Immobilization of nanovesicle

For the immobilization of nanoveislces, 0.1 mg mL^{-1} of PDL solution was added to the SWNT channel region and incubated for 2 h. Then, 1 μL of nanovesicle solution was added to the PDL-coated SWNT channel and incubated for 2 h. Nanovesicles were immobilized on the PDL-coated surface by a charge-charge interaction.

3.5.3 Immobilization of peptide receptor

For the immobilization of ORPs, 1.5 μL of ORP-suspended DW solution was placed on the SWNT channel region of the fabricated chip for 4 h. During that period, the ORPs were coated on the SWNTs with a monolayer *via* self-assembly. Finally, the chips were washed with DW 3~4 times to remove unbound ORPs.

3.5.4 Characterization of nanovesicle immobilization using atomic force microscopy (AFM)

The immobilization of nanovesicles was performed in dPBS solution. After the immobilization processes, the SWNT chennel was washed 2~3 times with dPBS. The dPBS solution was then gently dried by blowing N_2 gas onto it. The dried samples were subsequently used for the AFM imaging. The AFM imaging was carried out under ambient conditions using the AFM system (MFP-3D, Asylum Research, USA) in intermittent mode.

3.5.5 Characterization of nanovesicle immobilization using scanning electron microscope (SEM)

Nanovesicles on SWNT channels were fixed by the incubation in 1% OsO_4 solution for 30 min. After the fixation of the nanovesicles, the substrate was washed with deionized water and then dehydrated in ethanol with increasing concentrations. Finally, the prepared substrate was dried in a critical point dryer (CPD 030, Balzers, Germany) and coated with Pt (10 nm) by a sputter (SCD 040, Balzers, Germany). The image of fixed nanovesicles on the SWNT channel was taken by SEM (JEOL, Japan) with a 30 kV accelerating voltage and a 13000x magnification.

3.5.6 Characterization of peptide immobilization

The fluorescence, which was emitted from the four FITC-peptides immobilized on SWNT channels, was imaged using a fluorescence microscope (Oylmpus, Japan). The fluorescence intensities from the images were analyzed using ImageJ (NIH) and normalized by the maximum intensity. AFM imaging was performed under ambient conditions using the AFM system (MFP-3D, Asylum Research, USA) in intermittent mode.

3.5.7 Fabrication of gas-flow platform

A gas-flow platform consists of a fluidic channel part fabricated with polydimethylsiloxane (PDMS; Sylgard 184, Dow-Corning, USA) and a main frame fabricated with polycarbonate. The PDMS part was fabricated using standard soft lithography and replica molding techniques. A master mold was custom-made by Idea tech (Korea). The pattern in the mold for the fluidic channel has 2 mm of width and height. PDMS elastomer was mixed with its curing agent. The mixture was then poured onto the patterned mold and baked. The cured PDMS was peeled off from the master mold and punched to make hole. The top and bottom parts of the main frame were custom-made by Kistech (Korea). The top frame had inlet/outlet holes for the gas flow. The device was finally assembled by sandwiching the PDMS part and silicon wafer between polycarbonate-based top and bottom frames.

3.6 Preparation of sample

3.6.1 Liquid odorant

Odorant solutions (1 M; all from Sigma, USA) in dimethyl sulfoxide (Sigma, USA) were prepared and were serially diluted to 1:10 using PBS, Ca^{2+}-containing dPBS (140 mM NaCl, 8 mM Na_2HPO_4, 1.5 mM KH_2PO_4, 1 mM $CaCl_2$), deionized water (DW), or Ringer's solution according to the purpose of experiments. The diluted odorants were stored at 4 ˚C until they were used.

3.6.2 Gaseous odorant

Odorants in a liquid phase at room temperature were placed in 117 mL bottles sealed with a septum cap. To produce 1,000 ppm of gas samples, 0.32, 0.59, 0.32, 0.48, 0.29, and 0.38 μL of trimethylamine, triethylamine, dimethylamine, 3-methyl-1-propanol, acetic acid, and acetone solutions (all from Sigma, USA) were fully evaporated in the bottles. Gas samples with lower concentrations than 1,000 ppm were generated using odorant solutions which had been serially diluted with DW.

3.6.3 Blood plasma

For the preparation of blood plasma samples, blood was collected in heparin-coated blood collection tubes from a healthy human male in his twenties. The plasma was separated by centrifugation at 2000 g for 15 min, and the supernatant was stored at -20 ˚C until its use. This work was approved by the Seoul National University Institutional Review Board (SNUIRB No.1301/001-005, Seoul, Korea).

3.6.4 Spoiled food

For the preparation of spoiled milk, milk was purchased at a local market and incubated at 25 ℃ for different time periods. Before experiments, the milk was diluted to 1:100 in PBS containing Ca^{2+}. Oyster (South Korea), shrimp (Thailand), lobster (Canada), milk (South Korea), tomato (South Korea), broccoli (South Korea), and beef (South Korea) were purchased at a local market and subsequently ground. The samples were then stored in 15-mL Falcon tubes at 25 ˚C for different time periods. After the storage, 1 mL of DW was added into the Falcon tubes containing 1 mg of food samples, and the liquid fractions were diluted to 1:100 with DW before the experiments were performed.

3.7 Electrical measurement

3.7.1 Direct current (DC) mode

The electrical measurements were carried out using a Keithley 2636A sourcemeter (Keithley, USA) and a probe station (MS tech, South Korea). Figure 3.1 shows the equipment used for electrical measurements. For the measurements, 0.1 V DC was applied between the source and drain electrodes, whereas the gate voltage was grounded. 49.5 μL of dPBS containing Ca^{2+} or DW was added to the bioelectronic nose. Afterward, the current changes between the drain-source electrodes were measured. Then, 0.5 μL of the sample solution was added.

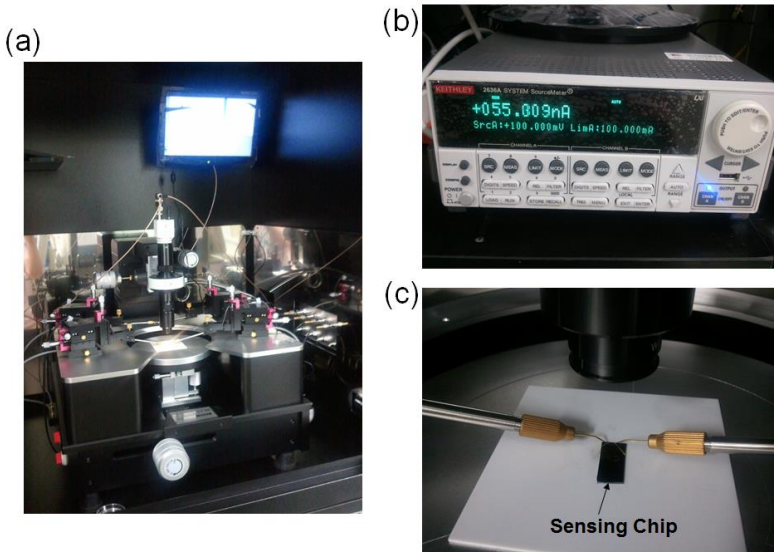

Figure 3.1 Equipment for electrical measurements. (a) Probe station and (b) sourcemeter were used for measuring the electrical conductance of the sensing chip. (c) The sensing chip was mounted on electric insulator, and the electrodes of the sensing chip were connected to the sourcemeter using probes of the probe station.

3.7.2 Alternating current (AC) mode

For the sensing experiments, a polypropylene-based liquid well around the sensing chip was prepared to keep the liquid environments. Then, a 9 μL of dPBS containing Ca^{2+} was placed on the well. The AC mode measurement using a lock-in amplifier was used to monitor the source-drain currents after injecting the odorant solutions. In the AC mode measurement, an alternating voltage (30 mV, 31 Hz) was applied to the source and drain electrodes by a function generator (Agilent Technologies, USA). A current through two electrodes was amplified using a low-noise current preamplifier (Stanford Research Systems, USA). Also, a lock-in amplifier (Stanford Research Systems, USA) was used to measure the intensity of the output response from the preamplifier. The AC mode operation using the lock-in amplifier enabled the highly accurate measurement without disturbances by environmental noises with different frequencies. The prime-number frequency was chosen as 31 Hz because 31 Hz is uncommon noise frequency (noise frequency is usually the multiples or divisions of 60 Hz). The lock-in amplifier was previously utilized for the measurement of the conductance on FET sensors and for the detection of biological and chemical responses. In this experiment, low operation frequency (31 Hz) was proper so that the SWNT-FETs can have electrical characteristics close to those of DC mode measurements.

Chapter 4.

Nanovesicle-based bioelectronic nose for the detection of lung cancer biomarker

Chapter 4. Nanovesicle-based bioelectronic nose for the detection of lung cancer biomarker

4.1 Introduction

In human blood, numerous compounds can be used for the diagnosis of diseases; hence, many types of sensors have been developed to easily and rapidly diagnose diseases.[95-97] Most sensors were functionalized with biomolecules such as antibodies and aptamers to improve their selectivity. However, such sensors commonly targeted relatively large-sized molecules such as proteins[98, 99] and DNA,[100-102] even though small chemicals can also be extremely effective biomarkers. One of the major reasons why chemical biomarkers have not been effectively used in diagnosis is the difficulty in determining proper methods which can selectively discriminate the chemical biomarkers. Consequently, a library of ORs can be an attractive candidate to be used to selectively detect chemical markers.[6, 38] Human nose selectively discriminates thousands of volatile compounds, and this ability is due to the selectivity of hORs expressed on the surface of the OSNs.[5] Therefore, the diverse ORs can open up the possibility of diagnosis by detecting chemical biomarkers in terms of a chemical-discriminating ability.

To utilize the selectivity of ORs, many researchers have recently developed various types of bioelectronic noses through functionalizing sensor platforms with OR proteins.[13, 73, 74, 103] However, a signaling pathway of the olfactory system was not used in such systems; thus, their fundamental limitation was their inability to mimic the real olfaction. In order to overcome this limitation, nanovesicles produced from animal cells can be a

superb alternative because they can generate cellular signals similarly to the olfactory system.[7] In addition, nanovesicles are suitable for applications to biosensor systems because they can be produced in large quantities and stored for a long period of time. By immobilizing olfactory nanovesicles on semiconductor-based sensors, highly sensitive and selective bioelectronic noses mimicking the olfactory system have been developed.[82, 83] This device is also able to solve the problems of typical electronic noses in terms of its sensitivity and selectivity.

However, another problem remains of overcoming the development of novel bioelectronic noses. The function of each OR has not yet been fully elucidated. Therefore, for this study, a screening process to find suitable ORs for intended purposes was carried out. In order to design an experiment demonstrating solutions of the whole issue, heptanal was chosen as a model compound in this study. Heptanal is a biomarker of non-small cell lung cancer.[104] The amount of heptanal in blood from lung cancer patients is conspicuously larger than that in blood from non-patients.[105, 106] The sensor that detects heptanal can be effectively used as a diagnostic tool for lung cancer. However, the amount of heptanal has still been analyzed using typical analytical methods such as gas chromatography-mass spectroscopy (GC-MS) and high-performance liquid chromatography (HPLC).[107, 108] These methods cannot be readily applied to rapid and easy diagnosis due to the requirements of intricate pretreatment processes, expensive instrumentations, and the long time required for analysis. Herein, a nanovesicle-based bioelectronic nose that mimics the human olfaction for the selective and sensitive detection of heptanal, a biomarker of lung cancer, is reported.

4.2 Screening of human olfactory receptor library

Olfactory signals are inceptively triggered by the activation of ORs expressed on the surface of OSNs. Once a certain OR binds with specific ligands, G-protein α-subunits and adenylyl cyclases are sequentially activated. Activation of adenylyl cyclases engenders an increase in the amount of intracellular cyclic adenosine monophosphate (cAMP), and finally results in an influx of Ca^{2+} ions.[56, 109] This olfactory signaling system could be reconstructed in culturable mammalian cells. Especially, HEK-293 cells endogenously contain all of the essential proteins required for the signal transduction; thus, the expression of ORs allows the cells to generate olfactory signals as depicted in Figures 4.1(a) and 4.1(b).[110, 111] Moreover, the signals can also be generated from the cell-derived nanovesicles because nanovesicles also possess membrane proteins and cytosolic components needed for the signal transduction (Figure 4.1(c)).[7] Therefore, a bioelectronic nose that can distinguish the odor of a target molecule could be fabricated by functionalizing a semiconductor-based transistor with the nanovesicles (Figure 4.1(d)) produced from artificial olfactory cells (Figure 4.1(c)).

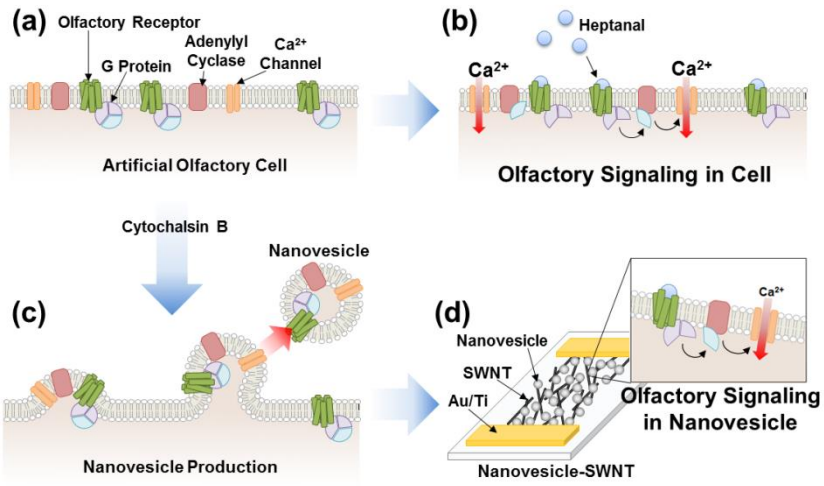

Figure 4.1 Schematic diagrams showing the olfactory signaling generated from cells and nanovesicles. (a) An artificial olfactory cell contains essential proteins for the olfactory signal transduction such as ORs, G proteins, adenylyl cyclases, and ion channels on the cellular membrane. (b) The binding of specific odorants to ORs triggers the olfactory signaling, and finally calcium ions flow into the cells. (c) Olfactory nanovesicles with all components for the olfactory signaling were produced from the artificial olfactory cells by a treatment of cytochalasin B. (d) A nanovesicle-based bioelectronic nose was fabricated by the immobilization of nanovesicles on SWNT-FETs. Specific odorants were detected through the olfactory signaling in nanovesicles.

For the development of a bioelectronic nose, a specific hOR binding with heptanal was first selected. By over-expressing 30 types of hORs in HEK-293 cells, a library of artificial olfactory cells was prepared. Then, it was examined which OR was affected by heptanal. If an OR specifically binds with heptanal, a signaling cascade induces an influx of Ca^{2+} ions. Also, intracellular Ca^{2+} ions bind to Fura-2, a fluorescence dye pre-loaded into the cells. The excitation wavelength of Fura-2 changes from 380 nm to 340 nm when Fura-2 binds to the Ca^{2+} ions. Therefore, as more Ca^{2+} ions bind to Fura-2, the fluorescence emitted by the 340 nm excitation becomes brighter. Thus, the increase in the amount of intracellular Ca^{2+} ions can be calculated by the ratio of fluorescence emissions (excitation at 340/380 nm).

Figure 4.2(a) shows the profiles of fluorescence ratio after the addition of 1 mM heptanal to various types of artificial olfactory cells. Among these 30 types of artificial olfactory cells, a significant influx of Ca^{2+} ions was observed from the OR1J2-expressing cells. This means that the OR1J2 protein specifically reacted to the stimulation by heptanal. The OR1J2-expressing cells were examined to determine whether they respond to other odorant molecules which have similar chemical structures to heptanal (Figure 4.2(b)). The OR1J2 was able to selectively discriminate heptanal among other analogous compounds such as hexanal, octanal, and nonanal.

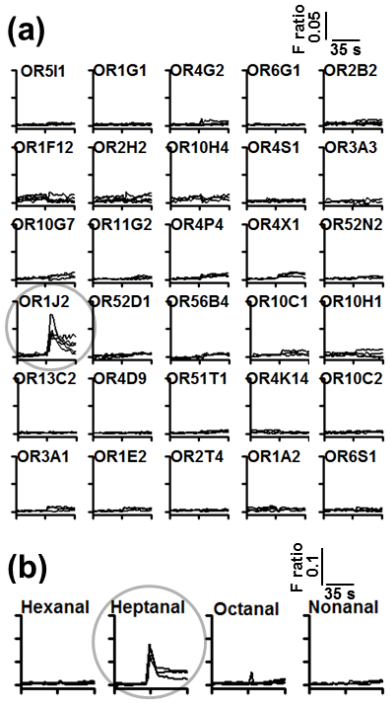

Figure 4.2 Selection of receptors from a library of human ORs. (a) Screening results to determine a specific olfactory receptor reacting to heptanal. 100 μM of heptanal was added to cells at 35 s in each set. In the case of OR1J2-expressing cells, a significant influx of Ca^{2+} ions was observed. (b) Selectivity of OR1J2. No remarkable influx of Ca^{2+} ions was observed when analogous compounds such as hexanal, octanal, and nonanal were added, whereas the addition of heptanal generated a sharp influx. 1 mM of odorants were added to cells at 35 s for each set.

4.3 Characterization of nanovesicle

Olfactory nanovesicles were produced from artificial olfactory cells by a treatment with cytochalasin B. Both the nanovesicles and the artificial olfactory cells were able to make olfactory signals using over-expressed ORs together with the endogenous signaling components, such as G proteins, adenylyl cyclases, and ion channels. In this work, $G\alpha_{olf}$ and RTP1S genes were co-transfected with OR genes, and their effects were examined. $G\alpha_{olf}$ protein is a major Gα subunit for olfactory signaling; hence, it is expected that the signal transduction would occur more effectively than in the case of utilizing endogenous $G\alpha_s$.[112] RTP1S assists the expression of OR proteins by acting as a kind of chaperone; thus, the OR expression level is expected to increase by the co-expression of RTP1S.[60, 113] Therefore, the co-expression of $G\alpha_{olf}$ and RTP1S together with ORs is expected to assist the cells and nanovesicles in amplifying olfactory signals.

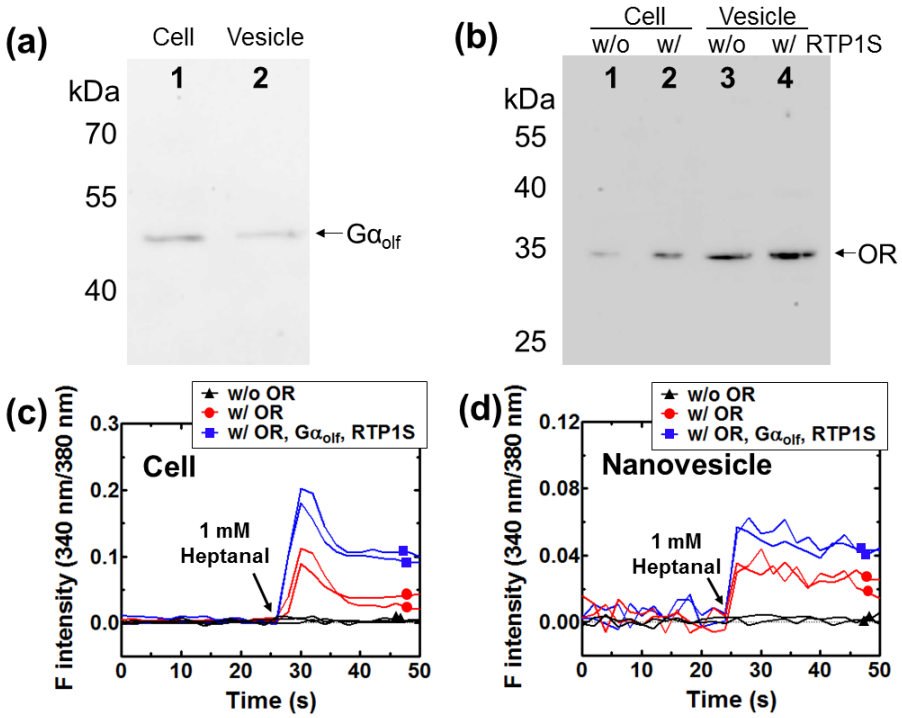

Figure 4.3 Characteristics of olfactory cells and nanovesicles. (a) Western-blot analysis of $G\alpha_{olf}$ proteins in cells and nanovesicles. When $G\alpha_{olf}$ genes were co-transfected with OR genes, $G\alpha_{olf}$ protein expression was observed both in cells (lane 1) and nanovesicles (lane 2). (b) Western-blot analysis of OR1J2 in cells and nanovesicles. Lanes 1, 2, 3, and 4 show the OR proteins expressed in cells without RTP1S, in cells with RTP1S, in nanovesicles without RTP1S, and in nanovesicles with RTP1S, respectively. The bands in lanes 2 and 4 were thicker than those in lanes 1 and 3, respectively, indicating that the expression level of ORs increased due to the co-expression of RTP1S. Ca^{2+} influx was measured in (c) cells and (d) nanovesicles. The signal intensities increased due to the co-expression of $G\alpha_{olf}$ and RTP1S in both cells and nanovesicles.

Figure 4.3(a) shows a Western blot image confirming the expression of $G\alpha_{olf}$ in cells (lane 1) and nanovesicles (lane 2). The bands in the image indicate that $G\alpha_{olf}$ proteins were over-expressed in cells, and that they also remained in nanovesicles. Expression of ORs and the effect of RTP1S on the expression level of ORs were also confirmed by a Western blot analysis. Four protein samples were prepared from cells and nanovesicles with and without RTP1S. They were loaded on lanes 1, 2, 3, and 4, respectively (Figure 4.3(b)). As shown in Figure 4.3(b), we could verify the expression of the OR1J2 proteins in both the cells and nanovesicles. The bands in lanes 2 and 4 were thicker than those in lanes 1 and 3, respectively, when the equal amount of total protein samples was loaded. This result clearly shows that the expression level of ORs was increased by the co-expression of RTP1S.

Next, we monitored the profiles of Ca^{2+} influx generated by the stimulation of 1 mM heptanal in cells and nanovesicles. As shown in Figures 4.3(c) and 4.3(d), cells and nanovesicles with $G\alpha_{olf}$ and RTP1S induced a larger influx of Ca^{2+} ions, compared to those without $G\alpha_{olf}$ and RTP1S. From these results, it was verified that the signals were obviously generated from the olfactory signaling pathway and effectively amplified in both cells and nanovesicles. The detailed signal profiles of the nanovesicles slightly differed to those of the cells. Presumably, this is because the nanovesicle is not an alive cell and contains only partial substances in and near the plasma membrane rather than all the signaling components and organelles. However, the nanovesicles maintained key activities such as a prompt increase in the amount of intracellular Ca^{2+} ions. This indicates that these nanovesicles can be effectively used for biosensor systems.

4.4 Fabrication of nanovesicle-based bioelectronic nose

The produced nanovesicles were used for the functionalization of SWNT-FETs. The nanovesicles were derived from animal cells, and their membrane has a negative charge similar to a cell membrane. Therefore, they could be easily immobilized on the transistor, which was pre-coated with poly-D-lysine (PDL) through a charge-charge interaction. The immobilization process was performed by placing a droplet of nanovesicle suspensions on the PDL-coated SWNT channels and incubating them for 2 h. Figure 4.4(a) is an AFM image showing nanovesicles adhering to a SWNT channel. The nanovesicles with a 100-200 nm diameter were immobilized on the SWNT channel, which was composed of random networks of SWNTs. Because the nanovesicles adhered very near to the SWNTs, the Ca^{2+} ions flowed into the nanovesicles would provide a positive potential to the SWNT channels. Since the SWNT-FETs exhibited *p*-type characteristics under ambient conditions (Figure 4.5), the conductance of SWNT channels is expected to be reduced by the activation of the olfactory signaling.

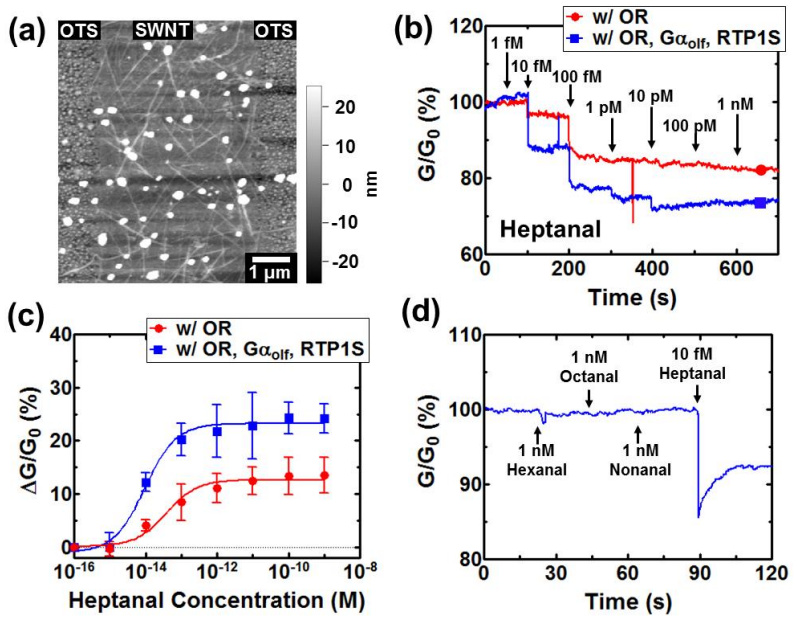

Figure 4.4 Sensitive and selective detection of heptanal using nanovesicle-based bioelectronic noses. (a) An AFM image of nanovesicles immobilized on a SWNT channel. (b) Real-time measurements of conductance changes generated by the addition of heptanal at concentrations ranging from 1 fM to 1 nM. A decrease in conductance was observed when 10 fM heptanal was added. The response intensity was much higher when $G\alpha_{olf}$ and RTP1S were co-expressed, compared with the expression of OR only. (c) Dose-dependent response curve of the sensor to heptanal. Each data point and error bar indicates the mean and standard deviation (SD), respectively (n=3-5). (d) Real-time recognition of heptanal. The addition of 10 fM heptanal induced a sharp decrease in the conductance of the bioelectronic nose, whereas the addition of 1 nM of other analogous compounds such as hexanal, octanal, and nonanal did not induce any changes in the conductance. Note that the heptanal concentration was much lower than other concentrations.

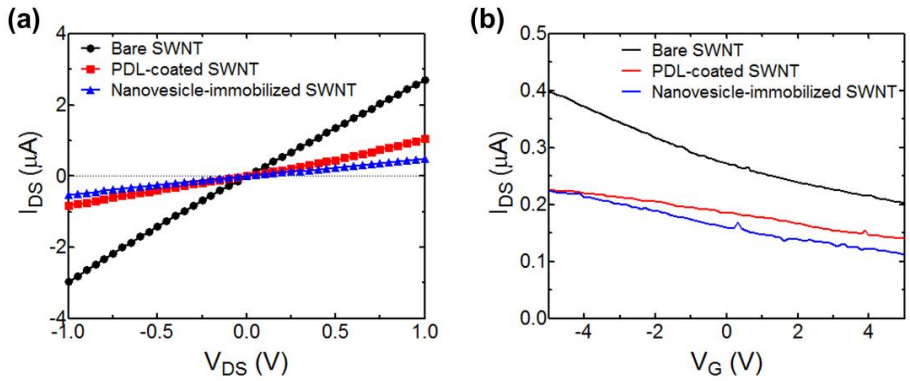

Figure 4.5 Electrical properties of bare, PDL-coated, and nanovesicle-immobilized SWNT-FETs. (a) Drain-source current versus drain-source voltage was plotted. Resistance of SWNT channels was increased by PDL coating and nanovesicle immobilization. (b) Characteristics of field-effect transistors obtained from bare, PDL-coated, and nanovesicle-immobilized SWNT devices. Data were plotted with drain-source current versus back-gate voltage. Drain-source currents were reduced with an increase in gate voltage at all devices. The fabricated SWNT-FETs showed linear IV properties. And the resistances of bare, PDL-coated, and nanovesicle-immobilized SWNT-FETs were calculated to be 3.36×10^5, 1.21×10^6, and 1.90×10^6 Ω, respectively. The increase in resistance indicates that some compounds were adhered on the surface. Also, the fabricated devices maintained *p*-type characteristics regardless of PDL coating and nanovesicle immobilization.

4.5 Detection of heptanal from standard solution

The produced nanovesicles were used for the functionalization of SWNT-based FETs. Fabricated nanovesicle-based bioelectronic noses detected heptanal based on the conductance change. A 49.5 μL of Ca^{2+}-containing dPBS droplet was placed on the SWNT channel, and the sample solutions were added. Figure 4.4(b) shows real-time conductance measurement data. The sensor exhibited a prompt decrease in the conductance after the addition of 10 fM heptanal, whereas no conductance changes were observed when the sensors without ORs were used or when the experiments were carried out in a Ca^{2+}-free environment (Figure 4.6). The response intensities from the sensors increased with the concentration of heptanal, until the intensity reached a plateau at a picomolar range as shown in Figure 4.4(c). These results demonstrated the high sensitivity of the sensor. The sensors were able to detect heptanal at a concentration as low as 10 fM in real-time. The decrease in conductance was caused by Ca^{2+} influx into the nanovesicle, which was induced by the binding of heptanal with ORs.

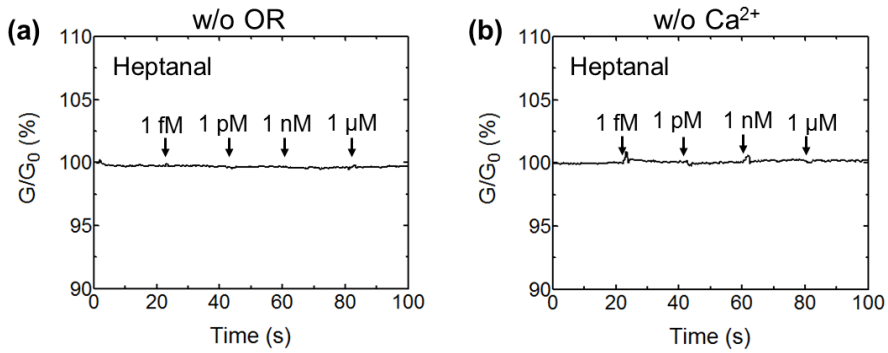

Figure 4.6 Real-time conductance measurements in the nanovesicle-based bioelectronic noses (a) using the nanovesicles without ORs or (b) in a Ca^{2+}-free buffer solution. In both cases, no signal change was observed with the addition of heptanal.

Additionally, in this experiment, two types of bioelectronic noses were used to again more clearly confirm the effects of $G\alpha_{olf}$ and RTP1S. The first bioelectronic nose was fabricated with the nanovesicles containing only ORs, and the second one was with the nanovesicles containing ORs, $G\alpha_{olf}$, and RTP1S. Both bioelectronic noses were able to generate significant responses to the stimulation with heptanal; however, the generated response intensities evidently differed. The bioelectronic nose with nanovesicles containing ORs, $G\alpha_{olf}$, and RTP1S induced much higher conductance changes. This tendency was almost identical to that analyzed by a calcium signaling assay as discussed previously. Moreover, a half maximal effective concentration (EC50), the stimulant concentration where 50% of the maximal effect is achieved, shifted from 3.73×10^{-13} M to 8.88×10^{-14} M; thus, the sensors became more sensitive with $G\alpha_{olf}$ and RTP1S. This shift was also observed in the cell-based calcium signaling assay as shown in Figure 4.7.

Figure 4.4(d) is real-time measurement data showing the conductance change generated by the addition of heptanal and other analogous compounds. The addition of 1 nM hexanal, octanal, and nonanal had no effect on the conductance, whereas the addition of 10 fM heptanal induced a prompt decrease in the conductance. This result shows that the chemical-discriminating ability of the original olfactory system was closely mimicked by the nanovesicle-based bioelectronic nose.

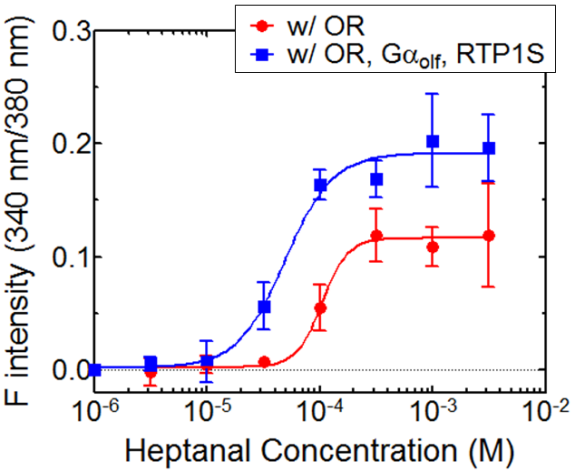

Figure 4.7 Dose-dependent response curves toward the stimulation of heptanal in cells expressing OR1J2. The cells with $G\alpha_{olf}$ and RTP1S as well as OR were more sensitive to heptanal than those solely with OR. The co-expression of $G\alpha_{olf}$ and RTP1S together with OR enhanced the olfactory signaling. The EC50 values of cells co-expressing $G\alpha_{olf}$ and RTP1S with OR and cells expressing only OR were 48.6 and 103.7 μM, respectively.

4.6 Detection of heptanal from human blood plasma

To verify the capability of the sensor for practical diagnosis, the detection of heptanal contained in human blood plasma was examined. Plasma samples were prepared from the blood of a healthy person. Human plasma naturally contains many compounds, and such compounds may non-specifically affect SWNTs and nanovesicles. Especially, a few hundred nM of heptanal is also contained in healthy human blood;[114] hence, the compounds in the plasma will affect the conductance change. To check the non-specific influence by the blood plasma, the plasma was diluted at different ratios with a buffer solution and was injected into the sensors. The result showed that $1/10^7$-diluted plasma samples did not affect the conductance of the sensor as shown in Figure 4.8(a). This result indicates that a small amount of non-patient plasma has no effect on the conductance of sensors, although the plasma was not pre-treated.

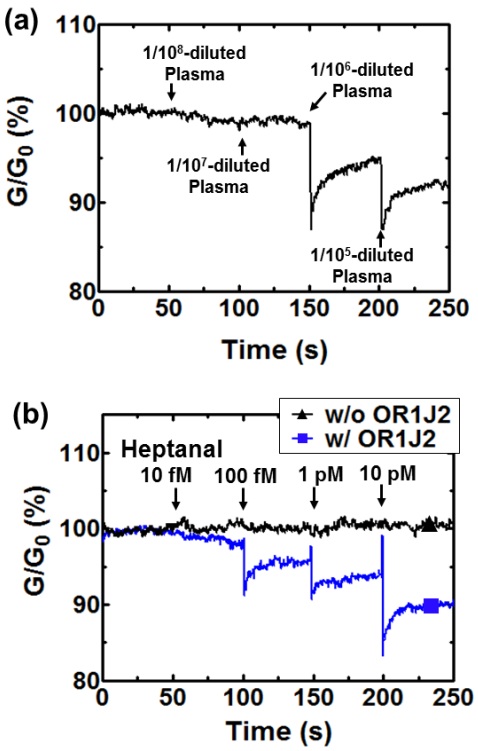

Figure 4.8 Detection of heptanal from human blood plasma using nanovesicle-based bioelectronic noses. (a) A real-time measurement for the influence of plasma on the conductance change in the sensor. The sensors were fabricated using nanovesicles with OR, $G\alpha_{olf}$, and RTP1S. Human blood plasma samples were diluted to different ratios. The $1/10^7$-diluted plasma did not show any effect on the conductance, which means that no pretreatment process is required when $1/10^7$-diluted plasma is used in the experiment. (b) The real-time detection of heptanal from $1/10^7$-diluted plasma using nanovesicle-based bioelectronic noses. A sensor fabricated based on nanovesicles with OR, $G\alpha_{olf}$, and RTP1S was able to detect 100 fM heptanal (square), whereas the sensor without ORs was not (triangle).

In order to confirm how well nanovesicle-based sensors could discriminate heptanal from other molecules included in the blood plasma, various concentrations of heptanal were spiked in the plasma samples prepared from a healthy person. Figure 4.8(b) shows real-time measurement data of conductance changes generated by the treatment with heptanal-spiked plasma samples. The treatment with plasma containing an additional 100 fM of heptanal induced a detectable decrease in the conductance of the sensor, whereas the conductance of the sensor without ORs was not affected. Compared with the results obtained using the standard solution (Figure 4.4(b)), the sensitivity slightly decreased due to various compounds in the real blood plasma; however, bioelectronic noses were still sensitive enough to recognize the patient's plasma, which contains a higher concentration of heptanal.

100 fM of heptanal was added in $1/10^7$-diluted blood plasma from a healthy person, and the sensor was able to recognize this concentration of heptanal. The concentrations of heptanal in the blood of non-patients and lung cancer patients are within the range of a few hundred nanomolar and several micromolar, respectively.[114] This means that even though the plasma is diluted to $1{:}10^7$, the heptanal concentration is still higher than 100 fM, which is a detection limit of this sensing system, in the case of patient's plasma. This suggests that the sensitivity of the sensor is sufficient to recognize the heptanal in the patients' plasma.

If the sensor is not sufficiently sensitive and selective, pretreatment processes are required to remove the compounds that may non-specifically affect diagnosis signals. The developed bioelectronic nose is able to detect a specific target ligand at an extremely low concentration range with high

selectivity, similar to the olfactory system. This is essential for the diagnosis of diseases by detecting biomarkers. These characteristics of bioelectronic noses will facilitate the rapid and easy diagnosis of lung cancer from human blood.

4.7 Conclusions

A bioelectronic nose for the diagnosis of lung cancer was developed through functionalizing SWNT-FETs with nanovesicles. A hOR, which specifically binds with a lung cancer biomarker, was selected by screening a library of hORs. Nanovesicles were then produced from mammalian cells that express the ORs on their membrane. Similar to the cell, the nanovesicles were able to make olfactory signals through a cellular signaling pathway. The olfactory signals were further amplified by co-expressing $G\alpha_{olf}$ and RTP1S. The nanovesicles were used to functionalize SWNT-FETs, and this strategy allowed us to develop a nanovesicle-based bioelectronic nose, a highly sensitive and selective biosensor system. The sensor mimicked the human olfactory system, and discriminated a chemical biomarker using an olfactory sense. Bioelectronic noses can selectively detect the biomarker at a concentration as low as 10 fM in real-time. This sensitivity and selectivity facilitated the detection of chemical biomarkers from human blood plasma without the need for any pretreatment processes. These results demonstrate that bioelectronic noses can be effectively applied for the rapid and easy diagnosis of lung cancer. Furthermore, this work provides an experimental method for the development of sensitive and selective bioelectronic nose systems that can be used for diverse purposes.

Chapter 5.

Nanovesicle-based bioelectronic nose for the assessment of food oxidation

Chapter 5. Nanovesicle-based bioelectronic nose for the assessment of food oxidation

5.1 Introduction

Effective sensing methods for the simple and rapid determination of quality of foods have been receiving a huge attention. Numerous volatile compounds are generated by the oxidation of foods; hence, the detection of such compounds can be one of the most effective strategies.[115-119] Typical techniques such as GC-MS and HPLC have been utilized for the analysis of volatile compounds.[120, 121] However, such techniques are unsuitable for the on-site measurement of quality of foods due to complex manipulations, a long analysis time, and labor-intensive pretreatments. Moreover, the large size of equipment is a critical drawback as a portable sensor. Therefore, various types of semiconductor-based platforms have been extensively studied.[122, 123] However, these devices were inferior to the natural olfactory system in terms of selectivity and sensitivity.

In the olfactory system, a specific odorant binds to ORs with high selectivity.[8] After the odorant binds to ORs, cellular signals are generated and transmitted to the brain. Through this mechanism, animals recognize odors. Many researchers have developed various strategies such as cell-based sensors and protein-based sensors to utilize the sensitivity and selectivity of the olfactory system.[13, 68, 69, 74, 79] However, these sensors did not use the signaling pathway of the natural olfactory system; thus, they had fundamental limitations.

A nanovesicle-based bioelectronic nose that mimics the canine nose was presented to sensitively and selectively detect hexanal, an indicator of lipid oxidation. Nanovesicles with cfOR5269, a specific canine olfactory receptor to detect hexanal,[124] were produced and immobilized on SWNT channels. The sensor detected 1 fM of hexanal in real-time. Significantly, the sensor could selectively detect hexanal with an excellent selectivity. Furthermore, hexanal in spoiled milk was easily detected without any pretreatment processes. This bioelectronic nose can be an effective device for the simple and rapid measurement of oxidation of foods.

5.2 Characterization of nanovesicle

Figure 5.1(a) shows a Western blot image confirming the expression of cfOR5269 in nanovesicles. Monomer, dimer, and multimer bands of cfOR5269 were observed. In other words, cfOR5269 proteins remained in nanovesicles.

Figure 5.1(b) shows the ratio of fluorescence intensity emitted from Fura-2 which had been pre-loaded in the nanovesicles. Fura-2 is a fluorescent dye that binds with intracellular Ca^{2+} ions, and the ratio of fluorescence (340 nm/380 nm excitation) indicates the amount of intracellular Ca^{2+} ions. No change of fluorescence ratio was observed when nanovesicles without OR were used. However, when nanovesicles with OR were used, the ratio of fluorescence remarkably increased by the injection of hexanal. This indicates the influx of Ca^{2+} ions into the nanovesicles. Thus, cfOR5269 and the olfactory signaling pathway were active in the nanovesicles.

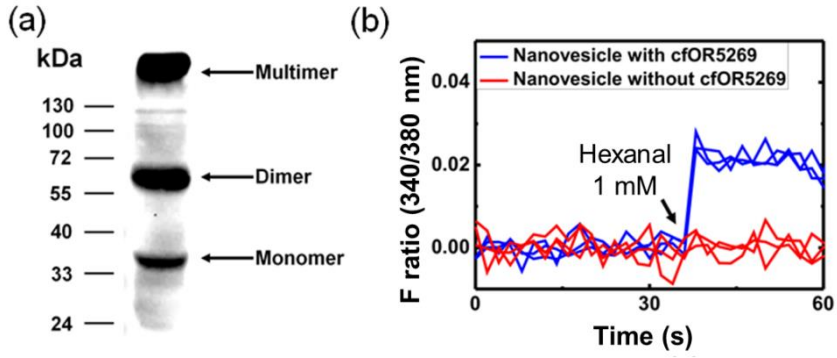

Figure 5.1 Characterization of nanovesicle. (a) A Western blot image of cfOR5269 protein expressed in nanovesicles. Monomer, dimer, and multimer bands of cfOR5269 were observed. (b) A real-time measurement of fluorescence ratio which represents the amount of Ca^{2+} ions. The ratio increased by the stimulation with 1 mM of hexanal when nanovesicles contained cfOR5269.

5.3 Fabrication of nanovesicle-based bioelectronic nose

Figure 5.2(a) shows a schematic diagram depicting the fabrication process of nanovesicle-based bioelectronic noses. The region of SWNT channels was first pre-coated with 0.1 mg mL^{-1} PDL solutions. Because PDL has a positive charge, nanovesicles could be easily immobilized using a charge-charge interaction. Nanovesicles can be active only in a liquid environment; thus, nanovesicle-based bioelectronic noses were not stored for over one day.

Figure 5.2(b) shows the sensing mechanism of nanovesicle-based bioelectronic noses. The binding event between hexanal and ORs activates G protein, adenylyl cyclase, and Ca^{2+} channels. The activated Ca^{2+} channels induce the influx of Ca^{2+} ions. The positive potential of Ca^{2+} ions acts as a gate potential to SWNT-FETs. Because the platform has *p*-type characteristic under an ambient condition, the increased positive potential results in the decrease in the conductance on SWNT transistor. In the case of nanovesicle-based bioelectronic noses, the binding of odorants to ORs triggers the cAMP signaling pathway, and the cellular signals were measured by the SWNT transistors.

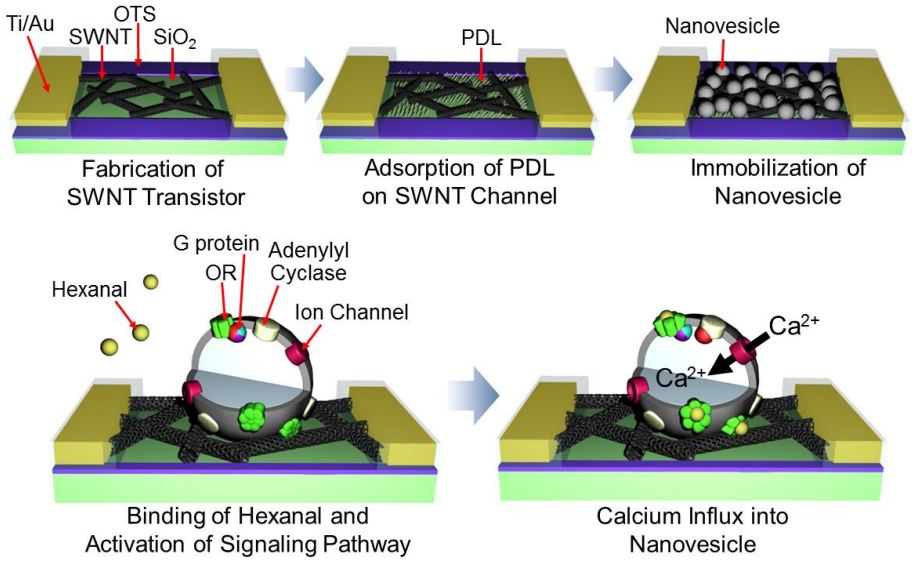

Figure 5.2 Fabrication process and sensing mechanism. (a) Schematic diagram showing a fabrication process of nanovesicle-based bioelectronic noses. (b) Schematic diagram showing a sensing mechanism of nanovesicle-based bioelectronic noses. The binding of hexanal to ORs results in the influx of Ca^{2+} ions. The accumulation of Ca^{2+} ions in the nanovesicles provides a positive gate-potential to SWNT transistors. Consequently, the increased potential results in a decrease in the conductance on the SWNT transistor.

5.4 Detection of hexanal from standard solution

Figure 5.3(a) is an SEM image of nanovesicles immobilized on the SWNT channel. Nanovesicles with 100-200 nm of diameter were attached on the SWNT channel. Figure 5.3(b) depicts the chemical structures of odorants which had been used in this study. Hexanal is a specific ligand of cfOR5269.[124] Chemical structures of odorants are very similar. The difference is their alkyl chain length or functional groups.

Data about the real-time detection of hexanal were obtained using nanovesicle-based bioelectronic noses (Figure 5.3(c)). Hexanal with different concentrations was injected to the sensor. Ca^{2+}-containing PBS solution was first placed on the chip. Then, the sample solutions were injected. The bioelectronic nose showed a remarkable change of the conductance by the introduction of 1 fM hexanal. This indicates high sensitivity of the nanovesicle-based bioelectronic noses.

Negative control experiments were conducted in Ca^{2+}-free environment (Figure 5.4(a)). The injection of hexanal had no effect on the conductance of SWNT transistors. This means that Ca^{2+} plays a critical role in the conductance change of SWNT transistor. The binding of hexanal on OR proteins in nanovesicles triggered the Ca^{2+} signaling pathway. As a result, the influx of Ca^{2+} occurred. The influx of Ca^{2+} ions resulted in an increase in the positive potential. Because SWNT transistor shows a *p*-type behavior, the increased potential consequently resulted in the decrease in the conductance of SWNT transistors.

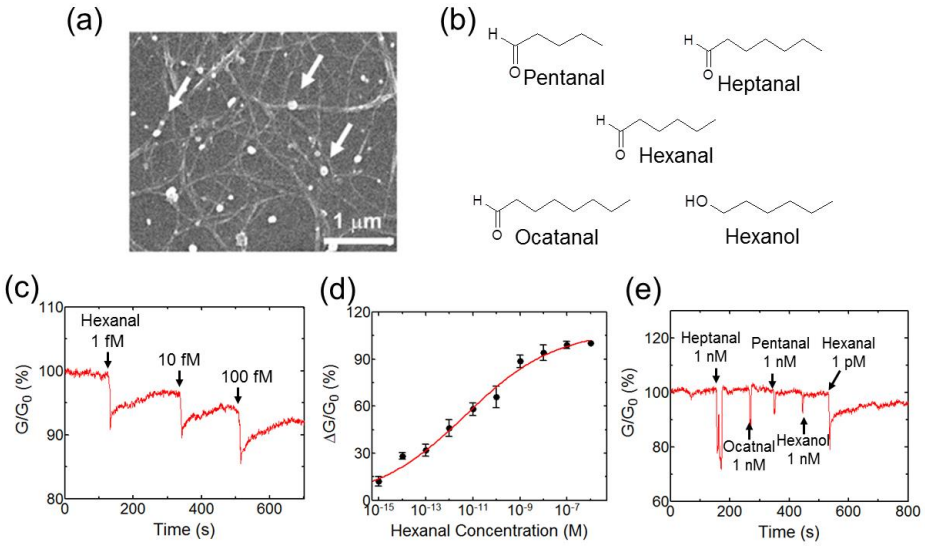

Figure 5.3 Detection of hexanal using nanovesicle-based bioelectronic noses. (a) SEM image of nanovesicles immobilized on the SWNT channel. White arrows point to nanovesicles. (b) Chemical structures of odorants that was used. (c) A real-time detection of hexanal using the bioelectronic nose. The conductance decreased by the injection of femtomolar range of hexanal. (d) Dose-dependent response curve to hexanal (n=5). (e) Selectivity of nanovesicle-based bioelectronic noses. The injection of 1 nM heptanal, octanal, pentanal, and hexanol had no effect on the conductance, whereas the injection of 1 pM hexanal induced a decrease in the conductance.

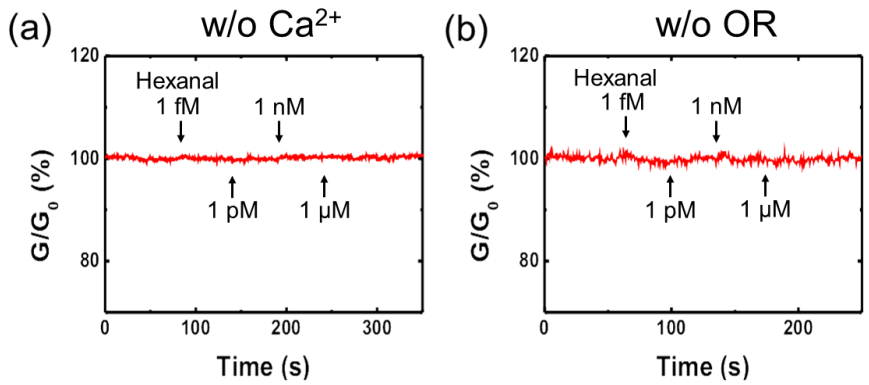

Figure 5.4 Negative control experiments for the demonstration of the sensing mechanism. (a) A real-time conductance measurement in Ca^{2+}-free PBS. No conductance change was observed by the addition of hexanal. (b) A real-time conductance measurement using the sensor based on nanovesicles without cfOR5269. There was no conductance change by the addition of hexanal.

Also, additional control experiments were conducted using nanovesicles without cfOR5269 (Figure 5.4(b)). In this case, no conductance change of SWNT channels was observed. This result also demonstrated the proposed sensing mechanism in Figure 5.2(b).

Figure 5.3(d) shows a dose-dependent response pattern toward hexanal. The conductance changes by the introduction of hexanal with different concentrations were measured. And the response intensity was normalized by the maximum intensity. Five response patterns were analyzed. The response intensities increased with the increase of hexanal concentrations. Finally, the response intensity was saturated at nanomolar range. The response patterns were fitted using Hill equation. Estimated EC50 value is 2.67×10^{-12} M.

Figure 5.3(e) shows selectivity of nanovesicle-based bioelectronic noses. The injection of 1 nM pentanal, heptanal, octanal, and hexanol had no effect on the conductance of the sensor, whereas the injection of 1 pM hexanal induced a remarkable decrease in the conductance. The difference between odorants used is very minor. Consequently, the developed sensor has an excellent selectivity capable of discriminating hexanal among analogous molecules.

5.5 Detection of hexanal from spoiled milk

Figure 5.5 shows the conductance changes generated by the injection of 1:100-diluted spoiled milk to bioelectronic noses. In order to prepare spoiled milk, fresh milk was stored at 25 ℃ for 0~5 days. Because milk contains fatty acids, hexanal can be produced by the oxidation of lipids.[115, 120] The bioelectronic nose based on nanovesicles without ORs had no effect on the conductance by the injection of spoiled milk. On the other hand, the bioelectronic nose based on nanovesicles with ORs induced significant changes in the conductance by the injection of spoiled milk. And the response intensity increased with the increase of spoilage time. Hexanal in the spoiled milk affected ORs and nanovesicles; thus, the conductance change of SWNT transistors occurred. This indicates that nanovesicle-based bioelectronic noses can be applied to the simple and rapid determination of degree of food oxidation.

Control experiments were also performed to confirm non-specific effects of other molecules in the spoiled milk (Figure 5.6). 1:100-diluted spoiled milk was injected to a bare SWNT transistor, while the conductance change of the sensor was monitored. The bare SWNT transistor was not affected to the injection of spoiled milk. Thus, it was demonstrated that the responses in Figure 5.5 were generated by the signals from the nanovesicles.

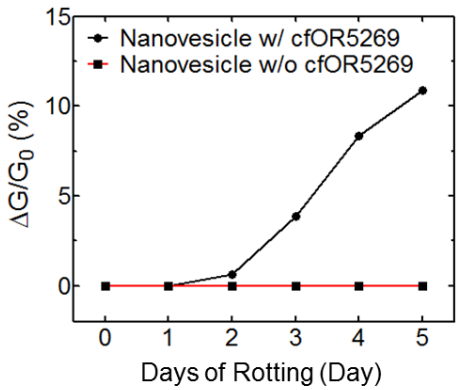

Figure 5.5 A response pattern generated by the addition of spoiled milk to nanovesicle-based bioelectronic noses. The bioelectronic nose based on nanovesicles with ORs induced conductance changes by the addition of spoiled milk. However, no conductance change was observed in the case of the bioelectronic nose based on nanovesicles without ORs. These results indicate that the conductance changes were induced by the binding event between hexanal in the spoiled milk and ORs in the nanovesicles.

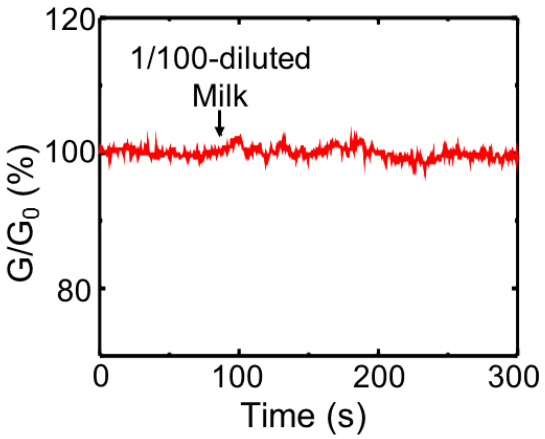

Figure 5.6 A real-time conductance measurement using a bare SWNT transistor toward spoiled milk. Milk spoiled for five days was injected to a bare SWNT transistor. The addition of spoiled milk had no effect on the conductance of the bare SWNT transistor.

5.6 Conclusions

A highly sensitive and selective nanovesicle-based bioelectronic nose was developed using nanovesicles and SWNT transistors. The bioelectronic nose detected hexanal, an indicator of the oxidation of foods. Hexanal was detected at a concentration as low as 1 fM with excellent selectivity. In addition, hexanal in spoiled milk was able to be simply and rapidly detected without any pretreatment processes. These results mean that nanovesicle-based bioelectronic noses can be used for the on-site measurement of food oxidations. Furthermore, the developed sensor platform will be extended toward the development of bioelectronic noses mimicking the natural olfactory system.

Chapter 6.

Improvement of nanovesicle stability using ion-channel-coupled olfactory receptor

Chapter 6. Improvement of nanovesicle stability using ion-channel-coupled olfactory receptor

6.1 Introduction

Animal noses are an effective chemical detector. The olfactory system can discriminate numerous odorous chemicals with great selectivity. Odorants first binds to ORs expressed in the surface of OSNs in the nasal cavity.[8] The binding event triggers the activation of α-subunit of G protein.[5] Adenylyl cyclases are subsequently activated, and cAMPs are synthesized using adenosine triphosphates (ATPs). The ion channels finally open, and ions are flowed into the cells.[56, 109, 111] This is a general cAMP signaling pathway that occurs for the perception of odors. This pathway can be reconstructed in culturable cells rather than original OSNs.[78-81] HEK-293 cells which artificially express ORs on their membrane have been commonly used as an alternative of OSNs because they contain all signaling components except ORs.[77] Cell-derived nanovesicles can also generate the olfactory signals.[7, 82] They are especially suitable to be applied to sensing systems because the size of nanovesicles is very small and nanovesicles can be produced in large quantities.[82, 83]

Bioelectronic noses based on OR-containing nanovesicles and FETs have been developed.[82, 83] Because such sensors have excellent sensitivity and selectivity, they could be utilized for the assessment of food oxidation and the diagnosis of diseases.[83] However, the most critical drawback of nanovesicle-based bioelectronic noses is stability. Nanovesicles can be stored for a long time in a frozen state.[7] However, in a non-frozen state, the

nanovesicles cannot be stable for more than one day. This weak stability is mainly because the olfactory signaling requires unstable signaling components, such as ATPs.[8] ATPs are easily hydrolyzed to adenosine diphosphates (ADPs), thermodynamically favorable compounds. Nanovesicles cannot synthesize ATPs because they do not contain cell organelles such as mitochondria; hence, the olfactory signaling pathway rapidly breaks.

In order to overcome the problem of instability, ion-channel-coupled receptors (ICCRs) can be a great solution.[125] It has been reported that the G protein-coupled receptors (GPCRs) which are fused with Kir6.2, a potassium channel, can generate an ion influx without the aid of ATPs.[126] The binding of ligands to GPCRs induces conformational change of GPCRs. Then, the conformational change directly results in the activation of Kir6.2 channels.[126] In this study, a stable nanovesicle-based bioelectronic nose was developed using ion-channel-coupled ORs (ICCORs).

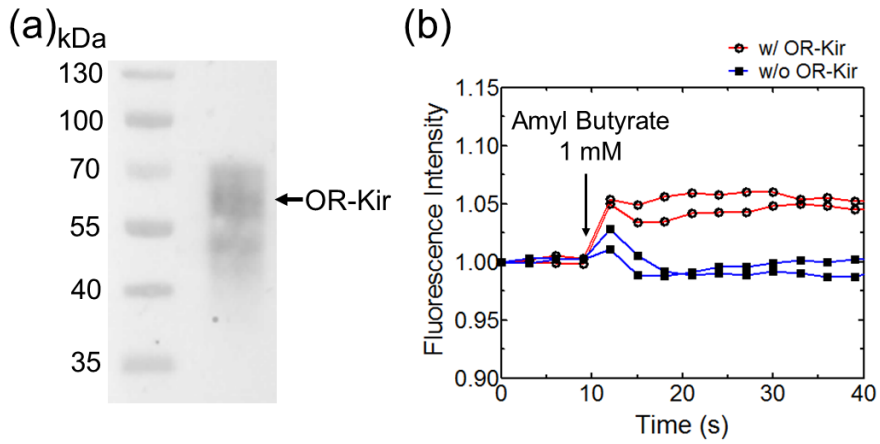

Figure 6.1 Characterization of nanovesicles containing Kir6.2-channel-coupled ORs (OR-Kir). (a) A Western blot image confirming the expression of OR-Kir in nanovesicles. (b) A real-time monitoring of an influx of positive ions into the nanovesicles. A fluorescence dye, which emits fluorescence by the influx of positive ions, was used. The addition of 1 mM of amyl butyrate induces the ion influx in nanovesicles containing OR-Kir.

6.2 Characterization of nanovesicle

Kir6.2 channel, one of inward-rectifier potassium channels, is originally coupled with sulfonylurea receptors, and modulates the movement of potassium ions.[127, 128] In this study, the Kir6.2 channel was covalently fused at the C-terminal end of hOR2AG1 instead of sulfonylurea receptors. hOR2AG1 is one of human ORs, and specifically interacts with amyl butyrate.[129] 25 N-terminal sequences of the Kir6.2 channel were excluded for the effective conformational change of the channel.[125] The ICCORs were over-expressed in HEK-293 cells. From the cells, nanovesicles were produced using cytochalasin B.[7]

The existence of ICCORs in nanovesicles was first demonstrated with Western blot analysis. Figure 6.1(a) shows a band of ICCORs, which represents the expression of ICCORs in nanovesicles. Then, an ion influx into the nanovesicles was checked (Figure 6.1(b)). FLIPR membrane potential dye which emits fluorescence by the influx of positive ions was used.[130] By the injection of 1 mM of amyl butyrate, fluorescence intensity increased in nanovesicles containing ICCORs. However, in the case of nanovesicles without ICCORs, the change of fluorescence intensity was not observed. This result clearly represents that ICCORs expressed on the surface of nanovesicles induced the influx of positive ions.

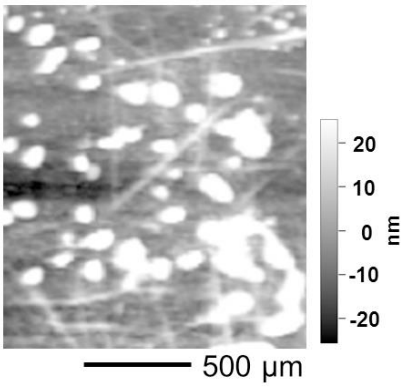

Figure 6.2 AFM image showing nanovesicles immobilized on the SWNT channel. Nanovesicles were absorbed very close to randomly-linked SWNTs.

6.3 Fabrication of nanovesicle-based bioelectronic nose

Produced nanovesicles were then immobilized on the SWNT-FETs. Because nanovesicles were derived from cells, surface membrane of nanovesicles has a negative charge. In order to simply immobilize the nanovesicles, SWNT channels were pre-coated with PDL. PDL is positively-charged molecules; thus, the immobilization was performed through a charge-charge interaction. Figure 6.2 shows the nanovesicles immobilized on the SWNT channel. SWNTs were randomly assembled on the SiO_2 surface, and the nanovesicles were absorbed very close to the SWNTs.

Figure 6.3 depicted the sensing mechanism. ICCORs expressed on the surface of nanovesicles first recognize the odorants. The binding event between ICCORs and odorants induces the direct activation of Kir6.2 channel as well as the original cAMP-mediated signaling pathway. As a result, positive ions were flowed into the nanovesicles. Positive ions act as a kind of gate-potential to the SWNT transistors.[82] Consequently, the conductance should decrease due to the *p*-type semiconducting property of SWNTs.[82, 83] Through monitoring the change of conductance of SWNT transistors, odorants were detected.

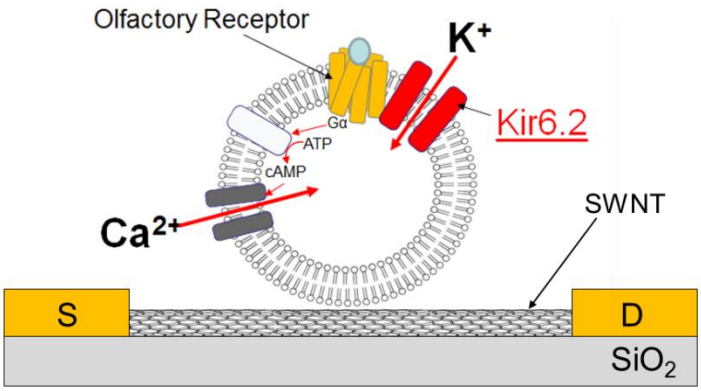

Figure 6.3 A sensing mechanism of nanovesicle-based bioelectronic noses using Kir6.2-coupled ORs. The activation of ORs induces the influx of K^+ through Kir6.2 channels as well as the influx of Ca^{2+}. Inflow of ions acts as a gate-potential; hence, the conductance on SWNT transistors decreases.

6.4 Characterization of nanovesicle-based bioelectronic nose

To confirm characteristics of the fabricated bioelectronic nose, the detection of odorants were conducted in four conditions (Figures 6.4(a) and 6.4(b)). The first condition had no calcium and potassium ions. When both ions were not contained in the buffer solution, the decrease in the conductance was not observed. The second condition had calcium ions without potassium ions, which means that the sensor can utilize the general cAMP signaling pathway. On the contrary to the second condition, the third condition had potassium ions without calcium ions. If there are no calcium ions in buffer solutions, the ion influx can only be generated using Kir6.2 channels fused with ORs. In both of second and third conditions, the addition of 1 fM amyl butyrate induced the prompt decrease in the conductance. However, the response generated by the potassium influx is much more intense than that by the calcium influx. In the last conditions, both ions were contained in buffer solutions. When both ions existed, the signal intensity was most enhanced. These results demonstrated that much more potassium ions were flowed into the nanovesicles compared to calcium ions. The intensive response indicates that it is easier to discriminate the specific responses among noise signals when the Kir6.2 channel was used. The difference of response intensities between four conditions can be more clearly compared in Figure 6.4(b). The conductance change generated by potassium influx is much larger than that by calcium influx.

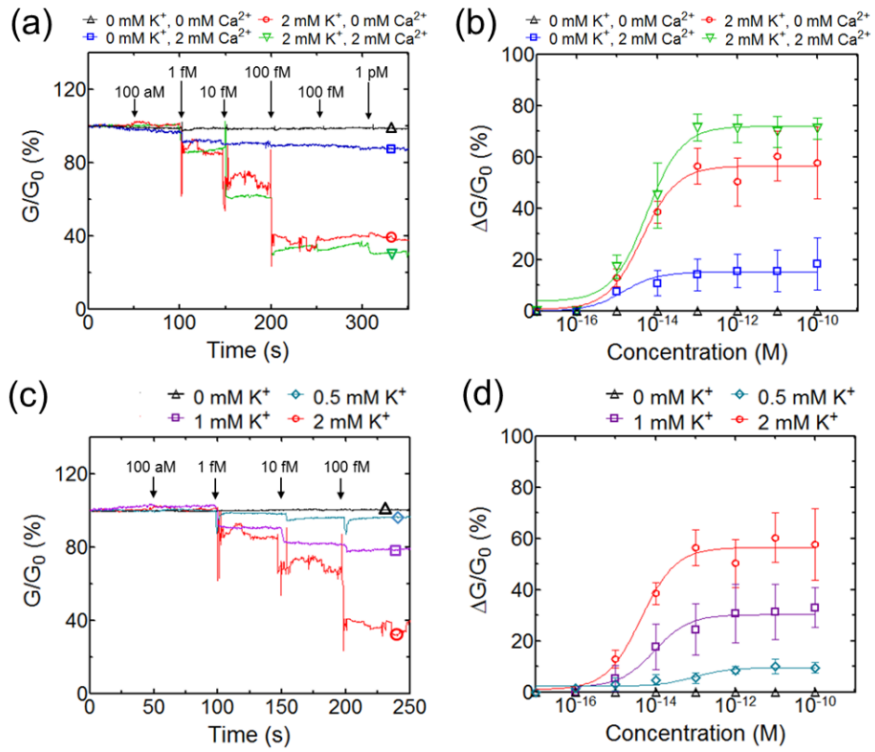

Figure 6.4 Characterization of bioelectronic noses using ICCOR-containing nanovesicles. (a) A real-time monitoring of conductance changes generated by the injection of amyl butyrate. (b) Dose-dependent response patterns of bioelectronic noses to amyl butyrate. The conductance change generated by the potassium influx is much larger than that by the calcium influx. (c) A real-time monitoring of conductance changes in the buffer solution with different concentrations of potassium ions. (d) The effect of K^+ concentrations on the response intensity. When larger amount of potassium ions existed in buffer solutions, larger conductance changes occurred.

Next, the potassium concentrations in buffer solution were changed (Figures 6.4(c) and 6.4(d)). It is also clear that when larger amount of potassium ions existed in buffer solutions, larger conductance changes occurred. In other words, when larger amount of external potassium ions existed, the ion influx more effectively occurred and the response intensity increased. When 2 mM of potassium ions were contained in the buffer solutions, the most intensive responses were observed. However, when the sensor was tested in higher concentrations than 2 mM, consistent results were not observed.

The selectivity of the sensor was also verified. In general, ORs have excellent selectivity. hOR2AG1 that was used in this study can specifically discriminate amyl butyrate from other analogous molecules.[13] It needed to be confirmed whether the selectivity of the OR well remained after Kir6.2 channels were coupled. As shown in Figure 6.5(a), chemical structures of compounds which were used for the confirmation of the selectivity are very similar to that of amyl butyrate. Moreover, the stimulated concentration of analogous compounds was much higher than that of amyl butyrate. Nevertheless, the sensor can precisely discriminate amyl butyrate (Figure 6.5(b)). This means that the selectivity of the hOR2AG1 intactly remained regardless of the fusion of Kir6.2 channels.

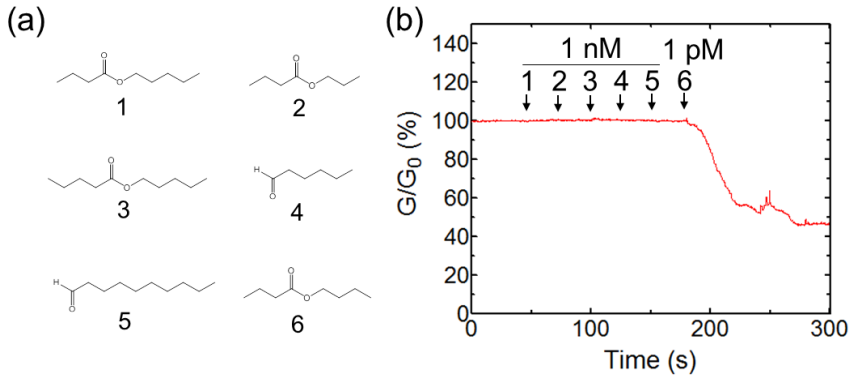

Figure 6.5 Selectivity of nanovesicle-based bioelectronic noses. (a) Chemical structures of amyl butyrate and its analogous compounds. Molecule names are (1) butyl butyrate, (2) pentyl valerate, (3) propyl butyrate, (4) hexanal, (5) decanal, and (6) amyl butyrate. (b) A real-time measurement of conductance changes by the injection of amyl butyrate and analogous compounds. The injection of 1 pM amyl butyrate induces the decrease in the conductance, whereas no changes were observed by the injection of 1 nM of other compounds.

6.5 Stability of nanovesicle-based bioelectronic nose

The cAMP-mediated signaling pathway requires ATPs. However, ATP is very unstable and easily hydrolyzed to ADP to get a low energy state. Cells can maintain a constant level of intracellular ATPs, but nanovesicles cannot due to the absence of cell organelles. Thus, the calcium signaling pathway easily and rapidly breaks in a non-frozen state. This fact indicates the instability of nanovesicles. However, Kir6.2 channel is physically opened by the conformational change of ORs without the aid of ATPs. Therefore, it was anticipated that the stability could be improved by the fusion of Kir6.2 channels.

The completely fabricated sensors containing nanovesicles were stored at 4 ˚C for several days. Figure 6.6 shows the remaining sensor activity after the storage. More than 85% of activity was maintained up to 8 days in the case of Kir-channel-mediated signaling, whereas ATP-mediated general calcium signaling was completely extinguished within 4 days. This result demonstrated that the stability of nanovesicles was remarkable improved.

The stability of sensor is one of the most essential properties for the practical applications. Although general nanovesicle-based bioelectronic noses exhibit a great sensitivity and selectivity, the stability was quite poor in a non-frozen state. In this study, the solution to overcome this problem was suggested. By coupling Kir6.2 channels with ORs, the stability of nanovesicle-based bioelectronic nose was able to be significantly improved.

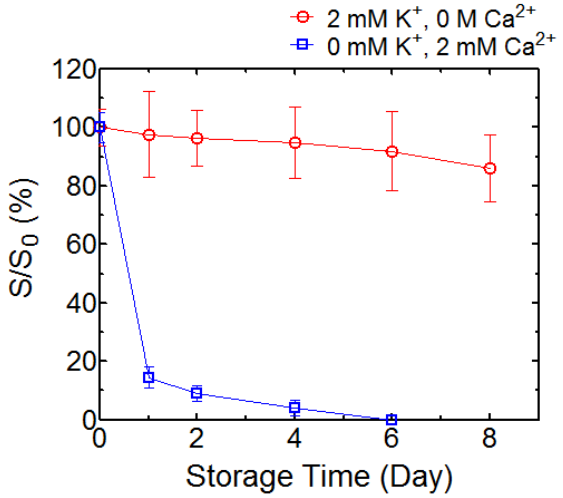

Figure 6.6 Stability of bioelectronic noses using ICCORs-containing nanovesicles in a non-frozen state. The fabricated nanovesicle-based bioelectronic noses were stored for different days at 4 ˚C. More than 85% of sensor activity was maintained up to 8 days when the Kir6.2-channel-mediated signaling was used. However, the ATP-mediated calcium signaling was extinguished within 4 days

6.6 Conclusions

Nanovesicle-based bioelectronic noses can be applied to various fields by virtue of their excellent sensitivity and selectivity. However, the stability of the nanovesicles needed to be improved. Kir6.2 channels covalently coupled with hORs can induce the ion influx without the aid of unstable signaling components; thus, nanovesicles containing Kir6.2-channel-coupled ORs were produced. Using the produced nanovesicles and SWNT transistors, a stable nanovesicle-based bioelectronic nose was developed. The amount of potassium ions flowed through the Kir6.2 channel was much larger than that of calcium ions flowed through the general signaling pathway. This means that the specific responses can be easily discriminated from noise signals. Also, the selectivity of the original OR remained after the Kir6.2 channel was coupled. Furthermore, the stability of nanovesicles was significantly improved because the activation of Kir6.2 channel does not require unstable signaling components. This ion-channel-coupling strategy enhances the potential for practical uses of nanovesicle-based bioelectronic noses.

Chapter 7.

Peptide-based bioelectronic nose for the determination of seafood decomposition

Chapter 7. Peptide-based bioelectronic nose for the determination of seafood decomposition

7.1 Introduction

Consumption of spoiled seafood can give rise to serious health problems, such as septicemia and gastroenteritis.[131, 132] Therefore, studies to develop methods for the on-site determination of seafood decomposition have been increasing. Such approaches should allow for the sensitive and selective detection of volatile compounds generated from spoiled seafood. Many research groups have reported that trimethylamine (TMA) can be used as an effective indicator of seafood decomposition because its amount is increased by the decomposition of trimethyl-N-oxide in seafood after death.[133-135]

In order to detect TMA, analytical techniques, such as GC-MS,[136, 137] ion mobility spectrometry (IMS),[138] and HPLC,[139] have been typically used. Although these techniques have the advantage of precise quantitative analysis, they cannot be readily applied to the on-site determination due to the requirements for complicated pretreatment processes, large instrumentations, and intricate detection methods. There have been significant advances in electronic[140-144] and bio-mimetic noses[145-147] that can be used for the on-site determination; however, there are still many limitations of these approaches, such as sensitivity and selectivity. More recently, OR-based bioelectronic noses have been demonstrated to be an effective solution to these limitations.[12, 13, 74, 103] However, ORs require lipid bilayer membranes for their proper function; hence, manufacturing processes of OR-based sensors were complicate and labor intensive. Furthermore,

because it is too difficult to thoroughly immobilize lipid bilayers on the chips, reusability and reproducibility could not be assured.

Herein, a peptide receptor-based bioelectronic nose is presented. This sensor can determine the degree of seafood decompostion in real-time through measuring the amount of TMA generated from spoiled seafood. Peptide-based bioelectronic noses were manufactured using SWNT-FETs functionalized with olfactory receptor-derived peptides (ORPs) which can selectively discriminate TMA. The functionalization was performed through a single-step process using the property of SWNTs which aromatic rings are stacked on the surface by π-π interactions.[75, 148] Additional phenylalanine (Phe) cluster was synthesized at the C-terminus of ORPs, which enabled us to simply cover the surface of SWNTs as a monolayer by a single-step process. The manufactured bioelectronic nose was able to sensitively and selectively detect TMA at a concentration of 10 fM and discriminate TMA from other similar molecules in real-time. Using the bioelectronic nose, TMA was successfully detected from three types of spoiled seafood (oyster, shrimp, and lobster) without any pretreatment processes. Also, the sensors were capable of discriminating spoiled seafood from other types of spoiled foods, because TMA is specifically generated from seafood decomposition.

Peptide-based bioelectronic noses were manufactured using small peptide rather than the whole protein; hence, it provides a new insight in biological aspects and a huge potential for applications in industrial fields. Although the peptide-based bioelectronic nose mimicked the olfactory reaction *via* membrane-translocated ORs, it was activated without lipid bilayers unlike the whole protein-based sensor due to the insignificance of tertiary structure. This results in an increase in the capability for practical

applications through improving reproducibility and reusability of the sensor as well as simplifying the manufacturing processes. It was demonstrated that the peptide-based sensor could be easily reused with a considerable reproducibility. Thus, peptide-based bioelectronic noses may be the most adjacent platform for practical uses. In addition, it was also produced on a portable scale making it effectively useful for the food industry where the on-site measurement of seafood decomposition is needed. Furthermore, the sensors could be used in a wide range of different applications because TMA is also a regulated air-pollutant[149] and an indicator of diseases, such as bacterial vaginosis[150, 151] and trimethylaminuria.[152]

7.2 Optimization of immobilization process

SWNT-based FET devices have high sensitivity to specific analytes with detection limits as low as the pico- or femto-molar range. Thus, they have been used in various applications by many groups. In most cases, biomolecules, such as enzymes,[153] receptors,[94, 154] antibodies,[155] and aptamers,[156] were immobilized on the surface of SWNTs to improve the selectivity of FET sensors. For the detection of TMA which emits an irritating and ammonia-like odor, ORP (NQLSNLSFSDLC) can be used.[157] ORP is a mutated α-helix peptide sorted out from a natural OR that can specifically recognize TMA. For the immobilization of the ORPs, one of the interesting properties of SWNTs was employed. Specific molecules with extensive π-systems can be stacked on the wall through π-π interactions. Thus, it was hypothesized that SWNTs could be non-covalently coated with specific ORP containing phenylalanines, a natural amino acid with π-systems

as depicted in Figure 7.1. In this article, it was aimed to exploit the biological analyte-selection ability in the development of a novel electronic sensor by conjugating ORPs onto SWNT-FETs through a single-step process.

First, it was verified that the additional attachment of Phe at the end of a small peptide facilitates the single-step immobilization on SWNTs. The line-patterned SWNT channels, which were uniformly distant apart, were fabricated on SiO_2 (Figure 7.2(a)). In order to clearly identify the effect of Phe, four types of synthetic peptides were used. These peptides consisted of fluorescein isothiocyanate (FITC), two glycines (Gly), and different numbers of Phe (ranging from zero to three). Glycine, an uncharged and non-polar amino acid, was the main component of the small peptides and was used as the linker between FITC and Phe. After the treatment with the peptide-suspended solutions and washing steps, green fluorescence was observed and a specific immobilization in the region of the SWNT channels was confirmed as shown in Figure 7.2(b). The immobilization efficiency was shown to be affected by the number of Phe in the peptide sequence. Figure 7.2(c) shows the normalized intensity of fluorescence emitted from each SWNT channel in Figure 7.2(b). The peptides with three Phe were more efficiently immobilized on SWNT channels over five-fold than those with only one Phe. These results indicate that the π-systems of aromatic rings of the three Phe were sufficient for the immobilization of small peptides.

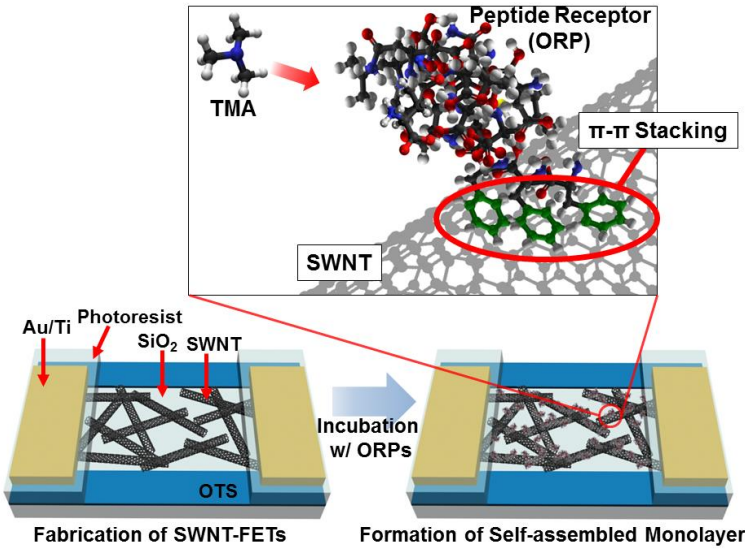

Figure 7.1 A peptide-based bioelectronic nose for the detection of TMA. ORPs were self-assembled on the surface of SWNTs during the treatment with ORP-suspended DW solutions. The ORPs were immobilized by π-π stacking of aromatic rings at their C-terminus and attracted TMA molecules very near to the SWNTs.

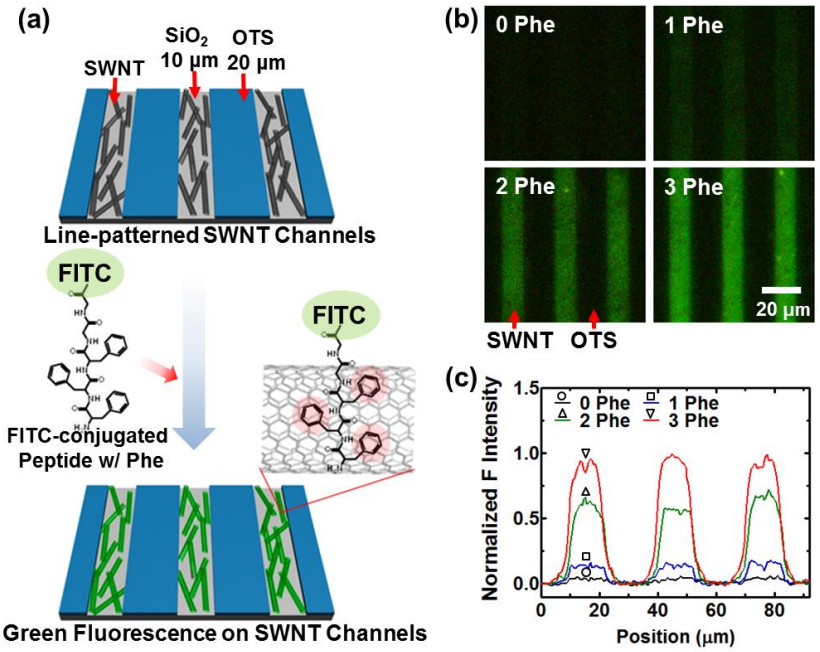

Figure 7.2 Peptide immobilization process using π-π stacking between SWNTs and aromatic rings of phenylalanines (Phe). (a) Schematic diagram describing the immobilization process of FITC-conjugated peptides on line-patterned SWNT channels. The peptide-immobilized SWNTs displayed green fluorescence due to immobilization of FITC, a green fluorescent dye. (b) Fluorescence microscopy images of SWNT channels after the immobilization of four kinds of FITC-peptides containing zero to three Phe residues. The sequences of 0 Phe, 1 Phe, 2 Phe, and 3 Phe are Gly-Gly, Gly-Gly-Phe, Gly-Gly-Phe-Phe, and Gly-Gly-Phe-Phe-Phe, respectively. (c) Normalized fluorescence intensity of each channel in Figure 7.2(b). The fluorescence intensity, which was used as a measure of the immobilization efficiency, increased with an increase in the number of Phe residues that were on peptides.

7.3 Functionalization of SWNTs through immobilization of ORPs

ORPs that possessed three additional Phe at the C-terminus were synthesized, and SWNT-FETs were fabricated. Before the immobilization of ORPs, the shape of the fabricated SWNT channels was assessed using AFM. Figure 7.3(a) shows the SWNT channel composed with random networks of many SWNTs. Then, the samples after the immobilization of ORPs were checked. ORPs were immobilized by placing a 1.5 μL droplet of DW containing Phe-attached ORPs on the SWNT channels. When the AFM images before and after the immobilization were compared (Figures 7.3(a) and 7.3(b)), the brightness of the ORP-immobilized SWNTs was more intense than that of bare-SWNTs, which indicates that the height of the ORP-SWNTs was increased by the immobilization process. The height of the cross section uniformly increased by 2~3 nm after the immobilization step as shown in Figure 7.3(c). Because the predicted height of ORP which consists of α-helix structure by 15 amino acids is approximately 2~3 nm, these results indicate that the ORPs uniformly coated the SWNTs as a monolayer. To further confirm immobilization, the electrical properties were measured. After the formation of monolayers, the resistance between the source and drain electrodes increased, but the FET property remained unchanged (Figures 7.4 and 7.5), both of which indicate successful immobilization of the ORPs.

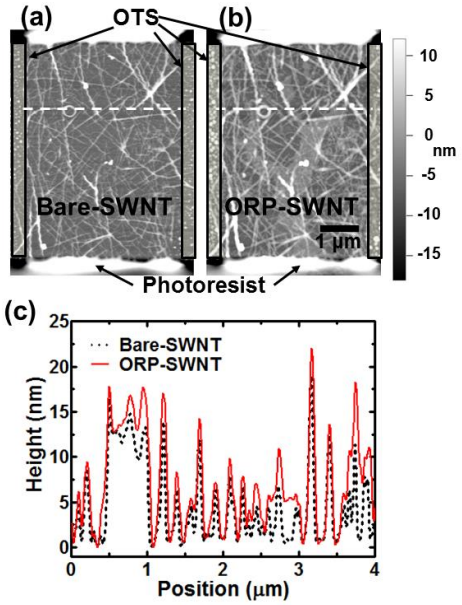

Figure 7.3 AFM images of (a) bare and (b) ORP-immobilized SWNT channels on the fabricated sensor devices. (c) Height profiles of specific cross sections (white dashed lines in (a) and (b)). The height of SWNTs increased by 2~3 nm after the immobilization of ORPs.

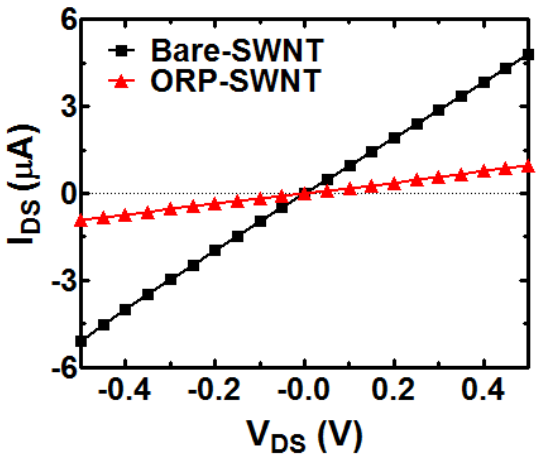

Figure 7.4 Electrical properties of bare and ORP-coated SWNT-FETs. Drain-source current versus drain-source voltage of each device was plotted. The resistance of the SWNT channels increased after the immobilization of ORPs. The fabricated SWNT-FETs exhibited linear IV properties and the resistance of bare and ORP-coated SWNT devices was calculated to be 9.8 × 10^4 and 53.5 × 10^4 Ω respectively. The increase in resistance after the immobilization indicates that compounds were attached on the surface of SWNTs.

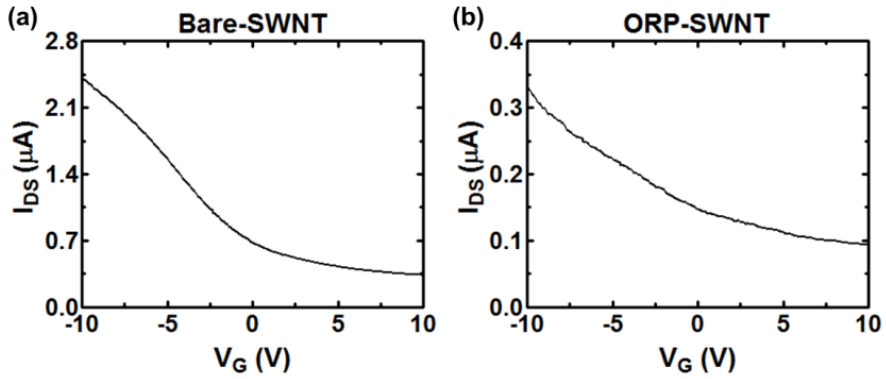

Figure 7.5 Properties of field-effect transistors obtained from (a) bare and (b) ORP-coated SWNT devices. Data were plotted with source-drain current versus back-gate voltage. Drain-source currents decreased with an increase in gate voltage. The fabricated devices maintained *p*-type characteristics after the immobilization of ORPs. This result indicated that both devices were good semiconducting transducers.

7.4 Detection of TMA from standard solutions

TMA was detected based on the conductance change on the SWNT transistor. TMA is an organic base and acts as a proton acceptor in water; thus, it provides a positive potential to *p*-type transistors.[158] An increase in the potential should result in a reduction of the conductance on the SWNT channels. In addition, a decrease in the conductance at extremely low TMA concentrations was expected due to the ORP-layer that absorbs TMA molecules very near to the surface of the SWNTs.

A 49.5 μL of DW droplet was placed on the SWNT channel of the FET device, and the sample solutions were added. The conductance change was then monitored. Figure 7.6(a) shows real-time conductance measurement data obtained from bare and ORP-coated SWNT-FETs after the addition of a solution containing various concentrations of TMA. The sensors exhibited a prompt conductance decrease after the addition of 10 fM TMA, whereas no change was observed in the case of the bare-SWNT device. The intensities of the responses increased with TMA concentration and reached a plateau at 100 μM as shown in Figure 7.6(b). The fitting line was calculated by the mean and standard deviation (SD) values of five duplicate sets. At concentrations higher than 100 μM, there was no more signal increase because all the binding sites of the peptide receptors were occupied by the TMA molecules. In addition, the responses were normalized by its saturated value and fitted to the Hill equation. The half maximal effective concentration (EC50) calculated from the Hill equation was 1.52×10^{-12} M. Based on these results, we verified that the sensor can sensitively detect TMA at concentrations as low as 10 fM in real-time.

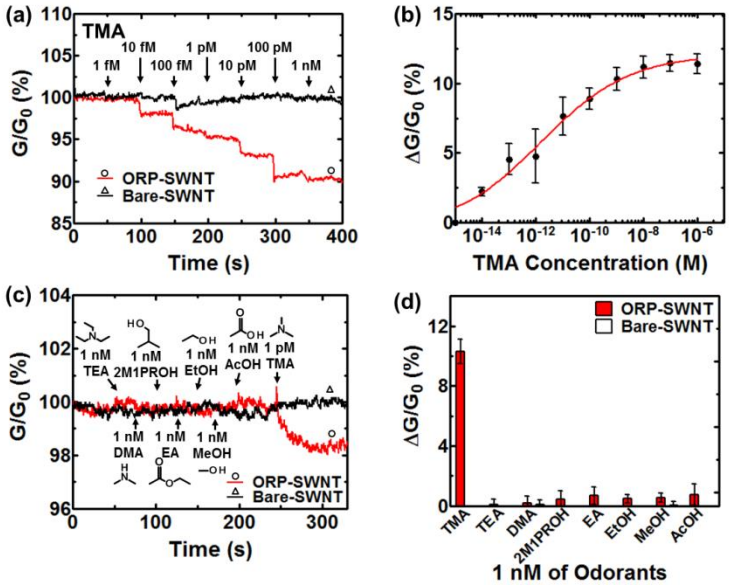

Figure 7.6 Detection of TMA from a standard solution using peptide-based bioelectronic noses. (a) Real-time measurements of conductance changes generated by the introduction of TMA using the bare and ORP-coated SWNT-FETs. A decrease in the conductance was visible after the introduction of 10 fM TMA, and the responses increased with an increase in TMA concentrations. (b) Dose-dependent response curve of the sensors to TMA. (c) Real-time recognition of TMA from other odorants using bare and ORP-coated SWNT-FETs. The addition of the 1 pM TMA solution caused a sharp decrease in the conductance of ORP-SWNT devices; however the addition of 1 nM of other molecules had no effect on the conductance. (d) Quantitative comparison of conductance changes after the injection of TMA and other molecules with a concentration of 1 nM (n=5). The abbreviations used are: TMA, trimethylamine; TEA, triethylamine; DMA, dimethylamine; 2M1PROH, 2-methyl-1-propanol; EA, ethylacetate; EtOH, ethanol; MeOH, methanol; AcOH, acetic acid.

Figure 7.6(c) shows real-time conductance measurements after the addition of TMA and other compounds. The addition of 1 nM triethylamine, dimethylamine, 2-methyl-1-propanol, ethylacetate, ethanol, methanol, and acetic acid did not affect the conductance on the bioelectronic nose, whereas the addition of 1 pM TMA caused a sharp decrease in the conductance. In addition, the intensity of the response after the addition of 1 nM TMA was compared with the intensities from 1 nM of other compounds to quantitatively assess the TMA-discriminating ability of the sensor (Figure 7.6(d)). The intensity generated from the TMA was higher at least by 10-fold than those from other compounds. Note that the difference between the TMA and the other compounds used in this experiment was very small in terms of chemical structure or irritating odor-property. These results show the excellent selectivity of peptide-based bioelectronic noses to discriminate TMA from analogous molecules.

7.5 Determination of seafood decomposition through detecting TMA in spoiled seafood

To verify the capability of the peptide-based bioelectronic nose for practical uses, TMA generated from real spoiled seafood was measured. In these experiments, three kinds of seafood samples were used; oyster, shrimp, and lobster. The fresh seafood samples were ground to reduce sampling errors and were stored in 15-mL Falcon tube at 25 ˚C. After storing for 0~4 days, 1 mL of DW per 1 mg of seafood samples was added to eliminate the liquid-squeezing step of spoiled seafood. The liquid fractions were additionally diluted to 1:100 with DW because 1:100-diluted samples did not affect the conductance of bare-SWNT devices as shown in Figure 7.7. The bare-SWNT transistors were first treated with the produced samples to check whether various compounds contained in spoiled seafood could non-specifically affect the conductance. Figure 7.8 shows the conductance measurement data after injecting the bare-SWNT transistors with three spoiled seafood samples. As a result, no detectable response was generated.

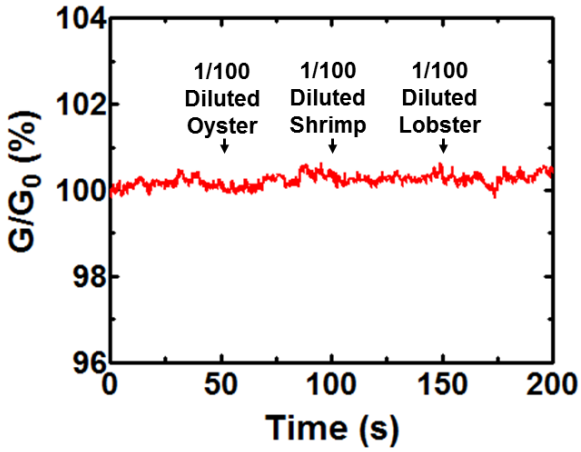

Figure 7.7 A real-time conductance measurement using bare SWNT-based devices after the introduction of 1/100-diluted seafood samples. The bare SWNT-FETs were not affected by 1/100-diluted samples.

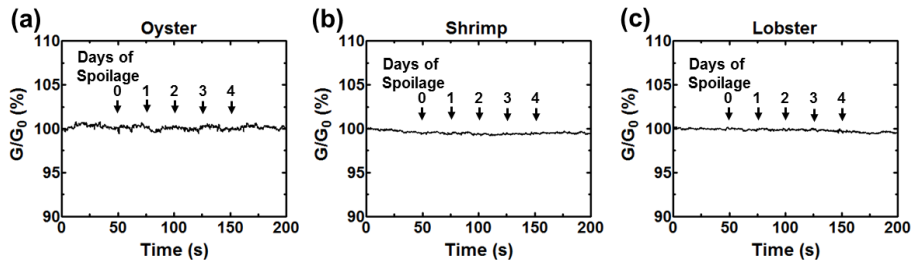

Figure 7.8 Real-time measurements of conductance changes after the introduction of (a) oyster, (b) shrimp, and (c) lobster samples that had been spoiled for 0~4 days using the bare SWNT-FET devices. No significant change in the conductance was observed after the introduction of spoiled seafood samples.

Peptide-based bioelectronic noses were then treated with the produced samples, and the conductance changes were monitored. Figure 7.9(a) shows the real-time measurement data. Changes in the conductance were observed after the addition of the oyster sample spoiled for two days. The shape of the rapid conductance decrease was similar to the response obtained from the standard TMA solution. This result demonstrates that the peptide-based bioelectronic nose was able to detect TMA from spoiled oyster in real-time. After the measurement was complete, the chip was washed with DW 3~4 times. Then, the washed chip was incubated with a DW droplet until the base line was re-stabilized. When this procedure was performed, the same sample could be measured four times, and consistent responses were observed. Especially, the SD value from the four response intensities was within 3%, indicating that the measurement was reproducible. However, when the sensor was reused more than five times, the signal was not quite reproducible. This is considered to be due to the damage accumulated by washing steps and also due to many contaminating compounds contained in the real samples.

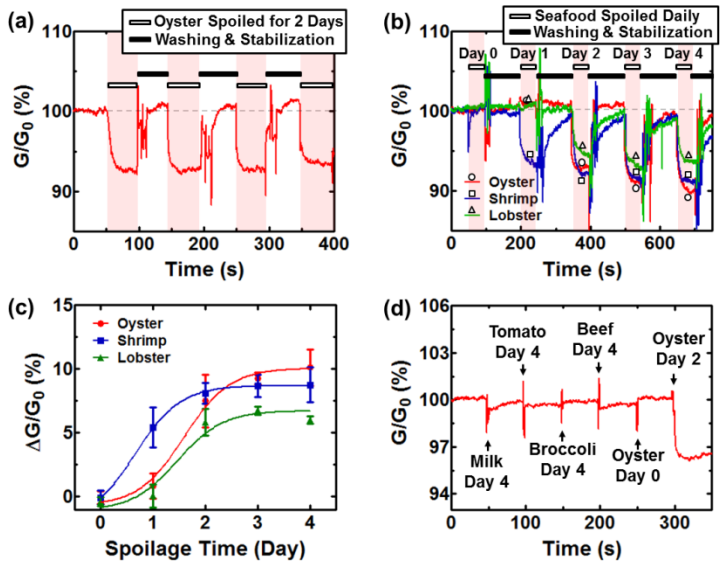

Figure 7.9 Detection of TMA from spoiled seafood. (a) A real-time measurement data exhibiting the conductance change generated by repetitive treatments with a spoiled oyster sample. Consistent and prompt responses were generated by four treatments. (b) Real-time measurements of conductance changes generated by treatments with oyster, shrimp, and lobster samples spoiled for different periods of time. Significant decreases in the conductance were observed for the 2 day-spoiled oyster, 1 day-spoiled shrimp, and 2 day-spoiled lobster. And the responses increased with an increase in the spoilage time. (c) Response patterns versus the degree of spoilage of the spoiled seafood samples. The generated responses tended to increase with the degree of spoilage. (d) A real-time recognition and distinction of spoiled oyster from other kinds of spoiled foods (milk, tomato, broccoli, and beef) and fresh oyster. The spoiled samples of milk, tomato, broccoli, and beef and fresh oyster had no significant effect on the conductance. However, the injection of the oyster sample that had been spoiled for two days caused a sharp decrease in the conductance.

Figure 7.9(b) shows real-time measurement data of conductance changes generated by treatment with oyster, shrimp, and lobster that had been spoiled for 0~4 days. A significant decrease in the conductance was observed when the 2 day-spoiled oyster, 1 day-spoiled shrimp, and 2 day-spoiled lobster samples were added. In addition, the response intensities increased with the degree of decomposition due to the increase in the TMA concentration. The increase in intensities were quantitatively plotted using 3~5 duplicated sets as shown in Figure 7.9(c). The saturation of responses was observed on the second or third day. This saturation may occur when the seafood was completely decomposed or the concentration of the target compound exceeds the detection range. If we compare the signal intensities in Figure 7.9(c) with the maximum signal intensity in Figure 7.6(b), the signal intensities in Figure 7.9(c) are in the detection range. This indicates that the saturation of the signal intensity is due to the complete decomposition of seafood samples. Based on the small SD value at each point in Figure 7.9(c), the sensors produced fairly reproducible responses. Moreover, peptide-based bioelectronic noses can be used to determine the degree of seafood decomposition. This is due to the ability to convert the response intensity into an estimated concentration of TMA in the sample solution (Table 7.1). The original samples were diluted to 1:10,000 with buffer solution. The fact that estimated TMA concentrations at the micro-molar level are similar to concentrations actually contained in real spoiled seafood clearly demonstrates the capability of the peptide-based bioelectronic nose to detect TMA in seafood samples.[137, 147]

Table 7.1 Estimated concentrations of TMA in seafood samples.

Seafood	Spoilage Time (Day)	Response Intensity (%)	Estimated TMA Concentration in Original Seafood Sample (M)
Oyster	0	< 2.22	$< 10^{-10}$
	1	< 2.22	$< 10^{-10}$
	2	7.51 ± 2.06	$(1.34 \pm 2.38) \times 10^{-6}$
	3	9.28 ± 0.45	$(3.08 \pm 2.52) \times 10^{-6}$
	4	10.11 ± 1.40	$(2.93 \pm 4.54) \times 10^{-5}$
Shrimp	0	< 2.22	$< 10^{-10}$
	1	5.41 ± 1.58	$(2.39 \pm 2.03) \times 10^{-8}$
	2	8.13 ± 0.82	$(7.37 \pm 7.76) \times 10^{-7}$
	3	8.67 ± 0.88	$(1.73 \pm 1.92) \times 10^{-6}$
	4	8.77 ± 1.39	$(3.31 \pm 4.45) \times 10^{-6}$
Lobster	0	< 2.22	$< 10^{-10}$
	1	< 2.22	$< 10^{-10}$
	2	5.82 ± 1.04	$(3.36 \pm 5.08) \times 10^{-8}$
	3	6.75 ± 0.30	$(6.93 \pm 2.61) \times 10^{-8}$
	4	6.02 ± 0.30	$(2.44 \pm 1.10) \times 10^{-8}$

TMA is specifically generated when seafood decomposes; therefore, bioelectronic noses can discriminate spoiled seafood from other types of foods by selectively detecting TMA. In order to verify the ability of the sensor to distinguish spoiled seafood, other types of spoiled foods (milk, tomato, broccoli, and beef) were prepared. Figure 7.9(d) shows real-time conductance measurement data after successively injecting four kinds of other food samples that had been spoiled for four days and oyster samples that were fresh and spoiled for two days. Injection of spoiled milk, tomato, broccoli, beef, and fresh oyster had no significant effect on the conductance. On the other hand, the injection of 2 day-spoiled oyster caused a sharp decrease in the conductance. These combined results clearly demonstrate that the sensor was able to specifically distinguish spoiled seafood from other spoiled food products and could be used for the determination of the degree of seafood spoilage.

Further improving the positive points of conventional OR-based sensors in terms of sensitivity and selectivity, the peptide-based bioelectronic nose possessed more advantages for practical uses. First of all, although the sensing mimicked the biological olfaction, it was actually conducted without lipid bilayers. ORs which have their own tertiary structures should be present in the lipid bilayers similar to the cellular membrane for maintaining proper functions. However, synthetic peptides can be activated without lipid bilayers due to the insignificance of their tertiary structure. This indicates the improvement of reusability and reproducibility of peptide-based bioelectronic noses.

Most sensors need to be functionalized by biomolecules to improve their selectivity. However, previously reported functionalization processes require

several complicated steps and labor intensive manipulations. This is also another obstacle to overcome. The most optimal process with a minimized step was provided in this study. The functionalization process was completed by placing a water droplet which contains peptides onto SWNT channels. Although the immobilization of peptide receptors occurred through non-covalent interactions by a single-step, the peptide receptors were strongly adhered to the surface of SWNTs, which allowed the peptide-immobilized sensors to be reusable. This easy but strong functionalization method will facilitate the advancement of other sensor platform, such as microfluidics-based sensors. Furthermore, it may be easily applied to the development of various other sensors that require functionalization of SWNTs through the immobilization of different types of specific peptides.

7.6 Conclusions

A bioelectronic nose was developed through the functionalization of SWNT-FETs with TMA-recognizing ORPs. The functionalization was conducted by a single-step process, and it was based on the π-system of the SWNTs, which can allow for the π–π stacking interactions. The ORP-layer selectively absorbed the TMA molecules very near to SWNT channels, and allowed immediate detection of TMA at a concentration as low as 10 fM with excellent selectivity. In addition, TMA generated from real spoiled seafood samples was reliably detected without any pretreatment processes. The peptide-based bioelectronic nose was also able to specifically recognize spoiled seafood by discriminating spoiled seafood from other types of foods. Moreover, the sensors were reusable and reproducible because they were manufactured using small peptides without lipid bilayers. These results demonstrate that peptide-based bioelectronic noses can be applied for the rapid and simple determination of seafood decomposition. Furthermore, this work provides a simple experimental method for the immobilization of biomolecules on SWNTs, which opens up the possibility for diverse applications.

Chapter 8.

Peptide-based bioelectronic nose for the detection of gaseous odorants

Chapter 8. Peptide-based bioelectronic nose for the detection of gaseous odorants

8.1 Introduction

Bioelectronic noses recognize odorants using two main parts. The first part is an odorant-recognizing element, and the second part is a signal transducer.[3] OR proteins produced from heterologous expression systems or cells expressing ORs on their surface membrane were generally used for the recognition of odorants.[13, 74, 78, 79, 81] ORs have great selectivity capable of precisely discriminating their specific ligands among other analogous molecules. By virtue of this selectivity, bioelectronic noses can perceive odorants similar to the human nose.

Even though OR-based bioelectronic noses exhibit good sensing performances, they have a problem to be applied to practical fields. First, a mass production of ORs is difficult due to high hydrophobicity and complex tertiary structures of ORs.[55, 65] Also, OR-based bioelectronic noses require a lipid membrane for the proper structure of ORs, which means low repeatability and reproducibility of the sensor. In order to overcome this issue, bioelectronic noses based on OR-derived peptides (ORPs) rather than the whole OR proteins have been developed.[54, 68, 157] Peptide-based bioelectronic noses also have excellent sensitivity and selectivity. And their capability to be utilized for the determination of seafood decomposition was demonstrated.[54]

Peptide receptors can be easily immobilized on the surface of SWNTs by a single-step process. It was demonstrated that a phenylalanine (Phe) cluster at the end of peptides induces the formation of a self-assembly monolayer.[54] Through this strategy, bioelectronic noses using peptide receptors and SWNT-FETs could be developed. This bioelectronic nose was able to detect odorants with excellent repeatability and reproducibility as well as high sensitivity and selectivity. The last remaining issue is whether the sensor can detect gaseous odorants. In this study, a gas-flow platform based on polydimethylsiloxane (PDMS) was fabricated and integrated with peptide-based bioelectronic noses. The peptide receptor, which is derived from canine ORs, specifically interacts with trimethylamine (TMA), an indicator of seafood decomposition.[70, 133-135, 137, 157] Using this sensing system, a potential of peptide-based bioelectronic noses for the detection of gaseous odorants and the determination of seafood decomposition was demonstrated.

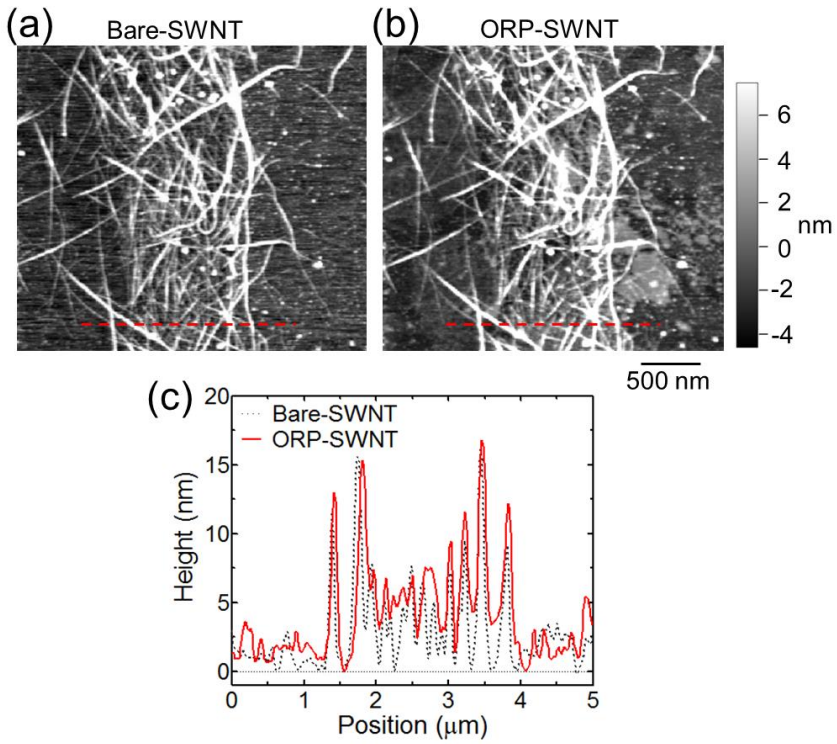

Figure 8.1 AFM images of (a) bare and (b) ORP-coated SWNT channels. (c) Height profiles of cross sections (red dashed lines in (a) and (b)). The heights of SWNTs were increased by the immobilization of ORPs.

8.2 Fabrication of peptide-based bioelectronic nose

Three Phe residues were attached at the C-terminal end of ORP (NQLSNLSFSDLCFFF). The π-system of three Phe induces the attachment of peptides onto the surface of SWNTs by π-π stacking interaction.[54, 75, 148] The immobilization of ORPs on SWNTs was confirmed with AFM (Figure 8.1). The heights of ORP-immobilized SWNTs were higher than those of bare SWNTs. This result demonstrated the successful immobilization of ORPs on the SWNTs. Electrical property of the SWNT-FETs was also measured. By the immobilization of ORPs on the SWNTs, the resistance between the source and drain electrodes increased (Figure 8.2). And, regardless of ORP immobilization, the sensor exhibits *p*-type properties (Figure 8.2). This means that the fabricated devices were good semiconducting transducers.

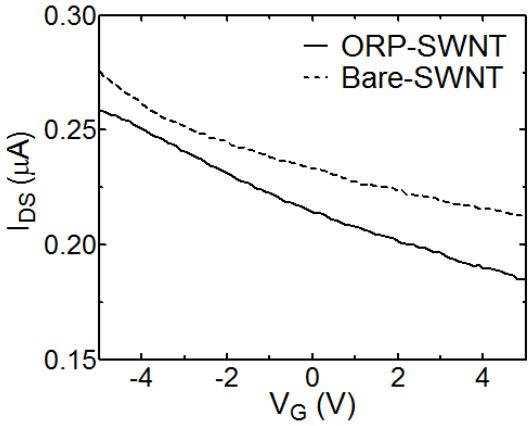

Figure 8.2 Field-effect properties of (a) bare and (b) ORP-coated SWNT devices. Data were plotted with drain-source current versus back-gate voltage. Drain-source currents decreased with an increase in the gate voltage. The *p*-type characteristic was maintained regardless of the immobilization of ORPs.

8.3 Fabrication of gas-flow platform

In order to supply accurate amounts of gas samples to the bioelectronic noses, gas-flow platform was fabricated using PDMS. The chip which had been completely fabricated was mounted on the gas-flow platform (Figure 8.3). Fluidic channels were formed with PDMS. The PDMS channel was firmly affixed to the sensing chip by a polycarbonate frame. For the actual detection of odorants, The PDMS-based fluidic channel was filled with gas samples. Gas samples with consistent concentrations were produced in bottles sealed with a septum cap, and supplied to the sensor using a syringe. In this system, 10 independent sensing channels were simultaneously stimulated by a single injection of the gas sample (Figure 8.4).

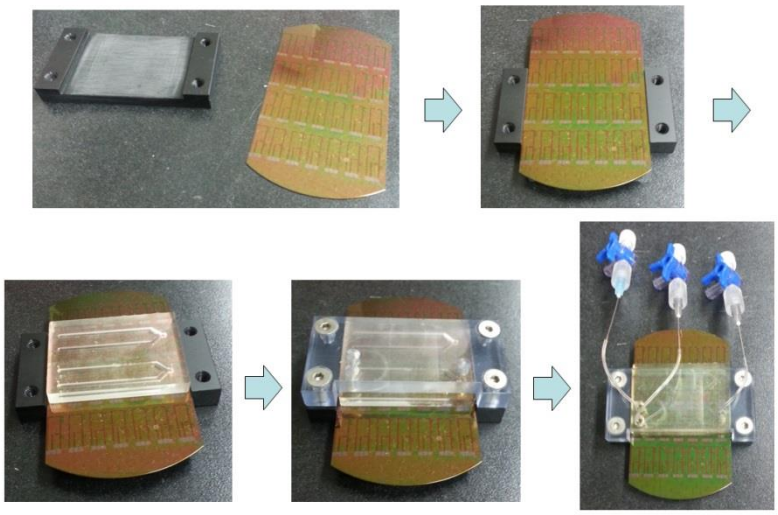

Figure 8.3 Mounting process of the sensing chip to the gas-flow platform. The 4-inch wafer of which edges had been cut was placed on the bottom part of a main frame. Then, a gas-fluidic channel based on PDMS and the upper parts of the frame were put on the sensing chip. The fluidic channel was finally filled with gas samples.

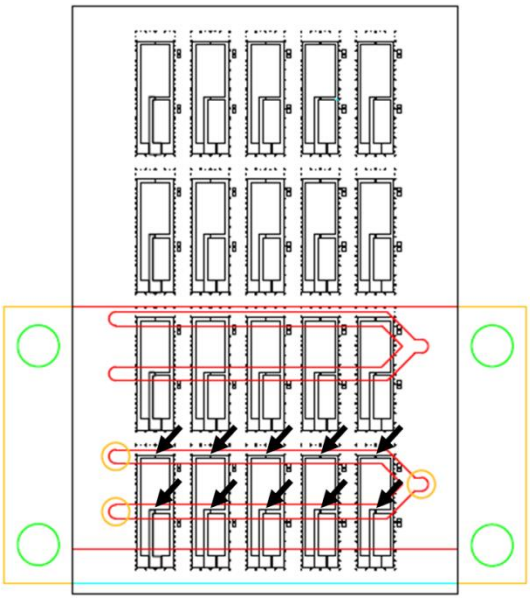

Figure 8.4 Schematic illustration of the gas-flow platform. Black lines represent gold electrodes deposited on the silicon wafer. Cyan and yellow lines represent bottom and upper parts of the frame, respectively. Red lines represent fluidic channels based on PDMS. Green circles are the position of screws to press the upper part of the frame. The frame was fabricated with polycarbonate. Black arrows point to sensing channels composed of SWNTs and peptide receptors.

8.4 Detection of gaseous TMA

The detection of TMA was conducted by monitoring the conductance change on the bioelectronic noses. TMA molecules, which are accumulated very close to SWNTs, can act as a kind of a positive gate potential because TMA accepts a proton from water vapor in air.[158] An increase in the positive potential results in a decrease in the conductance on the ORP-SWNT channels.

Gas samples containing TMA was injected to the sensing platform through the gas-flow channel, while the conductance change was monitored. Figure 8.5(a) shows conductance changes by the injection of TMA to the bare and ORP-coated SWNT-FETs. In the case of the ORP-coated device, the conductance promptly decreased by the treatment with 10 ppt of TMA. And the response intensity increased with an increase in the concentration of TMA (Figure 8.5(a)). However, no changes were observed when ORPs had not been immobilized on the SWNTs. These results indicate that the ORP layer could assist the accumulation of TMA close to the SWNT channels. Figure 8.5(b) shows a dose-dependent response pattern of the sensor. The response intensity was saturated at the ppb range.

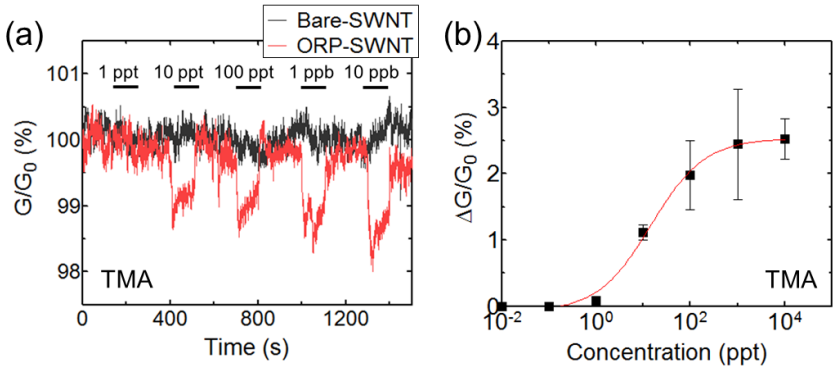

Figure 8.5 Detection of TMA using peptide-based bioelectronic noses. (a) Real-time measurements of conductance changes using bare and ORP-immobilized SWNT-FETs. Injection of 10 ppt TMA induced the prompt decrease in the conductance on the ORP-immobilized device. (b) A dose-dependent response pattern of peptide-based bioelectronic noses to TMA. The responses were generated by the treatment with 10 ppt of TMA, and reached a plateau at ppb level.

Peptide-based bioelectronic noses can be easily reused.[54] As shown in Figure 8.6, the peptide-immobilized device was able to be reused with high reproducibility. The sensor was treated with 1 ppb of TMA. After the measurement was completed, the TMA samples were displaced with fresh air. Then, the chip was incubated until the baseline of the sensor was re-stabilized. Through this procedure, the same sample was able to be detected four times, and reproducible responses were monitored (Figure 8.6). This indicates that the sensor could be repeatedly reused without the loss of activity.

This peptide-based bioelectronic nose can detect TMA with high selectivity because peptide receptors were used for the functionalization of SWNTs. The ORP that was used can discriminate TMA.[54, 157] In order to demonstrate the selectivity of the sensor, the effect of 5 odorants (triethylamine, dimethylamine, 2-methyl-1-propanol, acetic acid, and acetone) on the conductance of the sensor was measured. The response intensity by the injection of 10 ppb TMA was compared to the intensities from 10 ppb of other compounds (Figure 8.7). The responses generated from the TMA were more intensive than those from other molecules. Note that compounds that were used in this experiment have a similar chemical structure or irritating odor. The result in Figure 8.7 demonstrated the great selectivity of the peptide-based bioelectronic nose.

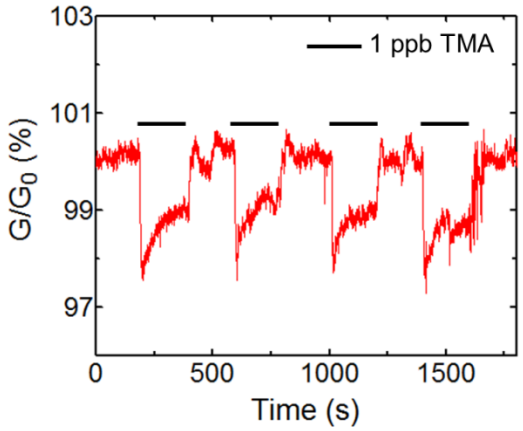

Figure 8.6 A real-time measurement showing the conductance change generated by repetitive stimulations with 1 ppb of TMA. Reproducible and prompt responses were observed by four treatments.

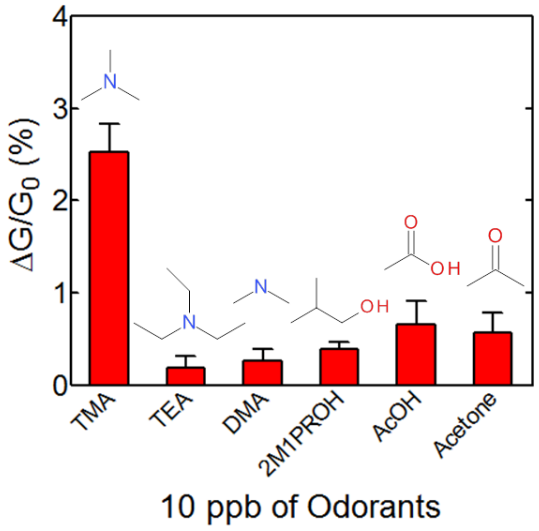

Figure 8.7 Conductance changes by the injection of TMA and other molecules with a concentration of 10 ppb (n=4). The most intensive responses were generated when TMA was injected. The abbreviations used are: TMA, trimethylamine; TEA, triethylamine; DMA, dimethylamine; 2M1PROH, 2-methyl-1-propanol; AcOH: acetic acid.

The sensitive detection of TMA is very important issue because TMA can be used as an indicator of seafood decomposition.[133-135] TMA is also one of regulated air-pollutants[149] and a biomarker of several diseases, such as bacterial vaginosis[150, 151] and trimethylaminuria.[152] Thus, numerous studies have been performed to develop sensitive TMA sensor. The limit of detection of other sensors which have been reported was mainly ppm or ppb level (Table 8.1). The peptide-based bioelectronic nose that was developed in this study was able to detect TMA at concentrations as low as 10 ppt. The human threshold of TMA odor has been reported as 0.00021 ppm.[159] Thus, the developed bioelectronic nose was much more sensitive than the human nose as well as other sensors. The high sensitivity means that TMA generated from very small amounts of spoiled seafood can be easily monitored. Furthermore, by using peptide receptors, selectivity of the sensor was significantly improved. The sensor can selectively recognize the spoilage of seafood by discriminating TMA among other molecules. The peptide-based bioelectronic noses can be effectively used in various fields where the sensitive and selective detection of TMA was required.

Table 8.1 Performances of various TMA gas sensors

Sensor Type	Limit of Detection (ppm)	Detectable Range (ppm)	Operation Temperature	Key Features
ORP-coated SWNT-FET (this study)	10^{-5}	10^{-5}-10^{-3}	Room temp.	Highly selective
Molybdenum trioxide thin films[160]	0.1	0.1-50	Room temp.	
Cr_2O_3 nanoparticles on ZnO nanowire[161]	0.05	0.05-5	400 ℃	
Y_2O_3-based catalytic chemiluminescent sensor[162]	10	10-42,000	320 ℃	
Microcantilever[163]	0.5	0.5-500	Room temp.	Long analyzing time (~4000s)
WO_3 hollow spheres[164]	0.05	0.05-5	450 ℃	Selective
Graphene-FET[158]	0.75	0.75-6.25	Room temp.	
WO_3 thin film[165]	200	200-1000	70 ℃	
SnO_2 thin film[166]	10	10-300	290 ℃	
ZnO nanoparticles[167]	0.2	0.2-0.8	Room temp.	

8.5 Conclusions

Peptide receptors were immobilized on the SWNTs through a single-step process. Three Phe residues at the end of the peptides were self-assembled on the surface of SWNTs by π-π stacking interaction. Because the peptide receptor specifically binds with TMA molecules, ORP-immobilized SWNT-FETs detected TMA with high sensitivity and selectivity. The limit of detection of the developed sensor is 10 ppt, which is the superb sensitivity compared to conventional TMA sensors. Moreover, the sensor has excellent selectivity. Furthermore, the interaction between peptides and SWNTs was quite stable; hence, repetitive measurements were also possible. This sensor can be used for the simple and rapid determination of seafood decomposition by sensitively and selectively monitoring the amount of TMA.

Chapter 9.

Overall discussion and further suggestions

Chapter 9. Overall discussion and further suggestions

The human nose can distinguish more than thousands of odorous molecules using ORs expressed in the surface of olfactory sensory neurons. Biding of odorants to ORs is the first event in the cellular mechanism for the odor perception. Sense of smell is one of the most effective tools to evaluate food quality, to monitor environmental pollutants, and to diagnose diseases. Many studies have recently attempted to mimic the olfactory system using electronic devices. However, it is realistically impossible to reconstruct the olfactory systems *in vitro* without the ORs because the ORs have a unique selectivity capable of precisely discriminating odorants among a mixture of other compounds. Therefore, novel sensing systems called a bioelectronic nose have been suggested. The bioelectronic noses were fabricated with ORs as well as electronic devices; hence, they can overcome limitations of conventional electronic devices.

In this thesis, carbon nanotube-based bioelectronic noses combined with olfactory nanovesicles and OR-derived peptides were presented. The nanovesicles and peptides recognize odorants with high selectivity, and SWNT-FETs transduce the biological recognition into sensitive signals that can be measured.

In chapter 4, a nanovesicle-based bioelectronic nose was presented. This bioelectronic nose can distinguish the odor of a lung cancer biomarker, heptanal, from human blood. Selective recognition of the biomarker was mimicked in the human olfactory system. A specific OR recognizing the chemical biomarker was first selected through screening a library of human ORs. The selected OR was expressed on the membrane of HEK-293 cells.

Nanovesicles containing the OR on the membrane were produced from these cells, and were then used for the functionalization of SWNTs. This strategy allowed the development of a sensitive and selective nanovesicle-based bioelectronic nose. This bioelectronic nose was able to selectively detect heptanal at a concentration as low as 10 fM, a sufficient level to distinguish the blood of a lung cancer patient from the blood of a healthy person. In actual experiments, the sensor could detect an extremely small increase in the amount of heptanal from human blood plasma without any pretreatment processes. This result offers a rapid and easy method to analyze chemical biomarkers from human blood in real-time and to diagnose lung cancer.

In chapter 5, a nanovesicle-based bioelectronic nose for the sensitive and selective detection of hexanal, an indicator of lipid oxidation in foods, was presented. This bioelectronic nose mimicked the function of the canine nose. The bioelectronic nose detected 1 fM of hexanal in real-time. Moreover, hexanal was detected with an excellent selectivity. The sensor could discriminate hexanal among analogous molecules such as pentanal, heptanal, and octanal. Furthermore, hexanal in spoiled milk was able to be detected without any pretreatment processes. This platform offers an effective strategy to easily and rapidly assess the degree of food oxidation.

In chapter 6, a method to improve stability of nanovesicle-based bioelectronic noses was presented. The activity of nanovesicles is easily extinguished due to the unstable signaling components such as ATP. Thus, potassium channels which can be directly modulated by the activation of membrane proteins were covalently coupled with ORs. The conformational change of ORs induced the influx of potassium ions through the fused channels. The ion influx was transduced into sensitive signals by SWNT-

FETs. By the coupling between ion channels and ORs, the discrimination of specific responses from noise signals could be easier. In addition, stability of nanovesicles in a non-frozen state was significantly improved. These results raise a possibility of nanovesicle-based bioelectronic noses for the practical uses.

In chapter 7, a peptide-based bioelectronic nose was presented. This bioelectronic nose can determine the degree of seafood decomposition in real-time through measuring the amount of TMA generated from spoiled seafood. The peptide-based bioelectronic nose was developed using SWNT-FETs functionalized with ORPs which can recognize TMA. The sensor sensitively and selectively detected TMA in real-time at concentrations as low as 10 fM. Utilizing these properties, the sensor was able to not only determine the quality of three kinds of seafood (oyster, shrimp, and lobster), but was also able to distinguish spoiled seafood from other types of spoiled foods without any pretreatment processes. Especially, the use of small synthetic peptides rather than the whole protein allowed the sensor to be simply manufactured through a single-step process and to be reused with high reproducibility due to no requirement of lipid bilayers.

In chapter 8, a peptide-based bioelectronic nose to detect gaseous odorants was presented. Peptide receptors that recognize TMA were immobilized on the SWNT-FETs by a single-step process. The functionalized SWNT-FETs were mounted on a gas-flow platform fabricated with PDMS and polycarbonate. Through the PDMS-based fluidic channel, gas samples were supplied to the sensor device. This sensor platform could detect 10 ppt of TMA. In addition, TMA was able to be selectively distinguished from other odorants. The use of peptide receptors rather than

cells or whole proteins allowed an easy fabrication process and high repeatability. The peptide-based bioelectronic nose can be extensively used for the determination of seafood decomposition by detecting the odor of spoiled seafood.

In this study, two kinds of biomaterials were used as a primary sensing element: cell-derived nanovesicles containing ORs on their membrane and OR-derived peptides. Each biomolecule has its own characteristics. The most important advantage of the nanovesicle is that they can mimic the olfactory signaling pathway. The nanovesicle generates olfactory signals through the original cellular pathway. Nevertheless, handling and storage of the nanovesicle were much easier than those of cells. Moreover, a mass production is possible. The most critical drawback of the nanovesicle is low stability in a non-frozen state. However, a method to improve the stability of nanovesicles was successfully demonstrated in this thesis. A peptide receptor is one of biomaterials closest to practical uses. OR-derived peptides have unique characteristics of OR proteins, such as high selectivity. In addition, the peptides can be synthesized in large quantities. Also, the fabrication process of peptide-based bioelectronic noses can be simplified. Most of all, it was, in this study, demonstrated that peptide-based sensors are active in a dry condition and can detect gaseous odorants. Thus, peptide-based bioelectronic nose will be a practical alternative to the human noses.

In spite of excellent performances as a sensing device, bioelectronic noses cannot yet be extensively used in all areas where a person can smell. This is because the functions of all ORs have not yet been fully revealed. 390 types of human ORs react to different odorants. Moreover, numerous odorants can affect ORs. Thus, incalculable combinations between ORs and

odorants exist, and the relationship should be investigated further.[168] Following the further investigation of the specific function of ORs, the application area of bioelectronic noses will continue to grow.

The most interesting thing in bioelectronic noses is that OR-based sensors can mimic the olfactory system. Types of odors have not yet been fundamentally and scientifically classified. Thus, there is no other choice but to recognize specific odors based on personal experiences. However, bioelectronic noses will offer a way to classify odors. Each odor has a unique response pattern with activated ORs.[38, 168] A sensor functionalized with a multi-array of all types of ORs can represent whole response patterns *in vitro*. This means that bioelectronic noses can classify types of odors without the help of the human nose. Thus, multi-array sensor platforms need to be developed to fundamentally understand the characteristics of odors.

In the case of peptide-based bioelectronic noses, they need to be utilized for various purposes besides the evaluation of seafood decomposition. Thus, a variety of peptide receptors are required. In order to effectively find novel peptide receptors, a phage display technique can be used. The phage display is an *in vitro* screening technique to identify high affinity biomolecules such as peptides. Through the discovery of novel peptide receptors, the applicability of the peptide-based bioelectronic nose will be improved.

In the case of TMA sensor, the detection of TMA was possible because target odorants acted as a base in water. However, if odorants are electrically uncharged, the detection through the same sensing mechanism as the TMA sensor is unavailable. This problem can be overcome by inducing the conformational change of peptide receptors. The bending of peptides caused by the odorant binding can modulate the distance between SWNTs and

charged amino acids which are located at the end of peptides. Consequently, the conformational change of peptides will be transduced into electrical responses through SWNT-FETs.

Other GPCRs such as taste receptors and hormone receptors can be utilized for the development of biosensor systems through the same strategy as that of the bioelectronic noses.[90, 91, 94, 169] Most GPCRs can be hybridized with sensor platforms. The hybridization between receptors and secondary transducers has facilitated the development of highly sensitive and selective biosensor systems. A bioelectronic tongue fabricated with human bitter taste receptors and FET devices was able to selectively detect bitter compounds at concentrations as low as 1 fM.[91, 94] Moreover, target tastants were efficiently detected in a mixture or in real food samples.[91] Human parathyroid hormone receptors (hPTHRs) were used for the functionalization of conducting polymer nanoparticle-based FETs.[90] The biosensor based on hPTHRs sensitively and selectively detected hPTHs. All these results indicate that the devices functionalized with GPCRs will allow us to develop not only bioelectronic noses and tongues, but also other biosensors for various purposes.

There are various fields where bioelectronic noses can be effectively utilized. First of all, the bioelectronic nose can be a perfect alternative to direct smelling. To this day, trained dogs play major roles in the detection of narcotics and explosives, such as their use in customs and airports as well as military institutions. Although dogs have an excellent smelling ability, they have critical limitations such as high costs for training and maintenance. Also, the natural olfactory system is easily and rapidly adapted to the repetitive exposure to odors; thus, the dogs cannot continuously search drugs

and explosives.[31] Hence, bioelectronic noses may replace the role of dogs within such industries.

Bioelectronic noses can be also utilized for the process monitoring using their excellent sensitivity and selectivity. For instance, they can selectively detect impurities that are contained in food and beverage products during mass production processes. Thus, the quality control of products can become remarkably easier. Also, a sensor, which detects the smell generated from coffee roasting, can accurately determine the degree of roasting. The volatile metabolites generated from bacterial fermentation processes can also be analyzed. Consequently, the progress of such processes can be easily monitored in real-time using the bioelectronic noses. Bioelectronic noses can be effectively applied to any fields where the process has a smell.

Bibliography

1. Persaud, K. and Dodd, G., Analysis of discrimination mechanisms in the mammalian olfactory system using a model nose. ***Nature*** 299, 352-355 (1982)
2. Rock, F., Barsan, N., and Weimar, U., Electronic nose: current status and future trends. ***Chem. Rev.*** 108, 705-725 (2008)
3. Lee, S.H. and Park, T.H., Recent advances in the development of bioelectronic nose. ***Biotechnol. Bioproc. E.*** 15, 22-29 (2010)
4. Göpel, W., Chemical imaging: I. Concepts and visions for electronic and bioelectronic noses. ***Sensor. Actuat. B-Chem.*** 52, 125-142 (1998)
5. Buck, L. and Axel, R., A novel multigene family may encode odorant receptors: a molecular basis for odor recognition. ***Cell*** 65, 175-187 (1991)
6. Malnic, B., Godfrey, P.A., and Buck, L.B., The human olfactory receptor gene family. ***P. Natl. Acad. Sci. USA*** 101, 2584-2589 (2004)
7. Pick, H., Schmid, E.L., Tairi, A.-P., Ilegems, E., Hovius, R., and Vogel, H., Investigating cellular signaling reactions in single attoliter vesicles. ***J. Am. Chem. Soc.*** 127, 2908-2912 (2005)
8. Firestein, S., How the olfactory system makes sense of scents. ***Nature*** 413, 211-218 (2001)
9. Zozulya, S., Echeverri, F., and Nguyen, T., The human olfactory receptor repertoire. ***Genome Biol.*** 2, 1-12 (2001)
10. Thaler, E.R., Kennedy, D.W., and Hanson, C.W., Medical applications of electronic nose technology: review of current status. ***Am. J. Rhinol.*** 15, 291-295 (2001)
11. James, D., Scott, S.M., Ali, Z., and O'Hare, W.T., Chemical sensors for electronic nose systems. ***Microchim. Acta*** 149, 1-17 (2005)

12. Lee, S.H., Kwon, O.S., Song, H.S., Park, S.J., Sung, J.H., Jang, J., and Park, T.H., Mimicking the human smell sensing mechanism with an artificial nose platform. ***Biomaterials*** 33, 1722-1729 (2012)
13. Kim, T.H., Lee, S.H., Lee, J., Song, H.S., Oh, E.H., Park, T.H., and Hong, S., Single-carbon-atomic-resolution detection of odorant molecules using a human olfactory receptor-based bioelectronic nose. ***Adv. Mater.*** 21, 91-94 (2009)
14. Park, S.J., Kwon, O.S., Lee, S.H., Song, H.S., Park, T.H., and Jang, J., Ultrasensitive flexible graphene based field-effect transistor (FET)-type bioelectronic nose. ***Nano Lett.*** 12, 5082-5090 (2012)
15. Zhang, X. and Firestein, S., The olfactory receptor gene superfamily of the mouse. ***Nat. Neurosci.*** 5, 124-133 (2002)
16. Godfrey, P.A., Malnic, B., and Buck, L.B., The mouse olfactory receptor gene family. ***P. Natl. Acad. Sci. USA*** 101, 2156-2161 (2004)
17. Quignon, P., Giraud, M., Rimbault, M., Lavigne, P., Tacher, S., Morin, E., Retout, E., Valin, A.-S., Lindblad-Toh, K., Nicolas, J., and Galibert, F., The dog and rat olfactory receptor repertoires. ***Genome Biol.*** 6, R83 (2005)
18. Ashton, E.H., Eayrs, J.T., and Moulton, D.G., Olfactory acuity in the dog. ***Nature*** 179, 1069-1070 (1957)
19. Moulton, D.G., Ashton, E.H., and Eayrs, J.T., Studies in olfactory acuity. 4. relative detectability of n-aliphatic acids by the dog. ***Anim. Behav.*** 8, 117-128 (1960)
20. Furton, K.G. and Myers, L.J., The scientific foundation and efficacy of the use of canines as chemical detectors for explosives. ***Talanta*** 54, 487-500 (2001)
21. Gazit, I., Lavner, Y., Bloch, G., Azulai, O., Goldblatt, A., and Terkel, J., A simple system for the remote detection and analysis of sniffing in explosives detection dogs. ***Behav. Res. Meth. Ins. C.*** 35, 82-89 (2003)

22. Cornu, J.-N., Cancel-Tassin, G., Ondet, V., Girardet, C., and Cussenot, O., Olfactory detection of prostate cancer by dogs sniffing urine: a step forward in early diagnosis. ***Eur. Urol.*** 59, 197-201 (2011)
23. Ehmann, R., Boedeker, E., Friedrich, U., Sagert, J., Dippon, J., Friedel, G., and Walles, T., Canine scent detection in the diagnosis of lung cancer: revisiting a puzzling phenomenon. ***Eur. Respir. J.*** 39, 669-676 (2012)
24. McCulloch, M., Jezierski, T., Broffman, M., Hubbard, A., Turner, K., and Janecki, T., Diagnostic accuracy of canine scent detection in early- and late-stage lung and breast cancers. ***Integr. Cancer Ther.*** 5, 30-39 (2006)
25. Bodyak, N. and Slotnick, B., Performance of mice in an automated olfactometer: odor detection, discrimination and odor memory. ***Chem. Senses*** 24, 637-645 (1999)
26. Clarke, S. and Trowill, J.A., Sniffing and motivated behavior in the rat. ***Physiol. Behav.*** 6, 49-52 (1971)
27. Uchida, N. and Mainen, Z.F., Speed and accuracy of olfactory discrimination in the rat. ***Nat. Neurosci.*** 6, 1224-1229 (2003)
28. Youngentob, S.L., Mozell, M.M., Sheehe, P.R., and Hornung, D.E., A quantitative analysis of sniffing strategies in rats performing odor detection tasks. ***Physiol. Behav.*** 41, 59-69 (1987)
29. Hu, J., Zhong, C., Ding, C., Chi, Q., Walz, A., Mombaerts, P., Matsunami, H., and Luo, M., Detection of near-atmospheric concentrations of CO_2 by an olfactory subsystem in the mouse. ***Science*** 317, 953-957 (2007)
30. Dalton, P., Psychophysical and behavioral characteristics of olfactory adaptation. ***Chem. Senses*** 25, 487-492 (2000)
31. O'Mahony, M., Sensory adaptation. ***J. Sens. Stud.*** 1, 237-258 (1986)
32. Freund, M.S. and Lewis, N.S., A chemically diverse conducting polymer-based "electronic nose". ***P. Natl. Acad. Sci. USA*** 92, 2652-2656 (1995)
33. Gardner, J.W., Shurmer, H.V., and Tan, T.T., Application of an electronic nose to the discrimination of coffees. ***Sensor. Actuat. B-Chem.*** 6, 71-75 (1992)

34. Pearce, T.C., Gardner, J.W., Friel, S., Bartlett, P.N., and Blair, N., Electronic nose for monitoring the flavour of beers. ***Analyst*** 118, 371-377 (1993)
35. Gardner, J.W., Hines, E.L., and Wilkinson, M., Application of artificial neural networks to an electronic olfactory system. ***Meas. Sci. Technol.*** 1, 446 (1990)
36. Ressler, K.J., Sullivan, S.L., and Buck, L.B., A zonal organization of odorant receptor gene expression in the olfactory epithelium. ***Cell*** 73, 597-609 (1993)
37. Ressler, K.J., Sullivan, S.L., and Buck, L.B., Information coding in the olfactory system: evidence for a stereotyped and highly organized epitope map in the olfactory bulb. ***Cell*** 79, 1245-1255 (1994)
38. Malnic, B., Hirono, J., Sato, T., and Buck, L.B., Combinatorial receptor codes for odors. ***Cell*** 96, 713-723 (1999)
39. Branca, A., Simonian, P., Ferrante, M., Novas, E., and Negri, R.M.n., Electronic nose based discrimination of a perfumery compound in a fragrance. ***Sensor. Actuat. B-Chem.*** 92, 222-227 (2003)
40. Oh, E.H., Song, H.S., and Park, T.H., Recent advances in electronic and bioelectronic noses and their biomedical applications. ***Enzyme Microb. Tech.*** 48, 427-437 (2011)
41. Capone, S., Siciliano, P., Quaranta, F., Rella, R., Epifani, M., and Vasanelli, L., Analysis of vapours and foods by means of an electronic nose based on a sol–gel metal oxide sensors array. ***Sensor. Actuat. B-Chem.*** 69, 230-235 (2000)
42. Cerrato Oliveros, M.C., Pérez Pavón, J.L., García Pinto, C., Fernández Laespada, M.E., Moreno Cordero, B., and Forina, M., Electronic nose based on metal oxide semiconductor sensors as a fast alternative for the detection of adulteration of virgin olive oils. ***Anal. Chim. Acta*** 459, 219-228 (2002)

43. Dutta, R., Hines, E.L., Gardner, J.W., Kashwan, K.R., and Bhuyan, M., Tea quality prediction using a tin oxide-based electronic nose: an artificial intelligence approach. ***Sensor. Actuat. B-Chem.*** 94, 228-237 (2003)
44. El Barbri, N., Amari, A., Vinaixa, M., Bouchikhi, B., Correig, X., and Llobet, E., Building of a metal oxide gas sensor-based electronic nose to assess the freshness of sardines under cold storage. ***Sensor. Actuat. B-Chem.*** 128, 235-244 (2007)
45. González Martín, Y., Cerrato Oliveros, M.C., Pérez Pavón, J.L., García Pinto, C., and Moreno Cordero, B., Electronic nose based on metal oxide semiconductor sensors and pattern recognition techniques: characterisation of vegetable oils. ***Anal. Chim. Acta*** 449, 69-80 (2001)
46. Crone, B., Dodabalapur, A., Gelperin, A., Torsi, L., Katz, H.E., Lovinger, A.J., and Bao, Z., Electronic sensing of vapors with organic transistors. ***Appl. Phys. Lett.*** 78, 2229-2231 (2001)
47. Doleman, B.J. and Lewis, N.S., Comparison of odor detection thresholds and odor discriminablities of a conducting polymer composite electronic nose versus mammalian olfaction. ***Sensor. Actuat. B-Chem.*** 72, 41-50 (2001)
48. Hatfield, J.V., Neaves, P., Hicks, P.J., Persaud, K., and Travers, P., Towards an integrated electronic nose using conducting polymer sensors. ***Sensor. Actuat. B-Chem.*** 18, 221-228 (1994)
49. Hao, H.C., Tang, K.T., Ku, P.H., Chao, J.S., Li, C.H., Yang, C.M., and Yao, D.J., Development of a portable electronic nose based on chemical surface acoustic wave array with multiplexed oscillator and readout electronics. ***Sensor. Actuat. B-Chem.*** 146, 545-553 (2010)
50. Gan, H.L., Man, Y.B.C., Tan, C.P., NorAini, I., and Nazimah, S.A.H., Characterisation of vegetable oils by surface acoustic wave sensing electronic nose. ***Food Chem.*** 89, 507-518 (2005)
51. García, M., Fernández, M.J., Fontecha, J.L., Lozano, J., Santos, J.P., Aleixandre, M., Sayago, I., Gutiérrez, J., and Horrillo, M.C.,

Differentiation of red wines using an electronic nose based on surface acoustic wave devices. ***Talanta*** 68, 1162-1165 (2006)

52. Li, C., Heinemann, P., and Sherry, R., Neural network and Bayesian network fusion models to fuse electronic nose and surface acoustic wave sensor data for apple defect detection. ***Sensor. Actuat. B-Chem.*** 125, 301-310 (2007)
53. Buck, L.B., Olfactory receptors and odor coding in mammals. ***Nutr. Rev.*** 62, S184-S188 (2004)
54. Lim, J.H., Park, J., Ahn, J.H., Jin, H.J., Hong, S., and Park, T.H., A peptide receptor-based bioelectronic nose for the real-time determination of seafood quality. ***Biosens. Bioelectron.*** 39, 244-249 (2013)
55. Kiefer, H., Krieger, J., Olszewski, J.D., von Heijne, G., Prestwich, G.D., and Breer, H., Expression of an olfactory receptor in *Escherichia coli*: purification, reconstitution, and ligand binding. ***Biochemistry*** 35, 16077-16084 (1996)
56. Ko, H.J. and Park, T.H., Dual signal transduction mediated by a single type of olfactory receptor expressed in a heterologous system. ***Biol. Chem.*** 387, 59 (2006)
57. Krautwurst, D., Yau, K.-W., and Reed, R.R., Identification of ligands for olfactory receptors by functional expression of a receptor library. ***Cell*** 95, 917-926 (1998)
58. Zhao, H., Ivic, L., Otaki, J.M., Hashimoto, M., Mikoshiba, K., and Firestein, S., Functional expression of a mammalian odorant receptor. ***Science*** 279, 237-242 (1998)
59. Wu, L., Pan, Y., Chen, G.-Q., Matsunami, H., and Zhuang, H., Receptor-transporting Protein 1 short (RTP1S) mediates translocation and activation of odorant receptors by acting through multiple steps. ***J. Biol. Chem.*** 287, 22287-22294 (2012)

60. Zhuang, H. and Matsunami, H., Synergism of accessory factors in functional expression of mammalian odorant receptors. ***J. Biol. Chem.*** 282, 15284-15293 (2007)

61. Zhuang, H. and Matsunami, H., Evaluating cell-surface expression and measuring activation of mammalian odorant receptors in heterologous cells. ***Nat. Protoc.*** 3, 1402-1413 (2008)

62. Kiely, A., Authier, A., Kralicek, A.V., Warr, C.G., and Newcomb, R.D., Functional analysis of a *Drosophila melanogaster* olfactory receptor expressed in Sf9 cells. ***J. Neurosci. Meth.*** 159, 189-194 (2007)

63. Matarazzo, V., Clot-Faybesse, O., Marcet, B., Guiraudie-Capraz, G., Atanasova, B., Devauchelle, G., Cerutti, M., Etiévant, P., and Ronin, C., Functional characterization of two human olfactory receptors expressed in the baculovirus Sf9 insect cell system. ***Chem. Senses*** 30, 195-207 (2005)

64. Minic, J., Persuy, M.A., Godel, E., Aioun, J., Connerton, I., Salesse, R., and Pajot-Augy, E., Functional expression of olfactory receptors in yeast and development of a bioassay for odorant screening. ***FEBS J.*** 272, 524-537 (2005)

65. Song, H.S., Lee, S.H., Oh, E.H., and Park, T.H., Expression, solubilization and purification of a human olfactory receptor from *Escherichia coli*. ***Curr. Microbiol.*** 59, 309-314 (2009)

66. Ko, H.J. and Park, T.H., Piezoelectric olfactory biosensor: ligand specificity and dose-dependence of an olfactory receptor expressed in a heterologous cell system. ***Biosens. Bioelectron.*** 20, 1327-1332 (2005)

67. Sankaran, S., Panigrahi, S., and Mallik, S., Olfactory receptor based piezoelectric biosensors for detection of alcohols related to food safety applications. ***Sensor. Actuat. B-Chem.*** 155, 8-18 (2011)

68. Sankaran, S., Panigrahi, S., and Mallik, S., Odorant binding protein based biomimetic sensors for detection of alcohols associated with Salmonella contamination in packaged beef. ***Biosens. Bioelectron.*** 26, 3103-3109 (2011)

69. Sung, J.H., Ko, H.J., and Park, T.H., Piezoelectric biosensor using olfactory receptor protein expressed in *Escherichia coli*. ***Biosens. Bioelectron.*** 21, 1981-1986 (2006)

70. Wu, T.-Z., A piezoelectric biosensor as an olfactory receptor for odour detection: electronic nose. ***Biosens. Bioelectron.*** 14, 9-18 (1999)

71. Benilova, I., Chegel, V., Ushenin, Y., Vidic, J., Soldatkin, A., Martelet, C., Pajot, E., and Jaffrezic-Renault, N., Stimulation of human olfactory receptor 17-40 with odorants probed by surface plasmon resonance. ***Eur. Biophys. J.*** 37, 807-814 (2008)

72. Vidic, J., Pla-Roca, M., Grosclaude, J., Persuy, M.-A., Monnerie, R., Caballero, D., Errachid, A., Hou, Y., Jaffrezic-Renault, N., Salesse, R., Pajot-Augy, E., and Samitier, J., Gold surface functionalization and patterning for specific immobilization of olfactory receptors carried by nanosomes. ***Anal. Chem.*** 79, 3280-3290 (2007)

73. Vidic, J.M., Grosclaude, J., Persuy, M.-A., Aioun, J., Salesse, R., and Pajot-Augy, E., Quantitative assessment of olfactory receptors activity in immobilized nanosomes: a novel concept for bioelectronic nose. ***Lab Chip*** 6, 1026-1032 (2006)

74. Yoon, H., Lee, S.H., Kwon, O.S., Song, H.S., Oh, E.H., Park, T.H., and Jang, J., Polypyrrole nanotubes conjugated with human olfactory receptors: high-performance transducers for FET-type bioelectronic noses. ***Angew. Chem. Int. Edit.*** 48, 2755-2758 (2009)

75. Lee, S.H., Jin, H.J., Song, H.S., Hong, S., and Park, T.H., Bioelectronic nose with high sensitivity and selectivity using chemically functionalized carbon nanotube combined with human olfactory receptor. ***J. Biotechnol.*** 157, 467-472 (2012)

76. Katada, S., Hirokawa, T., Oka, Y., Suwa, M., and Touhara, K., Structural basis for a broad but selective ligand spectrum of a mouse olfactory receptor: mapping the odorant-binding site. ***J. Neurosci.*** 25, 1806-1815 (2005)

77. Wetzel, C.H., Oles, M., Wellerdieck, C., Kuczkowiak, M., Gisselmann, G., and Hatt, H., Specificity and sensitivity of a human olfactory receptor functionally expressed in human embryonic kidney 293 cells and *Xenopus laevis* oocytes. ***J. Neurosci.*** 19, 7426-7433 (1999)

78. Lee, J.Y., Ko, H.J., Lee, S.H., and Park, T.H., Cell-based measurement of odorant molecules using surface plasmon resonance. ***Enzyme Microb. Tech.*** 39, 375-380 (2006)

79. Lee, S.H., Jun, S.B., Ko, H.J., Kim, S.J., and Park, T.H., Cell-based olfactory biosensor using microfabricated planar electrode. ***Biosens. Bioelectron.*** 24, 2659-2664 (2009)

80. Lee, S.H., Jeong, S.H., Jun, S.B., Kim, S.J., and Park, T.H., Enhancement of cellular olfactory signal by electrical stimulation. ***Electrophoresis*** 30, 3283-3288 (2009)

81. Lee, S.H., Ko, H.J., and Park, T.H., Real-time monitoring of odorant-induced cellular reactions using surface plasmon resonance. ***Biosens. Bioelectron.*** 25, 55-60 (2009)

82. Jin, H.J., Lee, S.H., Kim, T.H., Park, J., Song, H.S., Park, T.H., and Hong, S., Nanovesicle-based bioelectronic nose platform mimicking human olfactory signal transduction. ***Biosens. Bioelectron.*** 35, 335-341 (2012)

83. Park, J., Lim, J.H., Jin, H.J., Namgung, S., Lee, S.H., Park, T.H., and Hong, S., A bioelectronic sensor based on canine olfactory nanovesicle-carbon nanotube hybrid structures for the fast assessment of food quality. ***Analyst*** 137, 3249-3254 (2012)

84. Auge, J., Hauptmann, P., Hartmann, J., Rösler, S., and Lucklum, R., New design for QCM sensors in liquids. ***Sensor. Actuat. B-Chem.*** 24, 43-48 (1995)

85. Resa, P., Castro, P., Rodríguez-López, J., and Elvira, L., Broadband spike excitation method for in-liquid QCM sensors. ***Sensor. Actuat. B-Chem.*** 166–167, 275-280 (2012)

86. Shen, S., Liu, T., and Guo, J., Optical phase-shift detection of surface plasmon resonance. ***Appl. Optics*** 37, 1747-1751 (1998)

87. Hou, Y., Jaffrezic-Renault, N., Martelet, C., Zhang, A., Minic-Vidic, J., Gorojankina, T., Persuy, M.-A., Pajot-Augy, E., Salesse, R., Akimov, V., Reggiani, L., Pennetta, C., Alfinito, E., Ruiz, O., Gomila, G., Samitier, J., and Errachid, A., A novel detection strategy for odorant molecules based on controlled bioengineering of rat olfactory receptor I7. ***Biosens. Bioelectron.*** 22, 1550-1555 (2007)

88. Benilova, I.V., Minic Vidic, J., Pajot-Augy, E., Soldatkin, A.P., Martelet, C., and Jaffrezic-Renault, N., Electrochemical study of human olfactory receptor OR 17–40 stimulation by odorants in solution. ***Mat. Sci. Eng. C*** 28, 633-639 (2008)

89. Rao, S.G., Huang, L., Setyawan, W., and Hong, S., Nanotube electronics: large-scale assembly of carbon nanotubes. ***Nature*** 425, 36-37 (2003)

90. Kwon, O.S., Ahn, S.R., Park, S.J., Song, H.S., Lee, S.H., Lee, J.S., Hong, J.-Y., Lee, J.S., You, S.A., Yoon, H., Park, T.H., and Jang, J., Ultrasensitive and selective recognition of peptide hormone using close-packed arrays of hPTHR-conjugated polymer nanoparticles. ***ACS Nano*** 6, 5549-5558 (2012)

91. Song, H.S., Kwon, O.S., Lee, S.H., Park, S.J., Kim, U.-K., Jang, J., and Park, T.H., Human taste receptor-functionalized field effect transistor as a human-like nanobioelectronic tongue. ***Nano Lett.*** 13, 172-178 (2012)

92. Oka, Y., Omura, M., Kataoka, H., and Touhara, K., Olfactory receptor antagonism between odorants. ***EMBO J.*** 23, 120-126 (2004)

93. Jacquier, V., Pick, H., and Vogel, H., Characterization of an extended receptive ligand repertoire of the human olfactory receptor OR17-40 comprising structurally related compounds. ***J. Neurochem.*** 97, 537-544 (2006)

94. Kim, T.H., Song, H.S., Jin, H.J., Lee, S.H., Namgung, S., Kim, U.-k., Park, T.H., and Hong, S., "Bioelectronic super-taster" device based on taste receptor-carbon nanotube hybrid structures. ***Lab Chip*** 11, 2262-2267 (2011)

95. Ishikawa, F.N., Chang, H.-K., Curreli, M., Liao, H.-I., Olson, C.A., Chen, P.-C., Zhang, R., Roberts, R.W., Sun, R., Cote, R.J., Thompson, M.E., and Zhou, C., Label-free, electrical detection of the SARS virus n-protein with nanowire biosensors utilizing antibody mimics as capture Ppobes. ***ACS Nano*** 3, 1219-1224 (2009)

96. Star, A., Tu, E., Niemann, J., Gabriel, J.-C.P., Joiner, C.S., and Valcke, C., Label-free detection of DNA hybridization using carbon nanotube network field-effect transistors. ***Proc. Natl. Acad. Sci. USA*** 103, 921-926 (2006)

97. Stern, E., Vacic, A., Rajan, N.K., Criscione, J.M., Park, J., Ilic, B.R., Mooney, D.J., Reed, M.A., and Fahmy, T.M., Label-free biomarker detection from whole blood. ***Nat. Nanotechnol.*** 5, 138-142 (2010)

98. Chang, H.-K., Ishikawa, F.N., Zhang, R., Datar, R., Cote, R.J., Thompson, M.E., and Zhou, C., Rapid, label-free, electrical whole blood bioassay based on nanobiosensor systems. ***ACS Nano*** 5, 9883-9891 (2011)

99. Liu, S., Zhang, X., Luo, W., Wang, Z., Guo, X., Steigerwald, M.L., and Fang, X., Single-molecule detection of proteins using aptamer-functionalized molecular electronic devices. ***Angew. Chem. Int. Edit.*** 50, 2496-2502 (2011)

100. Castle, P.E., Gutierrez, E.C., Leitch, S.V., Maus, C.E., McMillian, R.A., Nussbaumer, W.A., Vaughan, L.M., Wheeler, C.M., Gravitt, P.E., and Schiffman, M., Evaluation of a new DNA test for detection of carcinogenic human papillomavirus. ***J. Clin. Microbiol.*** 49, 3029-3032 (2011)

101. Spain, E., Kojima, R., Kaner, R.B., Wallace, G.G., O'Grady, J., Lacey, K., Barry, T., Keyes, T.E., and Forster, R.J., High sensitivity DNA detection using gold nanoparticle functionalised polyaniline nanofibres. ***Biosens. Bioelectron.*** 26, 2613-2618 (2011)

102. Zhao, C., Wu, L., Ren, J., and Qu, X., A label-free fluorescent turn-on enzymatic amplification assay for DNA detection using ligand-responsive G-quadruplex formation. ***Chem. Comm.*** 47, 5461-5463 (2011)

103. Goldsmith, B.R., Mitala, J.J., Josue, J., Castro, A., Lerner, M.B., Bayburt, T.H., Khamis, S.M., Jones, R.A., Brand, J.G., Sligar, S.G., Luetje, C.W., Gelperin, A., Rhodes, P.A., Discher, B.M., and Johnson, A.T.C., Biomimetic chemical sensors using nanoelectronic readout of olfactory receptor proteins. ***ACS Nano*** 5, 5408-5416 (2011)

104. Deng, C., Zhang, X., and Li, N., Investigation of volatile biomarkers in lung cancer blood using solid-phase microextraction and capillary gas chromatography-mass spectrometry. ***J. Chromatogr. B*** 808, 269-277 (2004)

105. Fuchs, P., Loeseken, C., Schubert, J.K., and Miekisch, W., Breath gas aldehydes as biomarkers of lung cancer. ***Int. J. Cancer*** 126, 2663-2670 (2010)

106. Li, N., Deng, C., Yao, N., Shen, X., and Zhang, X., Determination of acetone, hexanal and heptanal in blood samples by derivatization with pentafluorobenzyl hydroxylamine followed by headspace single-drop microextraction and gas chromatography-mass spectrometry. ***Anal. Chim. Acta*** 540, 317-323 (2005)

107. Zhang, H.-J., Huang, J.-F., Lin, B., and Feng, Y.-Q., Polymer monolith microextraction with in situ derivatization and its application to high-performance liquid chromatography determination of hexanal and heptanal in plasma. ***J. Chromatogr. A*** 1160, 114-119 (2007)

108. Deng, C. and Zhang, X., A simple, rapid and sensitive method for determination of aldehydes in human blood by gas chromatography/mass spectrometry and solid-phase microextraction with on-fiber derivatization. ***Rapid Comm. Mass Sp.*** 18, 1715-1720 (2004)

109. Jones, D.T. and Reed, R.R., Golf: an olfactory neuron specific-G protein involved in odorant signal transduction. ***Science*** 244, 790-795 (1989)

110. Wetzel, C.H., Oles, M., Wellerdieck, C., Kuczkowiak, M., Gisselmann, G., and Hatt, H., Specificity and Sensitivity of a Human Olfactory Receptor Functionally Expressed in Human Embryonic Kidney 293 Cells andXenopus Laevis Oocytes. ***J. Neurosci.*** 19, 7426-7433 (1999)

111. Katada, S., Nakagawa, T., Kataoka, H., and Touhara, K., Odorant response assays for a heterologously expressed olfactory receptor. ***Biochem. Biophys. Res. Commun.*** 305, 964-969 (2003)

112. Katada, S., Tanaka, M., and Touhara, K., Structural determinants for membrane trafficking and G protein selectivity of a mouse olfactory receptor. ***J. Neurochem.*** 90, 1453-1463 (2004)

113. Saito, H., Kubota, M., Roberts, R.W., Chi, Q., and Matsunami, H., RTP Family Members Induce Functional Expression of Mammalian Odorant Receptors. ***Cell*** 119, 679-691 (2004)

114. Li, N., Deng, C., Yin, X., Yao, N., Shen, X., and Zhang, X., Gas chromatography–mass spectrometric analysis of hexanal and heptanal in human blood by headspace single-drop microextraction with droplet derivatization. ***Anal. Biochem.*** 342, 318-326 (2005)

115. Kim, Y.D. and Morr, C.V., Dynamic headspace analysis of light activated flavor in milk. ***Int. Dairy J.*** 6, 185-193 (1996)

116. Shin, M.G., Yoon, S.H., Rhee, J.S., and Kwon, T.-W., Correlation between oxidative deterioration of unsaturated lipid and n-hexanal during storage of brown rice. ***J. Food Sci.*** 51, 460-463 (1986)

117. Jadhav, S., Singh, B., and Salunkhe, D.K., Metabolism of unsaturated fatty acids in tomato fruit: linoleic and linolenic acid as precursors of hexanal. ***Plant Cell Physiol.*** 13, 449-459 (1972)

118. McClements, D.J. and Decker, E.A., Lipid oxidation in oil-in-water emulsions: impact of molecular environment on chemical reactions in heterogeneous food systems. ***J. Food Sci.*** 65, 1270-1282 (2000)

119. Kunau, W.-H. and Dommes, P., Degradation of Unsaturated Fatty Acids. ***Eur. J. Biochem.*** 91, 533-544 (1978)

120. Ulberth, F. and Roubicek, D., Monitoring of oxidative deterioration of milk powder by headspace gas chromatography. ***Int. Dairy J.*** 5, 523-531 (1995)

121. Sanches-Silva, A., Rodríguez-Bernaldo de Quirós, A., López-Hernández, J., and Paseiro-Losada, P., Gas chromatographic determination of glycerides in potato crisps fried in different oils. ***Chromatographia*** 58, 517-521 (2003)

122. Haugen, J.-E., Lundby, F., Wold, J.P., and Veberg, A., Detection of rancidity in freeze stored turkey meat using a commercial gas-sensor array system. ***Sensor. Actuat. B-Chem.*** 116, 78-84 (2006)

123. Sonia, E., GianFrancesco, M., Roberto, S., Ibanez, R., Agnese, T., Stefania, U., and Maurizio, S., Monitoring of virgin olive oil volatile compounds evolution during olive malaxation by an array of metal oxide sensors. ***Food Chem.*** 113, 345-350 (2009)

124. Benbernou, N., Tacher, S., Robin, S., Rakotomanga, M., Senger, F., and Galibert, F., Functional analysis of a subset of canine olfactory receptor genes. ***J. Hered.*** 98, 500-505 (2007)

125. Moreau, C.J., Dupuis, J.P., Revilloud, J., Arumugam, K., and Vivaudou, M., Coupling ion channels to receptors for biomolecule sensing. ***Nat. Nanotechnol.*** 3, 620-625 (2008)

126. Caro, L.N., Moreau, C.J., Revilloud, J., and Vivaudou, M., β2-adrenergic ion-channel coupled receptors as conformational motion detectors. ***PLoS ONE*** 6, e18226 (2011)

127. Isomoto, S., Kondo, C., Yamada, M., Matsumoto, S., Higashiguchi, O., Horio, Y., Matsuzawa, Y., and Kurachi, Y., A novel sulfonylurea receptor forms with BIR (Kir6.2) a smooth muscle type ATP-sensitive K+ channel. ***J. Biol. Chem.*** 271, 24321-24324 (1996)

128. Inagaki, N., Gonoi, T., Iv, J.P.C., Wang, C.-Z., Aguilar-Bryan, L., Bryan, J., and Seino, S., A family of sulfonylurea receptors determines the pharmacological properties of ATP-Sensitive K^+ channels. ***Neuron*** 16, 1011-1017 (1996)

129. Neuhaus, E.M., Mashukova, A., Zhang, W., Barbour, J., and Hatt, H., A specific heat shock protein enhances the expression of mammalian olfactory receptor proteins. ***Chem. Senses*** 31, 445-452 (2006)

130. Whiteaker, K.L., Gopalakrishnan, S.M., Groebe, D., Shieh, C.-C., Warrior, U., Burns, D.J., Coghlan, M.J., Scott, V.E., and Gopalakrishnani, M., Validation of FLIPR membrane potential dye for high throughput screening of potassium channel modulators. ***J. Biomol. Screen.*** 6, 305-312 (2001)

131. Gram, L. and Dalgaard, P., Fish spoilage bacteria - problems and solutions. ***Curr. Opin. Biotech.*** 13, 262-266 (2002)

132. Shapiro, R.L., Altekruse, S., Hutwagner, L., Bishop, R., Hammond, R., Wilson, S., Ray, B., Thompson, S., Tauxe, R.V., and Griffin, P.M., The role of Gulf Coast oysters harvested in warmer months in *Vibrio vulnificus* Infections in the United States, 1988–1996. ***J. Infect. Dis.*** 178, 752-759 (1998)

133. Dalgaard, P., Madsen, H.L., Samieian, N., and Emborg, J., Biogenic amine formation and microbial spoilage in chilled garfish - effect of modified atmosphere packaging and previous frozen storage. ***J. Appl. Microbiol.*** 101, 80-95 (2006)

134. Lone, G., Evaluation of the bacteriological quality of seafood. ***Int. J. Food Microbiol.*** 16, 25-39 (1992)

135. Veciana-Nogués, M.T., Mariné-Font, A., and Vidal-Carou, M.C., Biogenic amines in fresh and canned tuna. effects of canning on biogenic amine contents. ***J. Agric. Food Chem.*** 45, 4324-4328 (1997)

136. Milo, C. and Grosch, W., Detection of odor defects in boiled cod and trout by gas chromatography-olfactometry of headspace samples. ***J. Agric. Food Chem.*** 43, 459-462 (1995)

137. Veciana-Nogués, M.T., Albala-Hurtado, M.S., Izquierdo-Pulido, M., and Vidal-Carou, M.C., Validation of a gas-chromatographic method for volatile amine determination in fish samples. ***Food Chem.*** 57, 569-573 (1996)

138. Bota, G.M. and Harrington, P.B., Direct detection of trimethylamine in meat food products using ion mobility spectrometry. ***Talanta*** 68, 629-635 (2006)

139. Hyotylainen, T., Savola, N., Lehtonen, P., and Riekkola, M.-L., Determination of biogenic amines in wine by multidimensional liquid chromatography with online derivatisation. ***Analyst*** 126, 2124-2127 (2001)

140. Adhoum, N., Monser, L., Sadok, S., El-Abed, A., Greenway, G.M., and Uglow, R.F., Flow injection potentiometric detection of trimethylamine in seafood using tungsten oxide electrode. ***Anal. Chim. Acta*** 478, 53-58 (2003)

141. Alimelli, A., Pennazza, G., Santonico, M., Paolesse, R., Filippini, D., D'Amico, A., Lundström, I., and Di Natale, C., Fish freshness detection by a computer screen photoassisted based gas sensor array. ***Anal. Chim. Acta*** 582, 320-328 (2007)

142. Natale, C.D., Olafsdottir, G., Einarsson, S., Martinelli, E., Paolesse, R., and D'Amico, A., Comparison and integration of different electronic noses for freshness evaluation of cod-fish fillets. ***Sensor. Actuat. B-Chem.*** 77, 572-578 (2001)

143. O'Connell, M., Valdora, G., Peltzer, G., and Martín Negri, R., A practical approach for fish freshness determinations using a portable electronic nose. ***Sensor. Actuat. B-Chem.*** 80, 149-154 (2001)

144. Pacquit, A., Lau, K.T., McLaughlin, H., Frisby, J., Quilty, B., and Diamond, D., Development of a volatile amine sensor for the monitoring of fish spoilage. ***Talanta*** 69, 515-520 (2006)

145. Huang, X., Li, M., Xu, X., Chen, H., Ji, H.-F., and Zhu, S., Microcantilevers modified by specific peptide for selective detection of trimethylamine. ***Biosens. Bioelectron.*** 30, 140-144 (2011)

146. Li, N., Endo, H., Hayashi, T., Fujii, T., Takai, R., and Watanabe, E., Development of a trimethylamine gas biosensor system. ***Biosens. Bioelectron.*** 9, 593-599 (1994)

147. Mitsubayashi, K., Kubotera, Y., Yano, K., Hashimoto, Y., Kon, T., Nakakura, S., Nishi, Y., and Endo, H., Trimethylamine biosensor with flavin-containing monooxygenase type 3 (FMO3) for fish-freshness analysis. ***Sensor. Actuat. B-Chem.*** 103, 463-467 (2004)

148. Chen, R.J., Zhang, Y., Wang, D., and Dai, H., Noncovalent sidewall functionalization of single-walled carbon nanotubes for protein immobilization. ***J. Am. Chem. Soc.*** 123, 3838-3839 (2001)

149. Feldstein, M., Levaggi, D.A., and Thuillier, R., Odor regulation by emission limitation at the stack. ***Ann. NY Acad. Sci.*** 237, 309-314 (1974)

150. Chaim, W., Karpas, Z., and Lorber, A., New technology for diagnosis of bacterial vaginosis. ***Eur. J. Obstet. Gyn. R. B.*** 111, 83-87 (2003)

151. Wolrath, H., Stahlbom, B., Hallen, A., and Forsum, U., Trimethylamine and trimethylamine oxide levels in normal women and women with bacterial vaginosis reflect a local metabolism in vaginal secretion as compared to urine. ***APMIS*** 113, 513-516 (2005)

152. Chalmers, R., Bain, M., Michelakakis, H., Zschocke, J., and Iles, R., Diagnosis and management of trimethylaminuria (FMO3 deficiency) in children. ***J. Inherit. Metab. Dis.*** 29, 162-172 (2006)

153. Zhang, M., Smith, A., and Gorski, W., Carbon nanotube-chitosan system for electrochemical sensing based on dehydrogenase enzymes. ***Anal. Chem.*** 76, 5045-5050 (2004)

154. Sánchez-Acevedo, Z.C., Riu, J., and Rius, F.X., Fast picomolar selective detection of bisphenol A in water using a carbon nanotube field effect transistor functionalized with estrogen receptor-α. ***Biosens. Bioelectron.*** 24, 2842-2846 (2009)

155. Kim, J.P., Lee, B.Y., Hong, S., and Sim, S.J., Ultrasensitive carbon nanotube-based biosensors using antibody-binding fragments. ***Anal. Biochem.*** 381, 193-198 (2008)

156. Maehashi, K., Katsura, T., Kerman, K., Takamura, Y., Matsumoto, K., and Tamiya, E., Label-free protein biosensor based on aptamer-modified carbon nanotube field-effect transistors. ***Anal. Chem.*** 79, 782-787 (2006)

157. Wu, T.-Z. and Lo, Y.-R., Synthetic peptide mimicking of binding sites on olfactory receptor protein for use in ‘electronic nose’. ***J. Biotechnol.*** 80, 63-73 (2000)

158. Dan, Y., Lu, Y., Kybert, N.J., Luo, Z., and Johnson, A.T.C., Intrinsic Response of Graphene Vapor Sensors. ***Nano Lett.*** 9, 1472-1475 (2009)

159. Leonardos, G., Kendall, D., and Barnard, N., Odor threshold determinations of 53 odorant chemicals. ***J. Air Pollut. Control Assoc.*** 19, 91-95 (1969)

160. Pandeeswari, R. and Jeyaprakash, B.G., Nanostructured α-MoO_3 thin film as a highly selective TMA sensor. ***Biosens. Bioelectron.*** 53, 182-186 (2014)

161. Woo, H.-S., Na, C.W., Kim, I.-D., and Lee, J.-H., Highly sensitive and selective trimethylamine sensor using one-dimensional ZnO–Cr_2O_3 hetero-nanostructures. ***Nanotechnology*** 23, 245501 (2012)

162. Zhang, Z., Xu, K., Xing, Z., and Zhang, X., A nanosized Y_2O_3-based catalytic chemiluminescent sensor for trimethylamine. ***Talanta*** 65, 913-917 (2005)

163. Yang, R., Huang, X., Wang, Z., Zhou, Y., and Liu, L., A chemisorption-based microcantilever chemical sensor for the detection of trimethylamine. ***Sensor. Actuat. B-Chem.*** 145, 474-479 (2010)

164. Cho, Y.H., Kang, Y.C., and Lee, J.-H., Highly selective and sensitive detection of trimethylamine using WO_3 hollow spheres prepared by ultrasonic spray pyrolysis. ***Sensor. Actuat. B-Chem.*** 176, 971-977 (2013)

165. Tong, M., Dai, G., and Gao, D., WO_3 thin film sensor prepared by sol-gel technique and its low-temperature sensing properties to trimethylamine. ***Mater. Chem. Phys.*** 69, 176-179 (2001)

166. Zhao, S., Wei, P., and Chen, S., Enhancement of trimethylamine sensitivity of MOCVD-SnO_2 thin film gas sensor by thorium. ***Sensor. Actuat. B-Chem.*** 62, 117-120 (2000)

167. Tang, H., Yan, M., Ma, X., Zhang, H., Wang, M., and Yang, D., Gas sensing behavior of polyvinylpyrrolidone-modified ZnO nanoparticles for trimethylamine. ***Sensor. Actuat. B-Chem.*** 113, 324-328 (2006)

168. Saito, H., Chi, Q., Zhuang, H., Matsunami, H., and Mainland, J.D., Odor coding by a mammalian receptor repertoire. ***Sci. Signal.*** 2, ra9 (2009)

169. Kim, B., Song, H.S., Jin, H.J., Park, E.J., Lee, S.H., Lee, B.Y., Park, T.H., and Hong, S., Highly selective and sensitive detection of neurotransmitters using receptor-modified single-walled carbon nanotube sensors. ***Nanotechnology*** 24, 285501 (2013)

초 록

후각은 외부 환경을 인지는 중요한 감각이며 많은 연구진에서 후각 기능을 모사하는 장치들을 개발하여 이를 활용하고자 연구되어 왔다. 대부분의 인공 후각 장치는 휘발성 화학물질에 반응하는 센서들로 이루어지고, 특정 화학물질에 반응하는 센서들의 조합으로 냄새를 인지한다. 하지만 기존의 전자 장치들은 낮은 민감도와 선택도로 인하여 실질적인 활용이 어렵다. 그리하여 바이오 전자코라 하는 새로운 개념의 센서가 개발되었다. 냄새물질의 1 차적 검지를 위하여 생체물질을 이용하는 센서들을 바이오 전자코라 부르며, 이는 1 차 신호변환기와 2 차 신호변화기로 이루어진다. 1 차 신호변환기는 후각수용체와 같은 생체물질이며, 냄새물질을 인지하는 역할을 한다. 2 차 신호변환기는 1 차 신호변환기에서 만들어진 생체 신호를 우리가 검지할 수 있는 신호로 변환하는 역할을 한다.

본 연구에서는 후각수용체를 이용한 바이오 전자코를 개발하였다. 후각수용체는 G 단백질 결합 수용체이며, 사람은 390 여종의 수용체를 지닌다. HEK-293 세포에서 후각수용체를 발현하였고, 이를 후각 수용체의 기능을 밝히는데 활용하였다. 특별히, 폐암 진단용 마커 물질을 인지하는 후각수용체를 찾아 활용하였다. 세포는 후각 신경세포의 기능을 잘 모사할 수 있지만 큰 크기 때문에 나노소자 기반의 센서 플랫폼과 결합되기 어렵다. 따라서 세포를 대체하기 위한 세포 유래 나노베지클을 생산하였다. 나노베지클의 경우 세포 신호전달 과정에 필요한 모든 세포막 단백질과 세포질

물질을 포함하고 있기 때문에 세포를 대신하여 활용될 수 있다. 후각 수용체를 지닌 나노베지클을 단일벽 탄소나노튜브 트랜지스터에 고정화하여 바이오 전자코를 개발하였다. 냄새물질은 나노베지클의 세포막에 존재하는 후각수용체와 결합하고, 이는 세포 신호를 만드는 시작점이 된다. 나노베지클에서 만들어진 세포 신호는 탄소나노튜브 트랜지스터를 통하여 전기 신호로 변환되고, 이러한 원리를 통하여 폐암 진단용 지시물질을 높은 민감도와 선택도로 검지한다.

후각 수용체는 매우 높은 선택도를 지니고 있어, 특이적 냄새물질을 선택적으로 검지할 수 있다. 이러한 특성을 활용하여 식품의 질을 판별하는 바이오 전자코를 개발하였다. 식품 부패로 생성되는 냄새물질을 특이적으로 인지하는 후각수용체를 이용하였다. 후각수용체를 지닌 나노베지클을 탄소나노튜브 트랜지스터에 고정화하였다. 이러한 센서는 부패한 우유에서 식품 신선도 표지물질을 전처리 없이 쉽고 빠르게 검지한다.

나노베지클 기반의 바이오 전자코는 민감도와 선택도 측면에서 매우 훌륭한 특성을 지닌다. 하지만 낮은 안정성으로 인하여 실제 산업에서 활용하기 어렵다. 낮은 안정성은 세포 신호전달과정에 필요한 ATP 와 같은 물질들의 불안정성에서 비롯한다. 나노베지클의 안정성을 개선하기 위하여 신호전달 과정을 조작하였다. 칼륨 채널을 후각수용체 말단에 인위적으로 결합함으로써 ATP 없이 세포 신호를 만들 수 있는 시스템을 개발하였다. 이는 실제로 나노베지클의 안정성을 크게 향상시켰다.

후각수용체 단백질은 3 차원 구조를 이루기 위하여 지질막을 필요로 한다. 하지만 후각수용체에서 유래한 펩타이드 수용체는 3 차원 구조를 필요로 하지 않기에 지질막이 없는 상태에서도 후각 수용체와 같은 작용을 할 수 있다. 본 연구에서는 후각수용체에서 유래한 펩타이드 수용체와 탄소나노튜브 트랜지스터를 이용하여 해산물의 신선도를 측정하는 바이오 전자코를 개발하였다. 펩타이드 수용체는 해산물 부패를 나타내는 지시물질을 선택적으로 감지한다. 이러한 바이오 전자코는 해산물 부패 지시물질을 높은 민감도와 선택도로 검지할 수 있고, 실제 부패한 해산물에 존재하는 지시물질들 또한 전처리 없이 쉽고 빠르게 검출할 수 있다. 또한, 기체상태의 냄새물질 또한 쉽게 검지할 수 있다.

질병진단, 환경 모니터링, 식품 안전성 판별 등 다양한 분야에서 바이오 전자코를 활용할 수 있다. 본 연구에서 나노베지클과 펩타이드 수용체를 이용한 바이오 전자코를 개발하기 위한 연구 과정을 제시하였고, 바이오 전자코의 실질적 활용 가능성을 증명하였다.

주요어: 바이오 전자코, 나노베지클, 펩타이드, 탄소나노튜브, 질병 진단, 식품 안전성

학 번: 2008-21108